

Distribution unlimited.

The Snow Cover of the Arctic Basin

by V.F. Radionov, N.N. Bryazgin, and E.I. Alexandrov

*Arctic and Antarctic Research Institute,
a State Scientific Center of the Russian Federation,
Russian Federal Service for Hydrometeorology and Environmental Monitoring*

with foreword by Norbert Untersteiner, Chairman

*Department of Atmospheric Sciences, University of Washington,
Seattle, Washington, USA*

Technical Report
APL-UW TR 9701
March 1997

19970703 066

English translation sponsored by NASA Grant NAGW-4382

EXERCISE QUALITY CONTROLLED &

The Snow Cover of the Arctic Basin

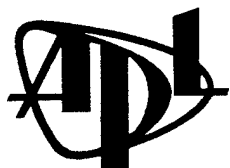
by V.F. Radionov, N.N. Bryazgin, and E.I. Alexandrov

*Arctic and Antarctic Research Institute,
a State Scientific Center of the Russian Federation,
Russian Federal Service for Hydrometeorology and Environmental Monitoring*

with foreword by Norbert Untersteiner, Chairman

*Department of Atmospheric Sciences, University of Washington,
Seattle, Washington, USA*

Technical Report
APL-UW TR 9701
March 1997



Applied Physics Laboratory University of Washington
1013 NE 40th Street Seattle, Washington 98105-6698

English translation sponsored by NASA Grant NAGW-4382

The Snow Cover of the Arctic Basin

A Monograph

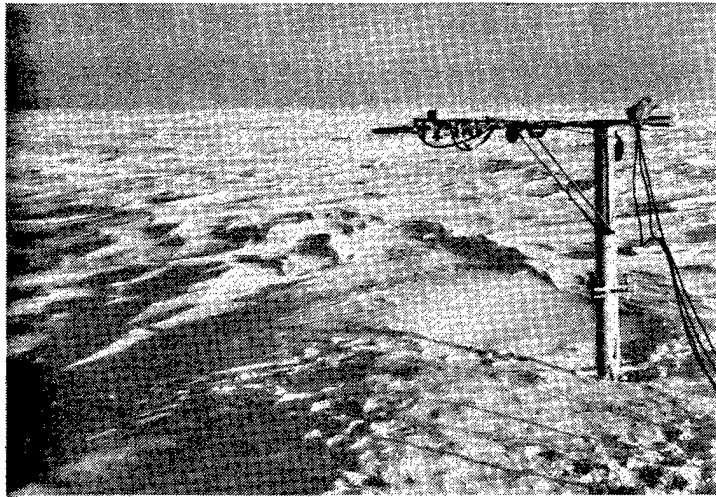
by

Vladimir Fyodorovich Radionov
Nicolay Nicolaevich Bryazgin
Evgeniy Ivanovich Alexandrov

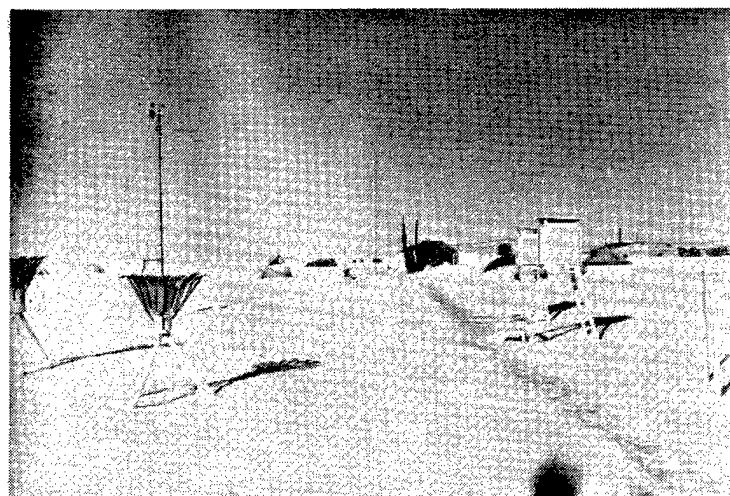
G. V. Alexeev, Editor

Gidrometeoizdat, 199397, 38 Bering Street, Saint Petersburg, Russia
Publishers

English translation by Irina Solovyova and T. C. Grenfell



Photographs by N. N. Bryazgin at drifting station NP-6 in 1957.
(top) Overview of station, (middle) albedo measurement, (bottom) snow-line measurement.



Photographs by N. N. Bryazgin at drifting station NP-6 in 1957. (top) Snow-density measurement, (middle) snow-accumulation gauge (left) and air temperature gauges (right), (bottom) anemometers.

FOREWORD

Norbert Untersteiner

Department of Atmospheric Sciences and Applied Physics Laboratory

A manuscript of this report was made available by Dr. Vladimir Radionov of the Arctic and Antarctic Research Institute in St. Petersburg to several researchers in the West who are engaged in arctic climate studies. The Russian version was published by Gidrometeoizdat Publishing House, St. Petersburg, in 1996 under the title "Snyezhnyi Pokrov v Arkticheskom Basseinye" by V. F. Radionov, N. N. Bryazgin, and E. I. Alexandrov. The present English version was prepared by Dr. Thomas Grenfell from a rough translation by I. Solovyova provided by Dr. Radionov.

The report describes a data set containing the most comprehensive collection of snow depths ever taken on Arctic sea ice, starting with the Soviet station NP-3 in 1954 and ending with NP-31 in 1991. While Russian drifting stations have always reported mean snow depth as part of their synoptic weather messages for the World Meteorological Organization, the present collection documents all snow depth readings and their statistics. The data collected here are also contained in a larger archive of all weather observations taken at Soviet (Russian) drifting stations. That archive is available on CD-ROM from the National Snow and Ice Data Center at www-nsidc.colorado.edu.

The help of all those involved in preparing this report, notably Dr. Radionov, Mr. R. Colony, Mr. I. Rigor, Drs. T. Grenfell and S. Warren, and the APL editorial staff, is greatly appreciated. Financial support for editing and printing was provided by NASA's Polar Research Program Office under Grant No. NAGW-4382.

TABLE OF CONTENTS

	<i>Page</i>
Preface.....	vi
Introduction.....	vii
1. Brief Characterization of the Climate of the Arctic Basin.....	1-1
1.1 Solar radiation.....	1-1
1.2 Atmospheric circulation and air pressure.....	1-2
1.3 Air temperature and humidity.....	1-3
1.4 Cloudiness.....	1-5
1.5 Characteristics of the wind.....	1-8
1.6 Atmospheric phenomena and the precipitation forming the snow cover....	1-10
2. Measurements of the Snow Cover and Data Processing.....	2-1
2.1 Snow-depth measurements at the standard meteorological sites.....	2-1
2.2 Snow-line survey (traverse) measurements.....	2-1
2.3 Dates of snow-cover formation and disappearance.....	2-3
2.4 Measurement of albedo.....	2-5
2.5 Comparison of the results of measurements of snow depth at the meteorological observation sites with those along the snow lines.....	2-5
3. Processes of Formation and Decay of the Snow Cover.....	3-1
3.1 Precipitation due to condensation and sublimation at the snow surface.....	3-1
3.2 Evaporation and melting of the snow cover.....	3-2
4. Physical Characteristics of the Snow Cover.....	4-1
4.1 Temperature of the snow cover.....	4-1
4.2 Density and hardness of the snow cover.....	4-3
4.3 Penetration of solar radiation into the snow.....	4-5

5. Albedo of the Snow Cover.....	5-1
5.1 Integrated albedo	5-1
5.2 Spectral albedo	5-4
6. Spatial Variability in the Characteristics of the Snow Cover in the Arctic Basin	6-1
6.1 Methods for cataloging the data and for calculating the climatological characteristics based on data from the drifting stations	6-1
6.2 Depth of the snow cover	6-3
6.3 Snow density	6-13
6.4 The water equivalent of the snow cover	6-13
6.5 Duration of the snow cover.....	6-15
6.6 Snow transport	6-17
7. Temporal Variability of Snow-Cover Characteristics in the Arctic Basin	7-1
7.1 Technique for producing continuous series of observations from the drift-station data	7-2
7.2 Interannual variability of snow-cover characteristics, precipitation, and air temperature	7-1
8. Summary	8-1
9. References.....	9-1
Appendix A.....	A1-A2
Appendix B	B1-B3
Appendix C	C1-C2
Appendix D.....	D1

PREFACE

In this monograph we present the results, reduction, and analysis of standardized observations of the precipitation and characteristics of the snow cover on the North Pole drifting stations from 1954 to 1991. The systematization of this unique set of observations and the resulting general conclusions, the completion of which involved the efforts of several dozen meteorologists, have made it possible for the first time to evaluate quantitatively the spatial and temporal variations of the parameters of the snow cover in the Arctic Basin. Along with cartographic materials, also presented in this monograph, this information can be used directly as input parameters in computer model to investigate a wide range of problems involving energy exchange in the ocean-atmosphere-cryosphere system and regional moisture exchange, as well as for climate research and the calculation of fresh water flux in the Arctic ocean.

The introduction and conclusion sections were written jointly by N. N. Bryazgin and V. F. Radionov, Sections 1 and 2 by E. I. Alexandrov, N. N. Bryazgin, and V. F. Radionov, Sections 3 and 4 by N. N. Bryazgin, Section 5 by V. F. Radionov, and Sections 6 and 7 by E. I. Alexandrov and N. N. Bryazgin. The authors wish to express their gratitude to the reviewers V. F. Zakharov and V. E. Borodachev for their thoughtful comments.

INTRODUCTION

The snow that covers the drifting ice in the Arctic Basin for 11 months, or sometimes throughout the entire year, is an important component of the regional climatic system. The high reflectivity of the snow surface significantly influences the radiation regime of the Arctic atmosphere.

The analysis and generalization of the results of actinometric observations at drifting, island, and coastal stations in the Arctic show that when the average annual albedo is more than 70%, the radiation balance is negative for all values of the total incident radiation. The zero isoline of the total annual radiation balance coincides with the boundary of the multiyear ice of the Arctic Basin.

The high infrared emissivity of snow is one of the causes of near-surface atmospheric temperature inversions. This, in turn, stimulates sublimation of water vapor from the atmosphere to the snow surface as hoar frost. In this case, the snow cover acts as an absorber of atmospheric moisture, and thus it is one of the factors influencing the global moisture exchange.

Since snow cover is one of the best heat insulators of all known natural surfaces, it has a considerable influence on the exchange of heat between the ocean and the atmosphere. At a snow-cover depth of more than 15 cm, the heat fluxes from the underlying ice surface are almost completely shielded by the snow cover. Consequently, the snow-cover parameters, primarily thickness, density, and their spatial distribution, have a pronounced effect on the thermal regime of the northern polar regions [58].

Pollutants falling out of the atmosphere accumulate in the snow cover. Their transport with drifting ice and subsequent entry into the surface water as the snow melts may have a significant effect on the hydrochemical characteristics of the upper ocean.

Even this brief list of the effects of the influence of the snow cover on climatologically important factors and environmental characteristics testifies to the importance of studying the parameters of the snow cover in the Arctic Basin.

The open-water area of the Arctic Basin under consideration is defined by the northern boundaries of the peripheral seas of the Arctic Ocean as well as the northern boundaries of Greenland and islands of the Canadian Arctic Archipelago. The geographical center of the Arctic Basin is a point with the following coordinates: 86°N latitude, 150°W longitude (point 7 in Figure 1). In summer and winter, this part of the basin is fully covered with ice, with an ice concentration between 8 and 10 tenths. In summer the area of open water is as much as 15–20%, and in winter up to 5% [6]. The thickness of the ice is considerable. Even the level undeformed first-year ice growing at low air temperatures during the course of many months reaches a thickness of 1.5 to 2 m. Ice that is driven by wind action can deform into hummocks whose height usually varies between 2 and 3.5 m. The portion of the total ice-covered area occupied by hummocks is about 13% in summer and 18% in winter.

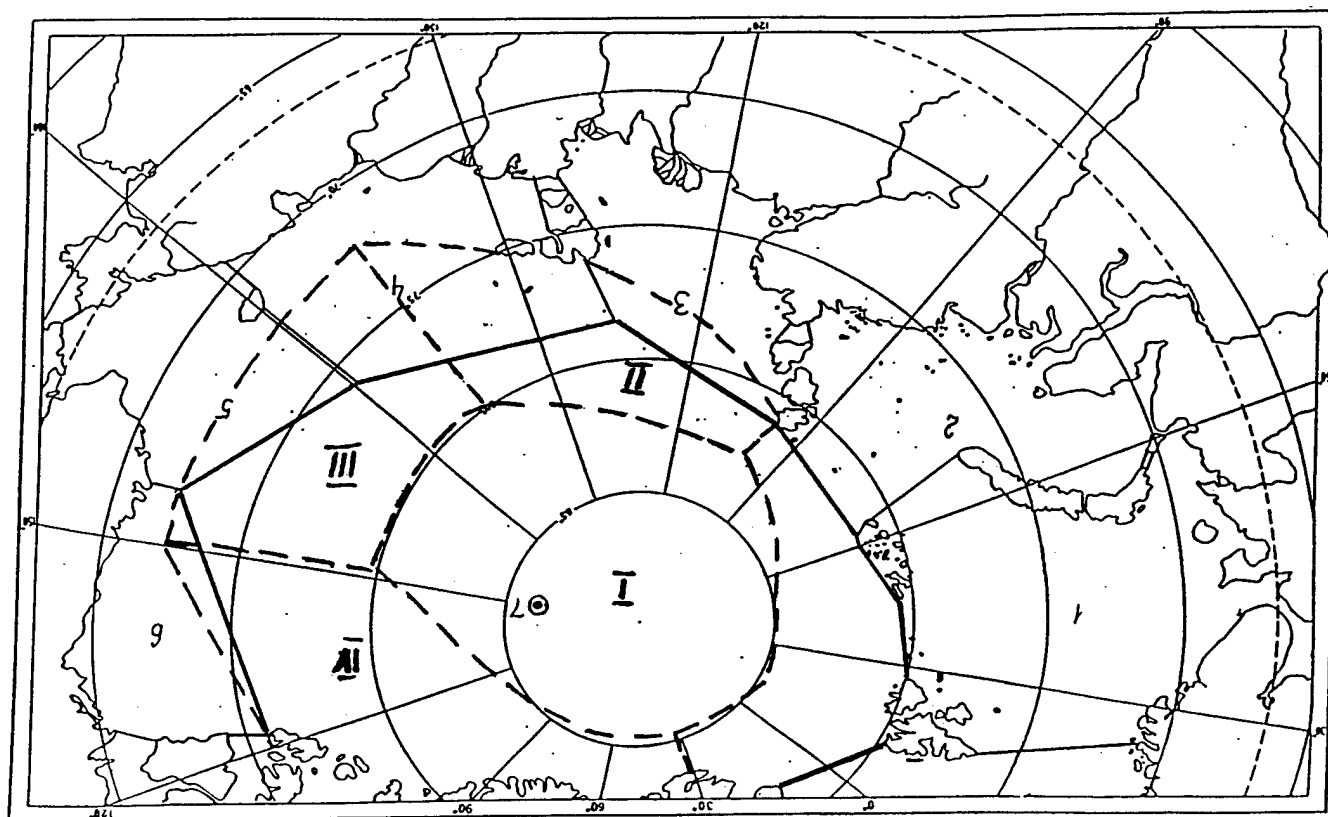


Figure 1. Boundaries of the Arctic Basin and adjacent Arctic seas. 1 - Barents Sea; 2 - Kara Sea; 3 - Laptev Sea; 4 - East-Siberian Sea; 5 - Chukchi Sea; 6 - Beaufort Sea; 7 - central point of the Arctic Basin. I - Central region, II - Siberian region, III - Pacific Ocean region, IV - Canadian region.

In wintertime, when air temperatures are below 0°C , the effect of the ice- and snow-covered areas on the atmosphere is not great. Seasonal variations in the air temperature over such areas are several tens of degrees, whereas over the open ocean variations usually do not exceed a few degrees. However, some ocean heat does reach the atmosphere through the ice. The confirmation of this is that the temperature of the snow cover's surface usually differs from the air temperature by less than $2\text{--}3^{\circ}\text{C}$, whereas over land in the Arctic and over glaciers, the difference is 7°C .

The sea ice is in constant motion as a result of the influence of the atmospheric circulation. In accordance with the air circulation, the principal direction of ice drift is from east to west toward the Greenland Sea. Some drifting stations experienced clockwise ice motion near the Canadian Arctic Archipelago (NP-2, NP-22). Station NP-7 was evacuated and left to travel into the strait between Greenland and Ellesmere Island. However,

the principal exit from the Arctic Basin is into the Greenland Sea, where the ice is transported by winds and by the East Greenland Current.

The study of snow cover on Arctic sea ice has received considerable attention. Fragmentary data on the snow cover are available that were obtained during the forced drift of the *Sedov* from 1937 to 1939. Measurements of the snow thickness over different ice types were performed by V. Kh. Buinitsky [14], N. I. Dem'yanov [17], V. A. Shamont'iev [51], and G. N. Yakovlev [53]. Additional investigations of the snow cover on Arctic sea ice have been carried out by N. N. Bryazgin [7], A. Ya. Buzuev et al. [13], R. Kh. Vaganov et al. [15], A. P. Koptev and B. L. Piatnenkov [28], and Yu. L. Nazintsev [39].

Episodic observations were performed at drifting station NP-1 in 1937 and at NP-2 in 1950–51. Regular measurements of the snow-cover characteristics were not started until 1954 at NP-3. Consistent techniques were used continually from then until October 1991, when NP-31 was decommissioned. In various years, measurements were carried out simultaneously at two and occasionally three stations drifting in different regions of the Arctic Basin. Some results of the analysis and summaries of a small number of the observations have been published. The annual variation of snow-cover depth and density was first obtained by V.S. Loschilov [32] using data from NP-6. Charts on the maximum snow-cover depths and on the extent of the snow cover in autumn and spring including the Arctic Basin are presented in the *Atlas of the Arctic* [3] and the *Atlas of the Oceans—The Arctic Ocean* [5]. They were based on the data obtained through 1975. Information about snow-cover depths over various types of ice topography encountered in the Arctic Basin are available in Ref. [36] and in the monographs by I. P. Romanov [47,48]. This monograph includes the first general results on snow-cover parameters from systematic observations carried out from 1954 (station NP-3) through 1991 (station NP-31).

1. BRIEF CHARACTERIZATION OF THE CLIMATE OF THE ARCTIC BASIN

1.1 Solar radiation

The radiation conditions in the Arctic Basin have certain unique characteristics compared with those in the temperate latitudes. They are connected with the presence of uniform surfaces for both snow and ice, with high atmospheric transparency, and with the alternation of extended periods of daylight and darkness (polar day and polar night, respectively). In summer the total incident solar radiation is greater than that in temperate latitudes. Table 1 gives the mean values of the various components of the solar radiation for the North Pole [33].

The yearly total for incident radiation at the Pole equals $2,836 \text{ MJ/m}^2$, and the maximum value has always been observed in July. In the Arctic Basin the direct solar radiation flux projected onto a horizontal surface (DSR) reaches its maximum value, 983 W/m^2 , in June through August. This is 70% of the solar constant. The yearly total of the DSR is 4 times less than that of the total radiation and 3 times less than that of the diffuse radiation. Maximum monthly values of direct radiation are recorded in June. Absorbed radiation is small, 670 MJ/m^2 per year, and the radiation balance for the whole year is negative. In April and September, and in the farthest southern regions of the Arctic during March and October, the radiation balance is nearly zero. From May to August the radiation balance is positive everywhere. Its distribution during this time is governed mainly by the surface albedo. The minimum values of the radiation balance are registered in the vicinity of multiyear ice and glaciers, and the maximum values are found in areas of open water [34].

Table 1. Monthly averages and yearly total values of the components of the solar radiation for the North Pole (MJ/m^2).

Component	Month						Yearly Totals
	Jan.	Apr.	Jul.	Oct.	Jun.-Aug.	Sep.-May	
Total Radiation	-	356	556	0	1697	1139	2836
Direct solar radiation projected onto a horizontal surface (DSR)	-	142	101	-	315	381	696
Diffuse radiation	-	209	465	0	1382	758	2140
Absorbed radiation	-	68	175	0	456	214	670
Radiation balance	-84	-29	151	-54	340	-478	-138

The duration of solar radiation reaching the surface in the Arctic Basin is short because of the frequent occurrence of clouds and is only about 22% of the theoretical maximum for cloudless skies (Table 2). The greatest duration of solar radiation occurs in April and is 360 hours. This is 58% of the theoretical maximum; in June through September, the value is only about 10%.

Table 2. Duration of solar irradiation at station NP-6 in 1958

Parameter	Month					
	Apr.	May	Jun.	Jul.	Aug.	Sep.
Duration, hours	380	240	102	73	66	45
Percentage of maximum possible duration	58%	33%	14%	10%	9%	8%

1.2 Atmospheric circulation and air pressure

The atmospheric circulation governing ice drift in the Arctic Basin also influences the solid precipitation that forms the snow cover. Precipitation usually occurs during the penetration of cyclones into the basin.

In the cold period from October to March, the pressure field can be characterized by a deepening of the Iceland Low and the development of its trough toward the northeast over the Atlantic sector of the Arctic. Over the Pacific Ocean sector, there is a zone of high pressure that joins the Siberian and Canadian anticyclones. During this period, the air pressure over the Arctic Basin fluctuates around 1020 hectopascals [1 hPa = 1 mbar] [42]. Near the North Pole, the air pressure is 5–10 hPa less than that value.

The most intensive cyclonic activity occurs in winter. Most of the cyclones are of Atlantic origin, and some of them come from the Pacific Ocean across the Chukchi Sea [43]. Most of the cyclone trajectories can be placed in four basic groups: (1) from the northern Atlantic across the Greenland and Barents seas; (2) to the east and northeast of these seas toward the Kara and Laptev seas; (3) from the Bering Sea across the Chukchi Sea; and (4) from Alaska to the north across the Beaufort Sea. In winter the trajectories of the anticyclones are directed from Siberia and Greenland to the Canadian sector of the Arctic Basin.

In March the pattern of the pressure fields starts changing slightly, but it still has the principal features of the winter regime. In April and May the winter pressure regime is completely disrupted. Instead of a high-pressure ridge over the Arctic Ocean, the Arctic anticyclone is established with its center near the northern coast of the Canadian Archipelago. The pressure is 1010 to 1020 hPa [22,41]. The trough of the Iceland Low starts to weaken, but it can be still seen in April. During this period the trajectories of the cyclones are also from the south, and most of them are concentrated near the North Pole. Anticy-

clones move into the Arctic Basin from Chukotka, but occasionally their paths shift to the south toward the Russian Arctic seas.

The summer air-pressure distribution differs significantly from that in the other seasons. Near the Pole an atmospheric depression can be clearly seen over the entire summer. This depression covers a large area but it is not deep. In this region, there is also an increase in the frequency of occurrence of low-intensity cyclones basically from the Eurasian continent [22]. In summer in the Arctic Basin large areas of open water are produced whose surface temperatures are about -1.5°C . This is accompanied by a large amount of ice melting and melt ponds with a temperature of about 0°C . Although not large, the aforementioned factors are apparently sufficient to create temperature contrasts which give rise to spontaneous generation of the cyclones in the Arctic Basin. Gradually, as the snow and ice melt, the polar depression increases and deepens: in July and August the pressure at the depression center decreases to 1008 hPa. Anticyclones then decrease in size and have a lower pressure: in July the pressure at the center of an anticyclone decreases to 1013 hPa and in August to 1012 hPa. In summer the greatest frequency of anticyclones occurs in the region to the north of Wrangel Island (up to three anticyclones per month). From there the anticyclones move to the east toward the Beaufort Sea. In summer, anticyclones reach the Pole from the Greenland Sea, usually about one per month.

The summer character of the pressure fields begins to decay in September, and by October the pattern of the pressure fields is already close to that of the winter. The summer depression near the Pole disappears, and there is a trend toward an increase in pressure. Only a branch of the trough of the Icelandic Low is preserved, with values of 1010–1012 hPa which are typical for winter. In autumn the polar maximum has not yet appeared, and there is only a modest rise in pressure, to 1014 hPa, in the northwestern part of the Canadian Arctic Archipelago.

In autumn a large number of cyclones from the northern part of the Pacific Ocean enter the central Arctic Basin across the Chukchi Sea. Other trajectories with weaker cyclones are directed from the Eurasian Arctic seas to the Pole. The greatest number of cyclones is observed in the Chukchi Sea (seven per month) and near the northern coast of Greenland (also seven cyclones per month).

In autumn, anticyclones enter the Arctic Basin from Siberia into the Chukchi Sea and reach the Pole. From the Pole, part of these Arctic anticyclones branch off toward the south in the direction of the Barents and Kara seas.

1.3 Air Temperature and humidity

Air temperature is an important, and the most evident, characteristic of climatic conditions of this region. A general representation of the air temperatures in the Arctic Basin is presented in Table 3, which gives the average air temperatures for various regions of the Arctic Basin for the period 1954–1991. (See Figure 1 for a map of the regions.)

Table 3. Monthly and annual mean air temperatures ($^{\circ}\text{C}$).

Region	Month												Year
	Jan.	Feb.	Mar.	Apr.	May	Jun.	Jul.	Aug.	Sep.	Oct.	Nov.	Dec.	
Pole	-32.3	-35.4	-33.8	-25.8	-12.1	-2.4	-0.5	-2.2	-9.5	-19.0	-28.1	-31.5	-19.4
Siberian	-31.5	-31.8	-31.4	-24.9	-10.8	-1.8	-0.1	-1.3	-7.2	-17.0	-25.3	-30.9	-17.8
Pacific	-30.8	-31.2	-29.7	-22.6	-10.5	-2.2	-0.1	-1.0	-6.5	-18.3	-25.7	-29.0	-17.3
Ocean													
Central	-32.4	-34.4	-32.8	-25.9	-12.1	-2.3	-0.3	-1.7	-8.9	-19.4	-28.3	-31.2	-19.1

In winter, from November to March, the character of the thermal field is determined by the trough and ridge patterns of the main thermobaric formations. The patterns of the isotherms and of the isobars are in good agreement with one another. In the Arctic Basin, the zone of the lowest temperatures is shifted from the Pole toward the Canadian Arctic Archipelago and Greenland. In February, the coldest winter month, the temperature there falls to -35°C .

During the spring, in April and May, a general and intensive increase in air temperature begins. From March to April there is an increase over the Arctic Basin, on average, of 8 to 10°C ; however, the pattern of the isotherms is close to that of the winter. As before, the zone of lowest temperatures is situated to the north of Greenland and the Canadian Arctic Archipelago. In May, a further reduction is observed in the temperature gradients, and the zone of low temperature (-12°C) covering the region adjacent to the Pole moves to the Chukchi Sea.

In summer, from June to August, the thermally uniform surface (melted snow and ice) in the Arctic Basin causes exceptionally stable air temperatures and very small horizontal temperature gradients. The lowest monthly average air temperatures from June (-3°C) to August (-2°C) are found near the Pole. In July the temperature at the Pole, as in the rest of the Arctic Basin, is only a few tenths of a degree below zero.

In September the monthly average air temperature decreases to -10°C . In October the pattern of the isotherms approaches the winter pattern. The lowest temperatures (-19°C) are recorded in the region near the Pole and to the north of Greenland.

The length of time when air temperatures are positive in the Central region is very short. The transition of the average daily air temperatures from negative to positive values occurs, on the average, on 15 July, and the transition back to negative values has already taken place by 21 July.

The annual variation in the water-vapor pressure is identical to that in the air temperature. In winter, from November to March, the variation is gradual without any well-pronounced minimum (only 0.5 hPa). In April the water-vapor pressure begins to grow rapidly, and the annual maximum (6 hPa) occurs in July and August.

In contrast to the water-vapor pressure, the relative humidity over the Arctic Basin undergoes negligible seasonal changes, and it can be described by the average monthly

values, which range from 75 to 95%. The amplitude of the annual variation is 15%. The greatest average relative humidity, 90–95%, is recorded during the warm period, July and August. As the air temperature decreases, the relative humidity begins to drop rapidly, and as early as November, it is 10–15% lower in the Arctic Basin than in July and August. At air temperatures below zero, further decreases in temperature can cause a supersaturation of up to 120% with respect to ice. As a result, hoar frost, rime, fog, ice needles and ice crystals occur frequently. According to the data from the drifting stations, the number of days from November to April when these phenomena occur varies between 20 and 31 each month. In certain years, the average frequency of occurrence of such days during the winter is between 82 and 90%.

To characterize the total duration when the atmosphere is supersaturated, we can use the percentage of time when the air temperature is lower than -25°C because the relative humidity is 100% during this time. The data given below show that thermal conditions favorable to supersaturation of water vapor in the air occur continuously over 80% of the time from January through March. The high relative humidity in the Arctic Basin is directly related to the frequent occurrence of solid precipitation and rime, which build up the snow cover.

Month	Oct.	Nov.	Dec.	Jan.	Feb.	Mar.	Apr.
Frequency of occurrence of $T_{\text{air}} < -25^{\circ}\text{C}$, %	20	60	75	83	89	88	53

1.4 Cloudiness

The deposition of solid precipitation, which gives rise to the snow cover, depends strongly upon cloudiness. The regime of cloudiness over the Arctic Basin is mainly governed by the state of the atmospheric circulation as well as the characteristics of the atmospheric temperature profile.

The spatial structure and physical characteristics of clouds in the Arctic differ from those in the other parts of the globe. In all areas of the Arctic, including the Arctic Basin, the maximum cloud cover, 9/10 to 10/10, is observed in the summer. The annual cloudiness in the Arctic Basin and the northernmost parts of the peripheral Arctic seas varies from 0/10 to as much as 4.5/10 to 5.0/10; in particular, the cloudiness is twice as high in summer as it is in winter. Throughout the year, stratus clouds are dominant, from 60% in winter to 80% in summer.

The vertical distribution of cloud layering depends on the season. In summertime, low clouds occur much more frequently than medium- and upper-level clouds, and the farther from the continent the greater the difference. In the summer, the frequency of occurrence of low-level clouds is 70–75% in the Arctic Basin, and it is 50–60% in the coastal zones.

The lowest cloud levels in the Arctic Basin are observed in summer. The base height of the stratus clouds is the lowest of all, 180–200 m over the peripheral Arctic seas and 150–170 m in the Arctic Basin (Table 4). The average height of stratus clouds in winter is about 400 m. The base of stratocumulus clouds is somewhat higher, between 600 and 700 m in winter and 450–550 m in summer [44].

Table 4. Base height (Z) and thickness (H), in meters, for different types of stratus clouds.

Cloud Type	Z (m)		H (m)	
	Winter	Summer	Winter	Summer
St	350	170	150	400
Sc	650	450	400	600
Ns	500		1500	
As, Ac	1600	2500	500	
Ci, Cs, Cc	5900	6600	1700	2100

St = stratus, Sc = stratocumulus, Ns = nimbostratus, A = altostratus, Ac = alto-cumulus, Ci = cirrus, Cs = cirrostratus, Cc = cirrocumulus.

Cloud base heights are subject to considerable seasonal variations. The base heights of medium- and upper-level clouds show pronounced annual variations, with maximum values in the summer. The winter cloud base is about 600–700 m. In wintertime, the frequency of occurrence of low clouds ($Z \leq 300$ m) is 15–20%. In summertime, the cloud base decreases to 100–300 m, and the frequency of occurrence increases to 60–65%.

A particular feature of Arctic clouds is that their internal liquid-water content is quite low. On average it is 40% less than that of similar-shaped clouds at temperate latitudes. The average cloud liquid-water content varies between 0.08 and 0.18 g/m³, depending on the underlying surface and cloud type (Table 5). The temperature dependence of the liquid-water content for stratiform clouds is given in Table 6 [44].

Table 5. Liquid-water content* (g/m³) of stratus and stratocumulus clouds for different underlying surface types.

Surface Type	Stratus			Stratocumulus		
	Max.	Min.	Ave.	Max.	Min.	Ave.
Ice	0.30	0.01	0.08	0.55	0.01	0.12
Open Water	0.55	0.02	0.12	0.60	0.02	0.18

*Total liquid water equivalent

Table 6. Temperature dependence of liquid-water content (g/m^3) for stratiform clouds.

Region	St, Sc			Ns		
	10 to 5°C	0 to -5°C	-10 to -15°C	10 to 5°C	0 to -5°C	-10 to -1°C
Arctic	0.13	0.10	0.07	0.21	0.13	0.09
Temperate latitudes	0.26	0.23	0.18	0.35	0.22	0.15

Because of their lower liquid-water content and because they consist of a different mixture of ice and liquid water, clouds in the Arctic have higher transparency than those in other regions (Table 7).

For continuous lower- and medium-level cloud cover, there is a great difference in the radiation attenuation in different seasons. Note that this difference is a result not only of the properties of the clouds but also of the characteristics of the underlying surface. Under cloudy skies, for example, the snow surface can be responsible for an increase in diffuse radiation and hence in the total radiation as well. As a result, two separate periods are designated in Table 7. The first one is from March to May, when the snow cover is stable throughout the Arctic regions. The other includes July to August, when the snow has melted except in the Arctic Basin, where a snow/ice cover still exists.

For continuous mid- or low-level Arctic cloud cover, the relative reduction in total radiation (Q/Q_0) is 2 to 3 times smaller than at the surface of open water in the Norwegian, Greenland, and Barents seas as well as in temperate latitudes.

Table 7. Relative reduction in total radiation (Q/Q_0) for continuous cloud cover at different layers, solar elevation = 30°.

Region	Season	Upper level	Mid level	Lower level
Arctic coastal zones	Mar.-May	0.92	0.82	0.67
	Jul.-Aug.	0.91	0.51	0.40
Arctic Basin	Mar.-May	0.97	0.83	0.79
	Jul.-Aug.	0.97	0.68	0.57
Northern European basin	Year	0.72	0.33	0.26
Temperate latitudes	Summer	-	-	0.21

In actual practice the incident solar radiation (Q) is determined by the atmospheric transparency (P), which determines the direct solar radiation (S') in the absence of clouds, by the degree of cloudiness (n), and by the albedo of the underlying surface (A). The results of a correlation analysis of sequences Q , P , n , A , and S' are shown in Table 8 [34].

Table 8. Correlation coefficients for Q , P , n , A , and S' .

Variable	P	n	A	S'
Q	0.12	-0.66	-0.03	0.79
P	-	-0.02	0.26	0.11
n	-	-	0.33	-0.88
A	-	-	-	-0.21

For a confidence level of 0.95, the crucial value of the correlation coefficient is 0.32. It is apparent that there is a close relationship only among the coefficients Q , S' , and n . The transmission coefficient (P) depends only weakly on them. This is shown by the fact that, in the periods when large reductions in atmospheric transparency took place (1964–65, 1982, 1992), there was no comparable reduction in Q .

There is a specific cloud formation characteristic of the Arctic—a cloudy veil consisting of a thin whitish layer of condensation products—called “Arctic haze” [8]. The frequency of occurrence of Arctic haze is presently rising compared with the levels in the 1950s as a result of anthropogenic pollution of the atmosphere. The height of the base of the haze most often ranges from 30 to 300 m, but sometimes it is higher, depending on the thickness of the inversion layer. It degrades slant-range visibility (although vertical visibility is relatively good) and makes it difficult to carry out an airborne visual search for a drifting station.

1.5 Characteristics of the Wind

The wind speed has a considerable effect on the depth and density of the snow cover. Snow that has fallen onto the surface is transported by wind action; as a result, it can accumulate at certain sites and be blown away from others. In some areas, the wind can compact the snow cover to such a degree that caterpillar-tractor treads make almost no visible marks on the snow surface.

The wind-speed regime in the Arctic Basin changes, depending on the season. The annual variation in the average velocities has a winter peak and a summer minimum during July and August; however, in the region of the Arctic Basin that is adjacent to the northern part of the East-Siberian Sea, the mean maximum velocity is observed in summer (Table 9). The anemometers at the drifting stations are set at heights between 6 and 8 m.

Table 9. Mean monthly and annual wind speeds (m/s).

Location	Month												Year
	Jan.	Feb.	Mar.	Apr.	May	Jun.	Jul.	Aug.	Sep.	Oct.	Nov.	Dec.	
Pole	5.1	4.4	4.4	4.3	4.3	4.3	4.3	4.3	4.3	4.4	4.4	4.5	4.4
85°N, 0°	5.1	5.0	5.0	4.3	4.3	4.2	4.2	4.2	4.4	4.7	4.7	4.9	4.6
85°N, 120°E	5.2	5.1	4.7	4.7	4.7	4.7	4.7	4.7	4.7	4.9	4.9	4.8	4.8
85°N, 120°W	5.1	5.4	4.1	4.2	4.4	4.4	4.5	4.4	4.5	4.4	4.0	4.3	4.4
80°N, 150°E	4.2	4.3	4.2	4.5	4.7	4.8	4.8	4.8	4.8	4.8	4.7	4.8	4.6
80°N, 180°E	4.1	4.5	4.2	4.7	4.7	4.7	4.7	4.7	4.8	4.7	4.4	4.8	4.6
80°N, 150°W	5.0	4.6	4.3	4.7	4.7	4.8	4.8	4.8	5.0	4.7	4.6	4.7	4.7
75°N, 150°W	5.3	4.8	4.8	5.0	5.1	5.3	5.3	5.3	5.4	5.2	5.2	5.2	5.2
Rudolf Island	7.2	7.4	7.1	6.7	6.0	4.8	4.2	4.6	5.8	6.8	6.6	6.9	6.2
Zhokhov Island	5.4	4.4	4.2	5.1	5.3	5.5	5.6	5.7	5.4	5.7	4.9	5.1	5.2
Wrangel Island	5.6	5.6	5.4	4.5	4.6	3.7	4.1	4.4	5.4	7.0	8.4	7.2	5.5

Table 10 gives the frequency of occurrence of wind speeds in different speed categories. Winds speeds in the Arctic Basin most frequently range from 3 to 7 m/s (more than 70% of the time). Storm-level wind speeds are seldom observed in the Arctic Basin, in contrast to the island and coastal stations.

Table 10. Frequency of occurrence of wind speed over the Arctic Basin as a percentage of the total occurrences.

Month	Wind speed, m/s											
	0-1	2-3	4-5	6-7	8-9	10-11	12-13	14-15	16-17	18-20	21-24	25-28
Jan.	12.2	28.1	29.9	14.7	8.7	4.1	1.4	0.8	0.3	0.1	0.04	0.04
Feb.	9.4	30.0	31.2	16.0	7.2	3.0	1.8	1.1	0.5	0.1	0.04	0.04
Mar.	11.9	29.6	32.1	15.0	6.2	3.3	0.9	0.5	0.2	0.1	-	-
Apr.	10.8	31.9	29.8	16.0	7.0	3.0	1.0	0.1	0.1	-	-	-
May	11.0	29.4	29.5	18.1	7.7	3.8	0.8	0.2	0.04	-	-	-
Jun.	9.0	28.0	29.9	20.6	8.0	3.7	1.5	0.2	0.1	-	-	-
Jul.	8.9	26.5	32.8	19.9	8.2	2.6	0.7	0.3	0.1	-	-	-
Aug.	8.8	27.5	30.7	18.0	9.0	3.8	1.6	0.2	0.2	0.04	-	-
Sep.	10.1	26.0	28.0	18.9	9.5	4.0	2.5	0.8	0.2	0.04	-	-
Oct.	10.5	27.0	26.4	18.5	9.8	4.3	2.8	0.7	0.3	0.05	0.04	-
Nov.	12.0	28.1	27.0	16.8	9.6	3.8	2.2	0.9	0.3	0.1	0.04	-
Dec.	11.2	29.1	28.2	15.0	10.0	3.8	1.9	0.7	0.1	0.04	-	-
Year	10.5	28.0	29.1	17.3	8.4	3.6	1.6	0.5	0.2	0.02	0.01	-

The peak wind speed observed at the drifting stations was 28 m/s. It was recorded south of 80°N latitude. The maximum wind speeds observed at the drifting stations during various time intervals were 19 m/s - 1 year, 23 m/s - 5 years, 25 m/s - 10 years, 26 m/s - 15 years, and 28 m/s - 20 years. It appears that the maximum wind speed of 28 m/s occurs very seldom, less than once every 20 years.

There are only few days with strong winds (≥ 15 m/s). On average, such winds occur less than 1 day per month, and the greatest number is 9 days (Table 11). Compared with the island and coastal stations, the number of days in the Arctic Basin with winds ≥ 15 m/s is, on the average, 7 times less. The most hazardous wind speeds (≥ 30 m/s) have not been observed in the Arctic Basin.

Table 11. Average and maximum number of the days with high winds (≥ 15 m/s) in the Arctic Basin.

Parameter	Month												Year
	Jan.	Feb.	Mar.	Apr.	May	Jun.	Jul.	Aug.	Sep.	Oct.	Nov.	Dec.	
Average	1	1	0.1	0.1	0.2	0.3	0.3	0.3	1	1	1	1	7
Maximum	7	6	4	3	3	3	4	4	5	4	9	5	57

Wind speed also influences the evaporation from the surface of the snow cover, particularly at small negative temperatures. The stronger the wind, the greater the evaporation.

1.6 Atmospheric phenomena and the precipitation forming the snow cover

In addition to precipitation, the snow-cover characteristics depend primarily on snow storms and blizzards, and in warm periods on fog as well. At wind speeds above 6 m/s, the snow cover begins to be influenced by wind. From this point on, drifting snow appears. However, blowing snow has an even stronger influence on the snow-cover distribution. Blowing snow appears at a wind speeds of 7 to 8 m/s, and the snow transfer occurs in an air layer several meters thick. The wind direction has a pronounced effect on the snow cover only if obstacles are present. Snow accumulates on the lee side of hummocks, and at the ice stations snowdrifts are observed on the lee sides of the huts and tents. Sastrugi, snow spits directed along the wind, form on free ice. As the wind direction changes, the direction of sastrugi also changes if the snow has not managed to densify sufficiently.

There are approximately 70 days of blowing snow per year in the Arctic Basin: in January through March up to 8 days, in April 6 days, in May 5 days, in June 4 days, in July 1 day, in August 2 days, in September 6 days, in October and November up to 8 days, and in December 9 days. Blowing snow is observed in this region throughout the year. In the summer (July and August) it occurs during snowfall events.

The duration of blowing snow is approximately 100 hours during the winter months and 1–5 hours in the summer. At these times, the wind speed most frequently (70%) falls in the ranges 10–13 and 14–17 m/s. Air temperatures are always higher during blowing-snow events than when they are absent. At temperatures of -30°C and below, blowing snow is recorded only 5% of the time. The greatest frequency of occurrence is observed

at air temperatures between -15 and -25°C . In the warm part of the year, blowing-snow events are most often observed at temperatures between 0 and -5°C , but occasionally they have also been seen when the air temperature was slightly above zero.

Fog in the Arctic is, for the most part, seen in the warm portion of the year, particularly in July and August (Table 12). The greatest number of days with fog is as high as 30 in August. In addition, the duration of fog is also significant in summer. It is as much as 100 hours per month in July and August, but in winter it is only 5 to 10 hours per month. On days with fog, the total duration is 5 to 6 hours. In summer, the snow cover disappears more quickly when fog is present. Polar explorers used to say: "fog makes the snow melt." Melting takes place when direct solar radiation is significant (particularly when the fog is transparent), the snow cover warms to 0°C , and the air temperature is above -4 to -5°C . For this type of fog, the relative humidity may be lower than 100%.

Table 12. Average and greatest number of days with fog in the Arctic Basin.

Parameter	Month												Year
	Jan.	Feb.	Mar.	Apr.	May	Jun.	Jul.	Aug.	Sep.	Oct.	Nov.	Dec.	
Average	1	2	3	4	6	15	23	19	16	7	3	2	101
Maximum	5	6	10	11	13	23	27	30	20	14	10	7	176

The minimum amount of precipitation (150 mm per year) occurs in the central part of the Arctic Basin. Most of this falls in solid form and builds the snow cover. Precipitation takes place there 152 days per year (Table 13). Precipitation is most often observed in autumn, in September and October (18 and 17 days, respectively). In late winter it occurs, on average, only 9 days per month. However, the maximum amount of precipitation, 24 to 25 mm per month, occurs during July and August, and the minimum, 7 to 8 mm, comes in late winter (Table 14). In the summer, the amount of liquid precipitation is greater than solid precipitation. The average monthly intensity of liquid precipitation is 0.15 mm/hour, and for solid precipitation it is 0.05 mm/hour. The daily mean maximum summer accumulation reaches 24 mm, but in winter it does not exceed 10 mm. The duration of precipitation is rather long, 150 to 200 hours on average, and the maximum is 400 hours per month. Fine-grained snow can fall continuously throughout an entire day.

Table 13. Average number of days with precipitation ≥ 0.1 mm.

Location	Month												Year
	Jan.	Feb.	Mar.	Apr.	May	Jun.	Jul.	Aug.	Sep.	Oct.	Nov.	Dec.	
Arctic Basin	12	10	10	9	11	12	13	15	18	17	13	12	152
Zhokhov Island	10	10	10	11	14	11	13	17	19	19	15	11	160
Wrangel Island	16	13	11	10	12	10	13	13	15	17	15	14	159

Table 14. Average precipitation (mm).

Location	Month												Year
	Jan.	Feb.	Mar.	Apr.	May	Jun.	Jul.	Aug.	Sep.	Oct.	Nov.	Dec.	
Arctic Basin	11	8	7	7	11	15	24	25	23	17	11	10	179
Rudol'fa Island	17	17	17	16	16	20	28	32	30	24	20	17	254
Zhokhov Island	13	8	8	9	14	21	39	33	22	16	13	10	206
Wrangel Island	16	10	10	8	13	15	34	35	32	24	17	15	229

Solid precipitation falls mainly in the form of snow and granular snow. Snow flurries, sleet, rimed ice crystals, and freezing rain are very infrequent in the Arctic Basin and are observable only in the warm period. During particularly cold weather in winter, ice needles (diamond dust) are common. Their accumulation rate is typically between 0.03 mm for 6 hours and 0.05 mm for 12 hours.

The speed of descent is 0.2 to 0.5 m/s for a snowflake in the Arctic Basin, and for ice crystals it is about 0.1 m/s [31]. If we assume an average wind speed of 1 m/s throughout the air column, a snowflake that leaves a cloud at a height of 400 to 600 m will be displaced laterally about 800 m before it lands on the surface. If the wind speed is 10 m/s, the snowflake will travel 8 km before falling to the surface.

2. MEASUREMENTS OF THE SNOW COVER AND DATA PROCESSING

Standard snow-cover observations include daily measurements snow depth at the standard meteorological sites as well as regular measurements of snow depth, density, and water equivalent along selected 1-km-long lines. The wavelength-integrated albedo of the snow was determined from measurements of the total incident and upward-scattered radiation at the meteorological sites and at irregular intervals at a variety of sites near the drifting stations using a portable albedometer.

2.1 Snow-depth measurements at the standard meteorological sites (meteosites)

Snow depth was measured daily using three fixed snow stakes installed at the meteosites. As a rule, the measurements were carried out each morning at a time as close as possible to 8 o'clock, local solar time. At the drifting stations the meteosites were usually located outside the zone of influence of man-made obstacles (huts, tents, etc.), where snowdrifts or wind-scoured bare spots occurred and snowdrifts and other disturbances could form. As supplementary information to aid in the interpretation of the observations, it was common practice to use visual observations of the characteristics of the snow cover in the vicinity of the meteosite: the snow coverage on a 10-unit scale and the character of the snow-cover relief [40]. Three gradations were used: a uniform surface without snowdrifts, a nonuniform surface with small snowdrifts to 40 to 50 cm in height, and a very nonuniform surface with large snowdrifts [27].

Snow depths were read off each of the three snow stakes in turn to within an accuracy of about 1 cm. The snow depth was taken to be the mean of these three readings. In analyzing the snow accumulation characteristics, as a rule, 10-day average snow depths are used for all the days when a snow cover is present at the meteosite. During transitional times, there can be up to several days when no snow is observed at the stakes. If the snow coverage in the vicinity is 6/10ths or above, the readings on these days are also taken into consideration for calculating the 10-day average snow depths, and the snow thickness is taken to be zero [40].

2.2 Snow-line survey (traverse) measurements

To determine the snow depth and density as well as the water equivalent of the snow in the areas adjacent to the station, snow measurements were carried out along lines 1000 m in length established outside the boundaries of the station. The orientation of a line could be set as desired relative to the structures at the station, but once established, the lines were not changed during the operation period of the station. Snow-line surveys were carried out when the average snow depth along the line was at least 5 cm and at least half of the area visible around the station was snow covered. Regular measurements

of the snow-cover characteristics were started in 1954 and carried out at all subsequent drifting stations.

Snow surveys were carried out on the 10th, 20th, and 30th day of each month. If there was a blizzard during those days, the snow surveys were carried out as soon as the storm was over. Snow depth along the lines was taken at 10-m intervals using a portable metal surveyor's rod marked to an accuracy of 1 cm. The measuring rod was inserted into snow down to the ice surface. The average of these 100 measurements was taken as the snow depth for the line. In addition, the maximum and minimum snow depths as well as the degree of snow coverage along the line were also determined.

Density of the snow cover was determined every 100 m with a model VS-43 snow-density gauge (Figure 2) whose cylinder has a cross sectional area of 50 cm². The cylinder was inserted through snow down to the ice surface, and the snow depth was read from the scale marked on the cylinder to an accuracy of 1 cm. The cylinder together with a snow sample were weighed using the balance of the snow gauge (see Figure 2) to an accuracy of 5 g (one gradation on the balance's scale). When the snow-cover depth was greater than 60 cm, the height of the cylinder, two snow samples or more as needed were taken by making a pit in the snow. The snow density was calculated to an accuracy of 0.01 g/cm³, using the formula

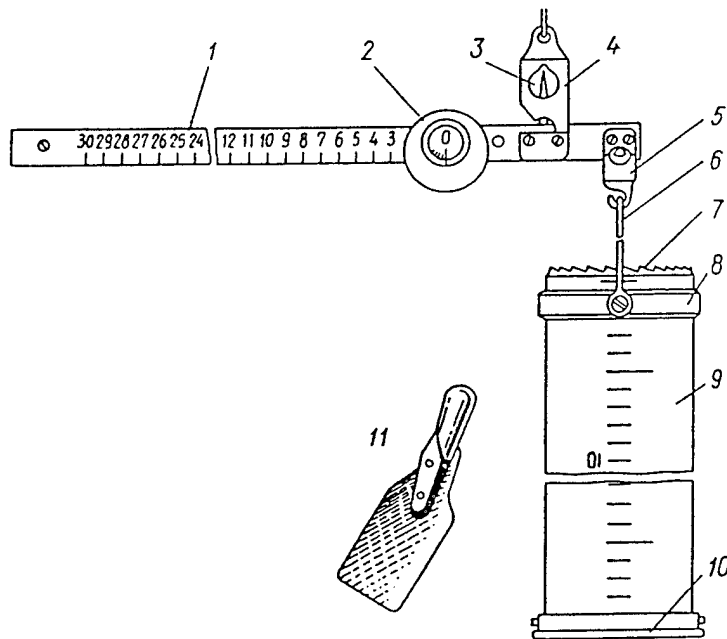


Figure 2. Model VS-43 snow-density gauge. 1 - index beam; 2 - movable weight; 3 - level indicator; 4 - fulcrum; 5 - hook; 6 - shackle; 7 - serrated cutting edge; 8 - movable ring; 9 - cylinder; 10 - cover; 11 - trowel.

$$\rho = n/(10 \cdot h),$$

where ρ is the snow density (g/cm^3), n is the number of the gradation on the snow gauge, and h is the snow depth in the snow gauge's cylinder.

The average of 10 measurements was taken as the snow density. A snow sample weighing 5 g forms a water layer 1 mm high in the cylinder of the snow gauge. The water equivalent of the snow cover is determined to an accuracy of 1 mm using the formula

$$Q = 10 \cdot H \cdot \rho,$$

where H is the average snow depth (cm) along the line, ρ is the average snow density (g/cm^3), and 10 is a scaling factor. When an ice crust was present, its thickness and density were measured as well. In that case, the water equivalent was recorded separately for the snow with and without the ice crust.

Measurements were registered in a "KM-5" record book. Table 15 gives an example of the observational data recorded from a snow survey at NP-6 on 20 November 1958 together with the results of the data reduction. This example is for snow with an ice crust, which is not typical for the Arctic.

2.3 Dates of snow-cover formation and disappearance

The time of the snow-cover formation and disappearance was determined by visual observations, which were recorded in the "KM-1" log book in the column titled "State of the snow cover." The procedure was as follows: for the *date of the snow cover appearance*, the date of the first autumn snow cover was taken regardless of the snow depth or the occurrence of subsequent melting events. A day with snow cover is considered to be a day when more than 50% of the area visible in a region is snow covered. *The date of the stable snow cover formation* is taken to be the day from which the snow covers at least 50% of the visible area in the vicinity of the station. If there is no snow on one subsequent day, it is not taken into account if it is preceded by at least 5 days of continuous snow cover. In addition, a 2- to 3-day interval is not considered either, as long as 10 days or more of snow cover precede it. *The date of disappearance of the stable snow cover* is considered to be the first day in spring when the snow cover occupies less than 50% of a visible area. If the snow cover reforms during the next 3 days and remains for at least 10 days, or if it reappears in a single day and lasts for at least 5 days, then the snow cover is considered to have been continuous, and another, later date of disappearance is determined.

2.4 Measurement of albedo

Values of the snow albedo are calculated using the results of the total incident and reflected (upward-scattered) solar radiation measured at the meteosites with a multipurpose M-80 shortwave pyranometer [54]. The receiving surface of the pyranometer was installed at a height of 1.5 m above the snow surface. The spectral range of the instrument is from 0.4 to 4 μm .

The error in the absolute calibration of the solar radiation flux is no greater than 7 W/m^2 . In this case, the relative error of an individual albedo measurement under actual conditions was within $\pm 5\%$.

The M-80 pyranometer measures relative changes, and it was calibrated using a Yanishevsky AT-50 actinometer [54]. When measurements were made, the sensitivity of the M-80 was compared monthly with that of the reference actinometer, which was used solely for this purpose. If the change in the pyranometer's sensitivity between two successive calibrations did not exceed 5%, the calibration coefficient used to calculate solar radiation from the recorded voltage was taken to be constant for the month until the next check was performed.

By careful selection and preparation of the instruments before the expeditions and by careful use in the field, the stability of their characteristics could be ensured for several years. Under the unusual circumstance that the sensitivity of the instrument changed 5% more more between two checks, the instrument was replaced by a spare one. In this way, the required measurement accuracy and uniformity in observational data sets were ensured.

The state of the active surface at the meteosite where the observations were carried out was described verbally on the basis of visual estimates. The structure of the snow cover was characterized by its age (fresh or old), its origin (deposited as precipitation or by wind transport), and the degree of pollution (clear, polluted, or dirty). The snow coverage of the meteosite was characterized by two following gradations: completely covered by snow or only partially covered. The type of the snow cover was characterized as dry, moist, with a frozen snow crust, or with an ice crust.

2.5 Comparison of the results of measurements of snow depth at the meteorological observation sites with those along the snow lines

In studying the snow-cover characteristics, it is common to make use of the two different data types—measurements of the snow depth at the meteosites and observations of the depth, density, and liquid equivalent of the snow along lines in the vicinity of the station.

From the viewpoint of how well the snow depth measurements at the meteosite represent the actual values in the local area, a comparison of the results of the measurements at the meteosite with those from the measurement lines is of direct interest. Figure 3

shows an example of the snow-depth measurements carried out in October 1974 and May 1975 along the snow line at station NP-22. It is apparent that the snow-cover depth along the measurement line varied significantly from one point to the next. In October the average snow depth along the line was 20 cm; the maximum value observed was 40 cm, the minimum was 4 cm, and the standard deviation (σ) along the line was 9 cm. In May the average snow depth along the line was 38 cm, the variability, σ , increased to 12 cm, and the maximum and minimum depths were 78 and 13 cm, respectively.

The average values for the snow-line thickness, however, compare very well with the thickness values at the meteosite. This can be seen in Figure 4, which compares the snow depths observed at the meteosite on NP-22 with the results of the snow-line surveys for the period October 1974 to June 1975.

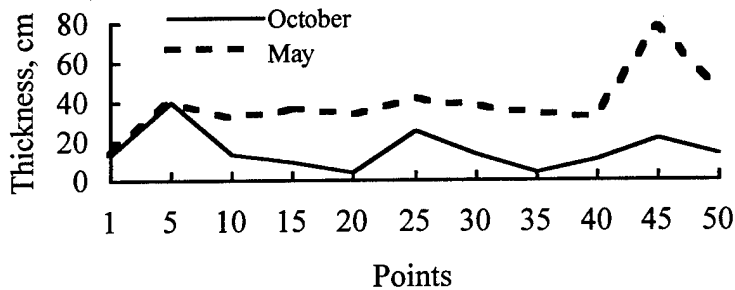


Figure 3. Snow depth data from the snow-line measurements at station NP-22.

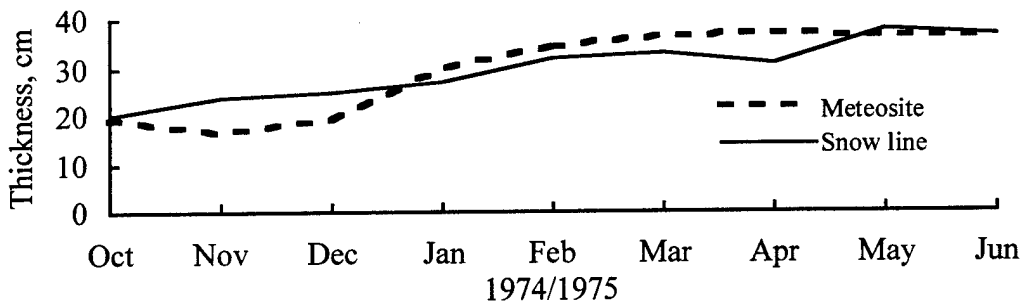


Figure 4. Snow-depth data from the meteosite and from the NP-22 snow-line survey for the period October 1974 to June 1975.

A general comparison of the snow depths observed at the meteosites and along the snow lines for all of the drifting stations is given in Figure 5 as a two-dimensional scatter diagram. The data correspond well. A quantitative comparison between the series of snow-depth observations at the meteosites and those from the snow surveys shows that the correlation between them is equal to 56% in October, 69% in January, and 61% in May.

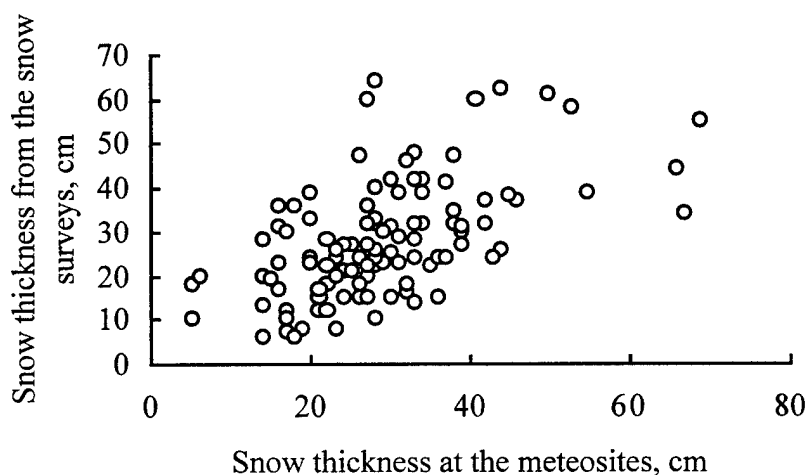


Figure 5. Two-dimensional scatter diagram of the snow-depth observations at the meteosites and along the snow lines.

Evaluation shows that the correlation among the snow-line data sets at the drifting stations is generally rather low. In 62% of all available January data sets, for example, it is less than 0.1; in 30% of the data, it varies between 0.11 and 0.2, and it is greater than 0.21 in only 8%.

The dependence of the errors (standard deviation) in the snow-depth measurements on the number measurements along the snow line in different regions of the Arctic Basin is given in Table 16. The table includes the average standard deviations for each region, obtained using the data taken from all drifting stations in the regions listed. At some stations the errors might be higher or lower than the average because of the interannual variations in weather conditions. Table 16 shows greater errors (by 20–30%) when the average snow depths are determined by 50 measurement points versus 100 points. Higher errors are typical for all regions at the end of the snow retention. The lowest errors are usually found in the Siberian and Canadian regions. This is caused by a combination of climatic conditions, primarily the features of the atmospheric circulation in these regions and the precipitation regime.

Table 16. Dependence of the error, σ , in measuring snow depth (cm) on the number of points sampled, n . The top values are for 100 points, and bottom for 50 points.

Region	October	January	May
Central	<u>1.1</u>	<u>1.4</u>	<u>1.7</u>
	1.6	1.8	2.3
Siberian	<u>0.7</u>	<u>1.2</u>	<u>2.0</u>
	1.0	1.6	2.3
Pacific Ocean	<u>1.0</u>	<u>1.4</u>	<u>1.6</u>
	1.2	1.9	2.2
Canadian	<u>n.a.</u>	<u>1.2</u>	<u>n.a.</u>
	1.2	1.8	0.9

To evaluate the reliability of the observations, Student t -coefficients for confidence intervals of the average snow cover characteristics are calculated according to

$$\sigma_x = \frac{\sigma}{\sqrt{n}},$$

$$\Delta\sigma = t_p \sigma_x,$$

where σ_x is the error of the mean, σ is the standard deviation, n is the number of observations, $\Delta\sigma$ is the absolute error of the average, and t_p is the Student's t -coefficient for the given confidence level.

Table 17 shows the statistical characteristics of the snow cover calculated on the basis of the snow-line measurements for the entire Arctic Basin and for its individual regions at a confidence level of $p = 0.95$. The data from all available snow-line surveys have been included in the calculations. The relative error of the calculated mean values varies between 1 and 10%.

Table 17. Average values of the snow-cover characteristics and their error at a confidence level of 0.95 for the number of observations shown; h_{ave} , ρ_{ave} , and Q_{ave} are the average values of the properties, σ is the corresponding standard deviation, $\Delta\sigma$ is the absolute error of the average, and n is the number of observations.

Region	Depth (cm)				Density (kg/m ³)				Water equivalent (mm)			
	h_{ave}	σ	$\Delta\sigma$	n	ρ_{ave}	σ	$\Delta\sigma$	n	Q_{ave}	σ	$\Delta\sigma$	n
Arctic Basin	27.5	10.1	0.80	600	300	4.6	0.39	533	85.2	35.2	3.00	530
Siberian	25.6	11.4	2.30	96	291	5.0	1.01	76	80.2	36.6	7.40	73
Pacific Ocean	27.1	9.2	1.58	131	303	4.6	0.79	124	87.2	34.5	5.93	124
Canadian	30.2	8.9	2.70	43	292	3.3	1.00	42	88.6	29.3	8.88	42
Central	27.8	10.2	1.10	330	302	4.7	0.51	291	85.1	36.0	3.88	291

3. PROCESSES OF FORMATION AND DECAY OF THE SNOW COVER

3.1 Precipitation due to condensation and sublimation at the snow surface

Solid precipitation from clouds in the form of snow and snow grains is the main factor influencing formation of the snow cover. When the air temperature is below freezing and rain falls, a glazed crust is formed on the snow cover. A glazed crust is observed for air temperatures in the range 0 to -8°C [9]. A surface glaze forms more frequently in summer when the snow cover is absent. The amount of the types of precipitation mentioned above is reliably measured by a precipitation gauge.

In addition, condensation and sublimation of water vapor on the snow surface contribute, to some extent, to the snow-cover formation in the Arctic Basin. Under foggy conditions with below-freezing air temperature, the fog droplets are deposited and freeze onto the snow surface. On average, more than 15–20 days with fog are recorded in the Arctic Basin during the warm season. The mean continuous duration of fog is 4.8 hours; the maximum duration was recorded in July 1976 when fog persisted for 78 hours. Both crystalline and granular rime are frequently observed in the Arctic Basin; hoar frost is less frequent, occurring at night when the air cools. In winter during cold weather (even under clear skies), ice needles (diamond dust) frequently occur, with a characteristic accumulation rate of 0.03 mm for 6 hours or 0.05 mm for 12 hours. None of these forms of deposition are detected by a precipitation gauge, but they occur frequently in the Arctic Basin.

Studies at the drifting stations have shown that the deposition rates of these types of precipitation are small, but the duration of these phenomena is considerable. For example, the deposition rate of rime on the snow surface is 0.0013 g/hour. The annual average duration of rime is about 1200 hours, and the amount of rime can reach $1200 \times 0.0013 = 1.6 \text{ g/cm}^2$. The increase in the snow depth, assuming the rime density is given by $\rho = 0.20 \text{ g/cm}^3$, will be

$$h = 1.6/\rho = 1.6/0.20 = 8.0 \text{ cm.}$$

This has a water equivalent of 16 mm. The intensity of deposited precipitation was measured with special instruments (see Section 2). The values for the various types are presented below.

	Cold Season (October–May)	Warm Season (June–September)
Rime	0.010	0.02
Diamond dust	0.003	-
Hoar frost	0.002	-
Fog water droplets	-	0.03

Of these, the deposition of rime and water droplets is most intense (Table 18). In total, the amount of deposited precipitation is considerable, 22.5 mm per year, or more than 10% of the total precipitation. In the winter months, deposited precipitation makes up 5% of the total, and in the summer months 10–15%. In certain years the fraction can reach 20–25%. The maximum in the deposited precipitation occurs at the beginning of autumn (September and October), when the occurrence of rime increases as a result of the sharp decrease in temperature while the absolute atmospheric humidity is still significant.

Table 18. Mean amount of deposited precipitation in the Arctic Basin (mm).

Type of Precipitation	Month												Win.	Sum.	Year
	Jan.	Feb.	Mar.	Apr.	May	Jun.	Jul.	Aug.	Sep.	Oct.	Nov.	Dec.	Oct.— May	Jun.— Sep.	
Rime	0.3	0.2	0.2	0.3	0.4	1.2	1.8	3.0	4.2	3.0	0.9	0.5	5.8	10.2	16.0
Diamond dust	0.6	0.7	0.3	0.2	0.1	0.0	0.0	0.0	0.0	0.2	0.3	0.4	2.8	0.0	2.8
Hoar frost	0.2	0.2	0.2	0.1	0.1	0.0	0.0	0.0	0.1	0.1	0.1	0.1	1.2	0.0	1.2
Water droplets	0.0	0.0	0.0	0.0	0.0	0.4	0.9	0.7	0.5	0.0	0.0	0.0	0.0	2.5	2.5
Total	1.1	1.1	0.7	0.6	0.6	1.6	2.7	3.7	4.7	3.3	1.3	1.1	9.8	12.7	22.5

3.2 Evaporation and melting of the snow cover

Evaporation from the snow surface is closely connected with weather conditions. Evaporation depends primarily on the atmospheric humidity deficit (relative to saturation) [19, 29]. The greater the humidity deficit, the more intense the evaporation. Measurements of evaporation from the surface of the snow pack were performed at drifting stations NP-6 in 1958 and NP-22 in 1976. The evaporator, made of Plexiglas, has a heat conductivity of $0.04 \text{ cal m}^{-1} \text{ s}^{-1} \text{ deg}^{-1}$, which is sufficiently close to the heat conductivity of dense snow. The instrument consisted of two parts. An upper, square cup 10 cm on a side with holes at the bottom to drain the melt water was inserted into a lower cup where the melt water collected. Snow samples were placed into the upper cup and weighed with a scientific precision scale to an accuracy of 0.1 g. The instrument, including the lower cup, was then buried in the snow with its upper edge at the same level as the snow surface. After exposures of different durations (from 2 to 6 hours), the upper cup was weighed again. The difference in the weights of the snow sample before and after exposure together with the duration of the exposure gave the rate of evaporation. If melt water accumulated in the lower cup, its amount was measured separately and taken into account.

Evaporation was noted most frequently from April to June, when sunny weather occurred most often. In July through August it was often foggy, at which times condensation rather than evaporation took place. In winter, measurements were often prevented by

frequent blizzards, drifting snow, and precipitation. According to data from the 38 sets of measurements that were completed, the mean rate of evaporation was 0.012 mm/hour (Table 19).

Table 19. Rate of evaporation from the snow cover surface in the Arctic Basin.

Station	North Latitude	Longitude	Number of Observations	Mean Air Temperature (°C)	Evaporation Rate (mm/hour)	Maximum Rate (mm/hour)
NP-6	81° 40' N	145° 32' E	17	-5	0.013	0.035
NP-22	83° 20' N	140° 30' W	21	-8	0.011	0.025

The maximum evaporation rate was 0.035 mm/hour. These measurements were performed at below-freezing air temperatures. When the snow cover was melting, individual measurements in July and August showed that the evaporation rate was 3 times as large.

For determining the decrease in the snow cover thickness from the amount of evaporation, the following empirical formula was proposed by Kuz'min [30] for calculating the daily evaporation rate:

$$E = 0.134(e_0 - e_2) \text{ mm/day,}$$

where e_0 is absolute atmospheric humidity (hPa) at the snow surface temperature, and e_2 is the absolute humidity (hPa) at a height of 2 m. For calculating the monthly evaporation rate, he proposes

$$E_m = 0.37 nd \text{ mm/month,}$$

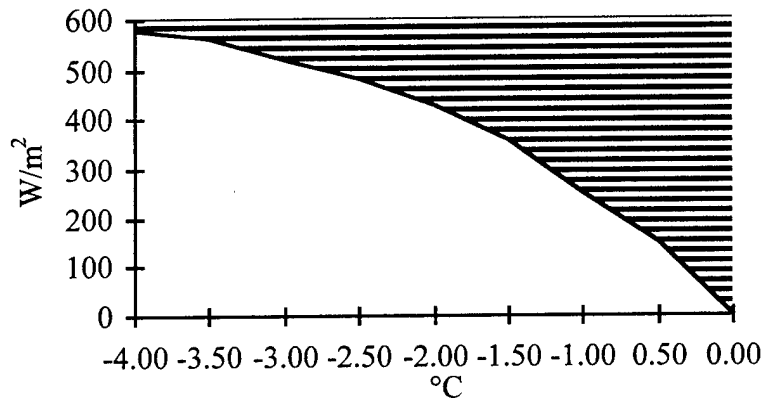
where n is the number of days per month and d is mean monthly humidity deficit (hPa). These formulae predict an annual decrease of 54 mm a year in the snow depth owing to evaporation (Table 20). On average, evaporation reduces the total snow accumulation by 20%.

It was shown by Dyunin [19] that evaporation from the snow is very strong during episodes of blowing snow. He suggested that because the effective surface area of the snow increases many times owing to snow particles rising into the air, the evaporation rate increases as a result. However, this has not been confirmed by observations at the drifting stations.

Melting of snow cover in the Arctic begins at below-freezing air temperatures owing to the influence of solar radiation. The process of melting is most intense in June when air temperatures increase to -5 or -4°C , and total solar radiation reaches values of 600 W/m^2 . With further increases in the air temperature, the role of solar heating in melting the snow decreases (Figure 6).

Table 20. Evaporation from the snow surface in the Arctic Basin (mm).

	Bryazgin, N.N. [4]	Khrol, V.P. [4]	Formulae [30]
Jan.	1.2	2	1
Feb.	1.3	2	1
Mar.	2.4	2	2
Apr.	3.6	3	3
May	5.7	9	8
Jun.	10.1	13	14
Jul.	9.2	10	11
Aug.	5.7	3	7
Sep.	4.1	4	3
Oct.	2.7	3	2
Nov.	1.4	2	1
Dec.	1.0	2	1
Warm Period, May–Aug.	30.7	35	40
Cold Period, Sep.–Apr.	17.7	20	14
Year	48.4	55	54


Figure 6. Onset of melting in the snow cover (shaded region) as a function of air temperature and the intensity of the incident solar radiation.

The main cause of intensive snow melting is above-freezing air temperatures. The duration of snow melting during a 24-hour period is closely related to the mean daily air temperature. When the mean daily air temperature reaches about $+2^{\circ}\text{C}$, snow melting occurs continuously over the entire 24 hours. Most of the snow melting occurs in July, especially during the second half of the month. There are between 5 and 15 days with a full

24-hour duration of melting in July and 2 to 3 days in August. Shown in Figure 7 is the decrease in snow thickness versus the number of days with a mean positive temperature. The correlation coefficient for linear regression (r) is equal to 0.91.

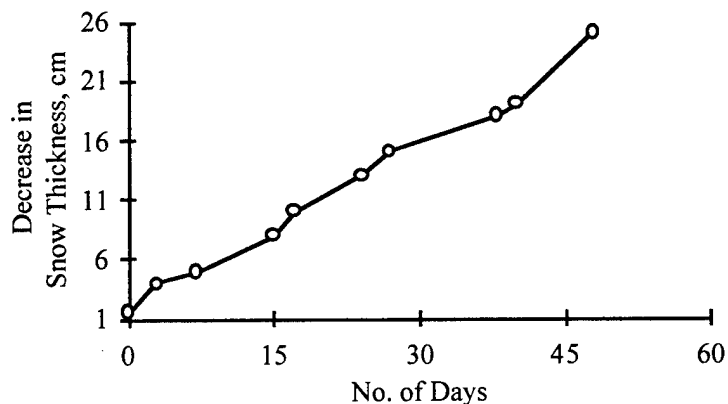


Figure 7. The relation between decrease in snow thickness and the total number of days with a positive mean temperature.

We emphasize that snow melting is an ablation process, since evaporation also occurs at the same time. In 1979 on NP-22 the mean rate of ablation was equal to 1.9 cm/day, or about 0.8 mm/hour. During the ablation period in the Arctic Basin, episodes of snowpack growth, instead of melting, can also take place at certain times as a result of solid precipitation. In total, from June to mid-August the snow cover depth decreases by 70% owing to positive air temperature and by 30% due to solar radiation.

After the snow cover melts completely, ice melting begins, and in some years ice melting from the upper surface is 30–40 cm. The snow cover in the Arctic Basin, however, does not melt completely every year, and the moist snow is transformed into firn. The melting maximum was recorded at NP-6 in 1958 and was 75 cm.

4. PHYSICAL CHARACTERISTICS OF THE SNOW COVER

The upper surface of the drifting ice on which the snow is deposited is characterized by a large variety of relief features of various sizes. Areas of young ice have the most level surface. Multiyear ice floes are distinguished by their strongly developed relief; ice hummocks alternate with level areas consisting of frozen melt ponds with elevated necks of ice between them. The ice floes are usually bordered by chaotic pressure ridges. Owing to the irregular relief, the snow cover on the ice floes is distributed nonuniformly. The snow that falls on the hillocks and hummocks is, as a rule, blown away, exposing the ice surface, and snow drifts are formed between the hummocks.

The snow surface changes not only owing to solid precipitation but also owing to snow redistribution under the influence of the wind and to rime deposition at the surface. Sometimes a strong rime layer is formed at the surface which prevents snow transport and the occurrence of low-level blowing snow even at a wind speed of 12 m/s.

The following snow types were distinguished during observations at the drifting stations: fresh fluffy snow, fresh sticky snow, loose old snow, dense old snow, moist old snow, snow crust, compact snow, moist snow, and wet snow. The snow cover is subdivided according to the character of the relief using the following gradations: uniform with slight accumulations of drifting snow, nonuniform, nonuniform with sastrugi and snowdrifts, and melting snow with melt ponds.

Also, snow hummocks and sastrugi are often formed at the drifting stations. They appear, then disappear, and form in different places depending on the wind direction. The snow hillocks are, on average, 14 m long and can be up to 10 cm tall. Sastrugi, which sometimes have peculiar forms, are formations of solid snow 1–5 m long and up to 50 cm tall. They are always elongated along the prevailing wind direction. The average area covered by sastrugi in the Arctic Basin is 20% [47]. The physical characteristics of the snow cover and their variation depend on the type of snow and the character of the surface relief.

4.1. Temperature of the snow cover

The temperature T_{surf} of the surface of the snow cover can differ significantly from the air temperature, which is measured at a height of 2 m; T_{surf} depends on the weather conditions, mainly on the presence of cloudiness.

Observations of snow temperature at the surface and at various depths were carried out continuously year-round at the drifting stations NP-6 in 1958–1959 and at NP-22 in 1976–1978. Measurements were made four times a day (at 0, 6, 12, and 18 hours) with a model AM-2M wire thermometer. Two-hundred and sixty measurement sets per month were carried out in winter (October to March), and 125 sets were made in summer (July to September).

In winter during the polar night when there was a continuous cloud cover, the snow surface temperature did not differ from the air temperature measured at a height of 2 m (at the meteorological hut). Under cloud-free conditions, however, the snow temperature decreased sharply compared with the air temperature owing to longwave radiative cooling. The difference between these temperatures reached 6–7°C (Table 21). A minus sign in Table 21 indicates that the snow temperature is lower than the air temperature, and a plus sign indicates that the snow temperature is higher than the air temperature. The mean value of the differences presented is equal to zero taken over the entire year, i.e., the annual heat balance between the snow surface and the air is close to zero.

Table 21. Differences between the temperature of the snow surface and the 2-m air temperature (°C).

ΔT	Mean Values	Minimum Values	Maximum Values	Number of Obs.
Jan.	-0.9	-5.0	0.0	260
Feb.	-1.1	-6.1	0.0	260
Mar.	-0.7	-5.1	0.8	260
Apr.	-0.4	-4.4	1.0	260
May	-0.2	-4.1	4.4	260
Jun.	0.1	-2.9	5.5	246
Jul.	-2.9	-6.9	3.3	125
Aug.	-0.5	-2.8	2.6	125
Sep.	0.3	-1.9	2.1	135
Oct.	0.0	-1.9	2.1	260
Nov.	-0.3	-4.5	0.0	260
Dec.	-0.7	-5.5	0.0	260
Warm Period Jun.–Aug.	-0.7	-6.9	0.0	631
Cold Period Oct.–May	-0.6	-6.1	4.4	2080
Annual	-0.1	-6.9	5.5	2711

Before the onset of intensive snow melting, positive values of $T_{\text{snow}} - T_{\text{air}}$ are often recorded owing to heating of the snow by solar radiation in the presence of thin stratus clouds and fog. This occurs at air temperatures below 0°C (in the range -10 to 0°C). In June the difference is +0.1°C, on average. In September the snow temperature is also higher than the air temperature, by 0.3°C, on average, because the air temperature decreases more rapidly than the snow temperature (Figure 8).

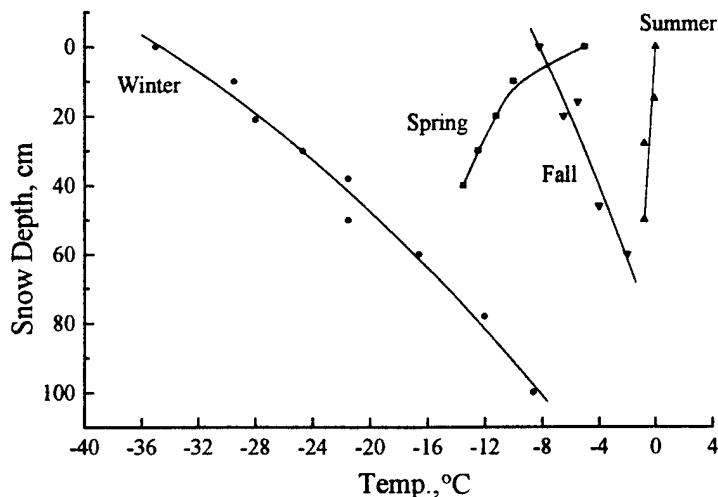


Figure 8. Changes in surface temperature versus snow depth.

The depth dependence of the snow temperature varies, depending on the season. After the snow cover becomes established in autumn, the snow temperature increases with depth, from -9°C at the surface to -2°C at a depth of 60 cm (see Figure 8). In winter the temperature changes from -35°C at the surface to -9°C at a depth of 100 cm. With the onset of spring, heating of the snow begins from the top, and the temperature gradient in the snow changes sign (see Figure 8). During summer melting, the temperature differences are very small.

4.2 Density and hardness of the snow cover

In the established snow cover, the process of regelation can take place—melting of the snow particles followed by repeated freezing. In addition, within the snow cover there is persistent recrystallization due to transfer of water vapor molecules from one crystal to another. Growth of large snow crystals also occurs at the expense of the smaller ones. The freshly fallen snow quickly loses its initial structure (in 2–5 days). Also, in the Arctic, the snow cover becomes constantly more dense owing to the influence of the wind. The snow density is not constant with depth. It changes layer by layer as a result of the physical processes occurring in the snow [24].

Density basically increases with depth in the snow cover. Figure 9 presents variations of mean snow density as a function of depth using the observations from a 3-m-thick snowdrift on NP-6. An analysis of measurements of the snow density versus depth allowed us to determine the depth distribution and to obtain the following formula for determining the snow density versus depth:

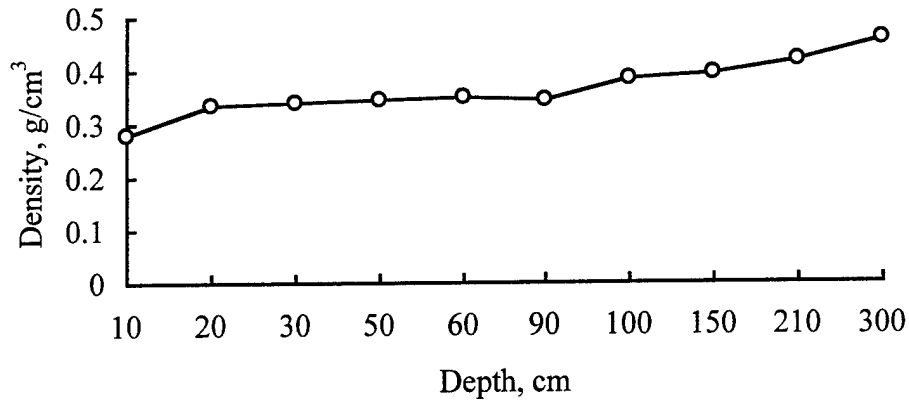


Figure 9. Mean snow density versus depth from the observations at NP-6.

$$\rho = 0.216 h^{0.123} \text{ g/cm}^3,$$

where ρ is the snow density and h is the snow depth in centimeters.

This formula, which takes into account the nonlinear dependence of snow density on depth, is more suitable than previous formulas [19, 37, 58] which were based on a linear representation for snow density changes with depth.

The density of moist snow varies from 485 to 681 kg/m³. Table 22 presents snow densities versus snow type for different depths. Fresh snow has the lowest density and melting snow the highest.

Table 22. Snow density (kg/m³) versus type of snow cover and depth (cm) from special observations at NP-22.

Depth, cm	Fresh, Dry	Fresh, Moist	Old Compact	Wet and Melting	Firn	Ice Crust
0-5	150	230	280	480	-	-
6-10	190	260	330	530	-	-
11-30	240	290	350	530	-	-
31-40	-	-	360	-	-	860
41-70	-	-	380	-	630	-
> 70	-	-	440	-	-	-
Entire Layer	190	260	370	530	-	-

An increase in snow density also results in an increase in its bearing capacity and hardness. By hardness we mean the increase in the load per unit area that the ice cover can endure without breaking. Its value was determined by means of a cone pressed in the snow by a vertical load. The hardness was calculated as the ratio between the load applied to the cone and the indentation area in the snow. The indentation area was calculated from the depth of the loaded cone in the snow.

The snow cover hardness depends on its density. Measurements at NP-6 in the winter of 1958 showed a linear dependence between the snow cover hardness and its density (Figure 10). At a density of 300 kg/m^3 , the snow supported a pressure of 0.095 kg/cm^2 , and at a density of 450 kg/m^3 , 0.80 kg/cm^2 . Thus 1 m^2 of snow cover can support approximately 8 tons. The influence of the snow temperature on its hardness was not investigated.

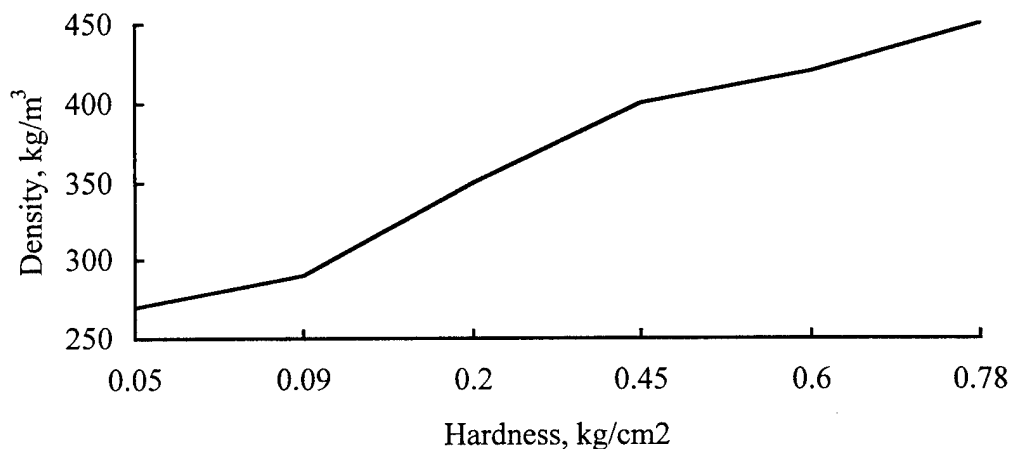


Fig. 10. Changes in the snow-cover hardness depending on its density.

4.3 Penetration of solar radiation into the snow

Many investigators have studied the penetration of solar radiation into the snow beginning as early as the 1960s [21, 28, 29, 55, 57]. Measurements of the radiation fluxes at the surface as well as different depths in the snow were performed with a pyranometer mounted with the receiving surface directed upward or downward. Table 23 presents mean values of solar radiation penetrating to a depth of 5 cm as a function of the elevation of the sun above the horizon for different types of the snow cover.

Table 23. Mean solar radiation values in snow at a depth of 5 cm under clear skies (W/m^2).

Snow State	Solar Elevation (deg.)		
	10°	20°	30°
Dry	14.0	55.0	111.5
Moist	34.9	83.7	195.2
Wet	55.8	160.5	230.0

It is evident that the amount of energy penetrating the snow layer increases with the elevation of the sun above the horizon, and the transmissivity of the snow increases as the wetness increases. An analysis of the observations has shown that shortwave radiation does not penetrate deep into the snow: 90% of the incident radiation is absorbed in the upper 5 cm. In dry snow, the radiation flux is 4% of the incident radiation at a depth of 10 cm and then decreases with depth, but at a considerably slower rate. Solar radiation penetrates to greater depths in moist melting snow than in dry snow (Table 24).

Table 24. Percentage of solar radiation penetrating into the snow as a function of depth and snow state.

Snow Depth, cm	Dry Snow	Moist and Melting Snow
0	100	100
3	25	35
5	10	25
10	4	12
30	2	5
50	1	3

The fluxes of outgoing solar radiation, as with radiation penetrating into the snow, are greater for moist snow than for dry snow (Figure 11). At the surface of dry snow, the outgoing solar radiation equals almost half the incident radiation (47%); at the surface of moist snow, it equals 65%. At a depth of 5 cm, the upward radiation flux is 6% and 18% in dry and moist snow, respectively. For penetrating radiation, the corresponding values are 10% and 25% (see Table 23).

In spite of the small amount of solar radiation penetrating into the snow layer, heating of the snow by the sun during the polar day persists throughout the entire day. This contributes to internal heating of the snow. In the presence of local pollution (lowered albedo) due to activities on the station or to deposition of contaminants advected by the atmosphere, solar heating contributes to intensive formation of cavities in the snow. These cavities are filled with a mixture of water and ice crystals, which is transformed into melt ponds. As an aside, we note that there were unsuccessful attempts at long-term storage of food in the ice pits. Without additional screening from solar radiation penetrating the ice, the food spoiled even at below-freezing air temperatures.

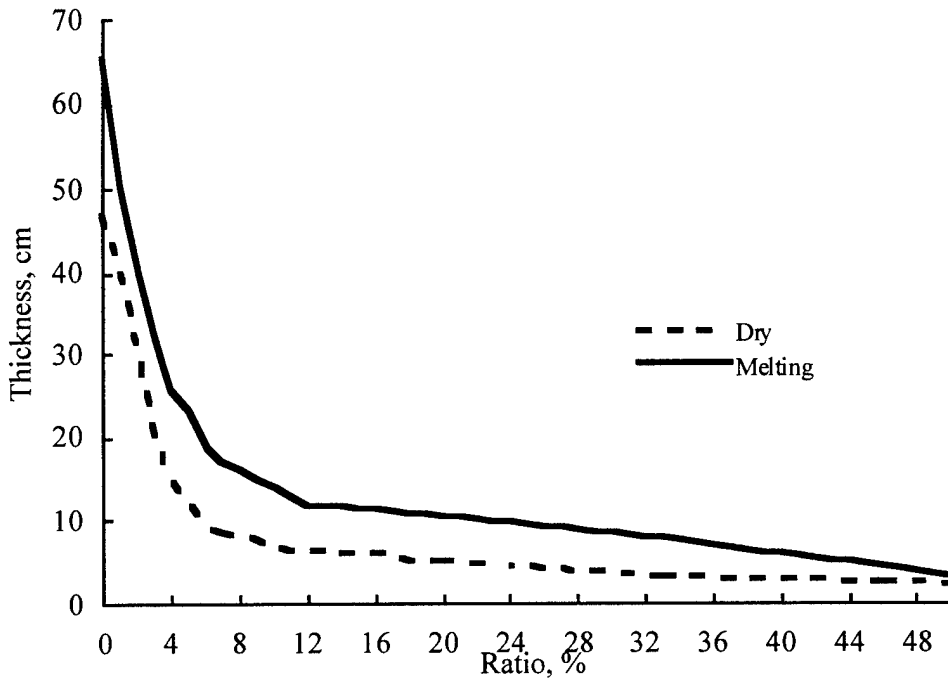


Figure 11. Snow depth versus ratio of outgoing to incident solar radiation (%)

5. ALBEDO OF THE SNOW COVER

The surface albedo is one of the basic climate-determining factors. Its value defines the ratio of the solar radiation absorbed and reflected by the surface. Thus the albedo directly influences the radiation regime of the ice-ocean-atmosphere system. The albedo of the snow depends on the structure and state of the snow cover, the degree of contamination, the snow density, and its moisture content. All these characteristics change continuously under the influence of meteorological conditions and solar radiation, whose influence results in a large variety of snow types and snow cover relief. These, in turn, cause significant variations in albedo values.

In principle, variations in wavelength-integrated snow albedo can also be related to the illumination conditions for clear or cloudy skies as well as to changes in the spectral composition of incident solar radiation, depending on the elevation of the sun.

5.1 Integrated albedo

Measurements of the integrated albedo of the snow cover were carried out at all drifting stations starting with NP-2 as a standard meteorological observation. The results of the data analysis and its generalization are published in part in the works of Bryazgin [7], Chernigovskiy and Marshunova [52], and Timerev [50]. A large amount of the snow-cover albedo observations in various regions of the Earth, including the Arctic, is generalized in the monographs by Kondrat'yev [2, 46] and by Kukla and Robinson [57]. The values characterizing the albedo of varying types of snow surfaces [7] are given in Table 25. As can be seen from the table, the albedo varies over a very wide range, depending on the snow's structure, age, and moisture content.

Table 25. Albedo of various types of the snow surface, %.

Snow State	Moisture and Color	Ave.	Max.	Min.
Fresh snow	Dry, bright-white, clean	88	98	72
	Moist, bright-white	80	85	80
Fresh drifted snow	Dry, clean, slightly compacted	85	96	70
	Moist, gray-white	77	81	59
Snow which fell or drifted 2-5 days previously	Dry, clean	80	86	75
	Moist, gray-white	75	80	56
Compact snow	Dry, clean	77	80	66
	Moist, gray-white	70	75	61
Recrystallized snow and ice	Moist	63	75	52
	Dry, gray-white	65	70	58
Saturated with water	Light-green	35	-	28

A visual description of the state of the snow cover is, of course, very subjective. It is not possible to determine the changes in the physical parameters of the snow cover in this way. This makes it much more difficult to explain the causes for the variability of the snow reflectivity when analyzing the standard measurements carried out earlier.

Annual variations of mean monthly albedo values, the limits of their variability, and their standard deviations are presented in Figure 12 [33]. These values were obtained by averaging over the entire set of standard observations at all the drifting stations for the period 1950 to 1991. On the whole, from October to April the mean albedo values of snow/ice in the Arctic Basin vary only from 80% to 86%. The basic changes in albedo occur during the period of intensive snow-cover decay from May into July and through establishment of the new snow cover in September.

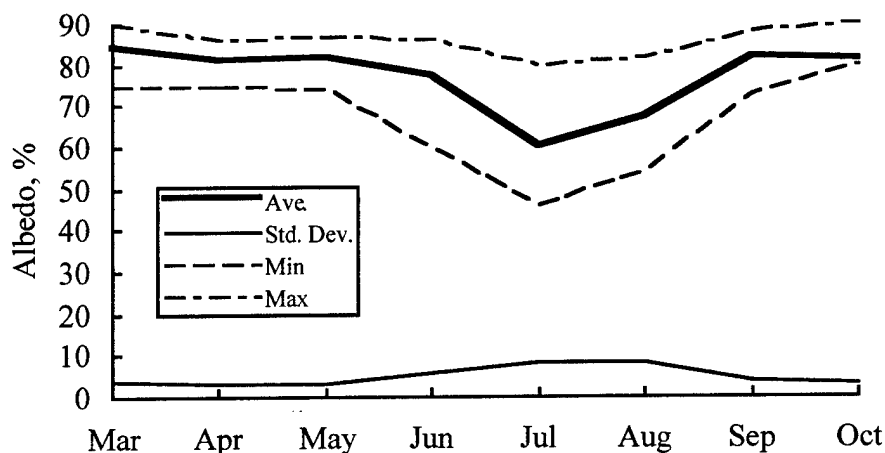


Figure 12. Annual variations of mean monthly albedo at the drifting stations, 1950–1991.

The maximum albedo values of 96–98% are characteristic of fresh, dry, new-fallen snow. The minimum albedo values, close to 30%, are observed during intensive snow melting, especially when the snow is saturated with water.

The temporal variation of the integrated albedo in the presence or absence of clouds is presented in Figure 13 (the data used here are from Timerev [50]). It is apparent from Figure 13 that the snow albedo is greater under cloudy conditions than under clear skies by 3–6%. A careful data analysis has also shown that under conditions of complete cloudiness the albedo values measured under low-level stratus clouds systematically exceed the albedos measured under mid-level stratus clouds by 2–3% [50]. On the whole, taking into account the accuracy of the albedo measurements (± 4 –5%), we conclude that the influence of clouds on the multiyear mean albedo values is not significant and does not as a rule exceed the observation accuracy.

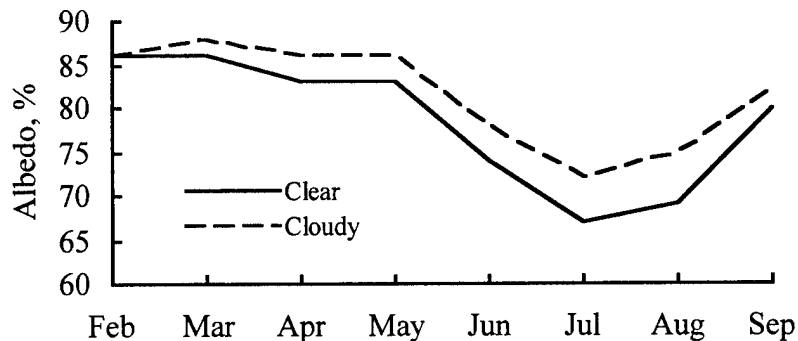


Figure 13. Multiyear mean monthly albedo values for clear and cloudy skies versus month.

Observations carried out on the ice of Dickson Inlet in May 1949 [52] showed that the albedo values were 12% greater, on average, under conditions of continuous cloudiness than on sunny days. This difference is 4 times as large as the standard deviation of the multiyear mean snow albedo on the drifting ice in May (see Figure 12).

On the basis of the observations at the standard times, diurnal variations of the snow albedo, i.e., the dependence of albedo values on the solar elevation, occurred, as a rule, on sunny days in the spring. The albedo maximum was most often recorded in the middle of the day. It has already been mentioned that the reflectivity of the snow surface measured at the meteorological sites depends on the snow's structure and type and the surface relief. These parameters are governed by the meteorological conditions preceding and at the time of the measurements. In the Arctic, cloud-free days are most common in the spring, and large values of the solar radiation flux incident on the snow-covered surface are characteristic of these days. In the afternoon when the air temperatures are slightly below freezing, the upper layers of the snow can melt and form a film of water on the grains, and the albedo decreases significantly. The results of observations at drifting station NP-4 in May 1955 [52] are presented in Figure 14. The amplitude of the albedo change in the course of a day was 13%. Daily albedo variations of this sort were observed in May 1957 on NP-7 [52] and on NP-22 in June 1979 [45]. At NP-22 the difference between the maximum and the minimum albedo was 16%.

During overcast conditions, daily variations in albedo were, as a rule, not particularly pronounced. But during the period before the onset of intensive snow melting in May, the characteristics of the daily variation were, on the whole, the same on cloudy days as on sunny days. The variation did not, however, exceed 6% [52]. The mechanism remained the same as on sunny days: melting and moistening of the surface layer of the snow.

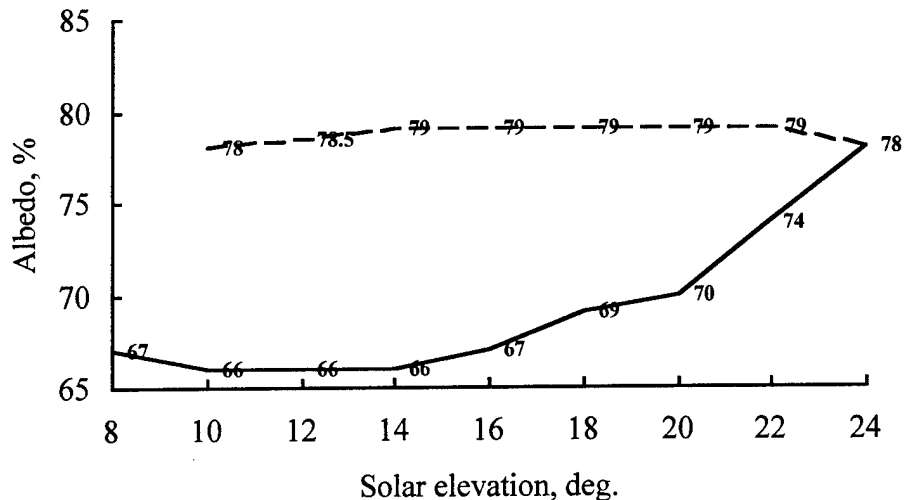


Figure 14. Albedo versus solar elevation at the beginning of spring snow melting (NP-4, May 1957). The dashed line designates measurements made before noon, and the solid line designates after noon.

In some cases, the albedo maximum was recorded in the morning and evening hours. On days when there was melting, an ice crust could form, owing to longwave radiative cooling as the solar elevation decreased, that smoothed the surface roughness. It produced a well-pronounced mirror effect at relatively large solar incidence angles. As a result, albedo maxima could be observed both in the morning and in the evening.

When averaging is performed over extended time intervals, these effects are smoothed out. On the whole, we conclude that the integrated albedo values averaged using a large observation set change little for solar elevations from 10° to 35° . The observed variability does not exceed the accuracy ($\pm 5\%$) of the standard measurements.

5.2 Spectral albedo

The spectral albedo, A_λ , is calculated as the ratio of the values of hemispheric fluxes of the reflected and incoming solar radiation within the sufficiently narrow wavelength range. The relative error of the spectral albedo values is estimated in [2] to be 6 to 8%.

One of the first sets of spectral albedo measurements for different types of snow surfaces was performed by Kalitin [20]. Similar observations were carried out again in 1957 [25], in 1961, and in 1963 [26] in the Leningrad region. Detailed tables of the observation results are given in the appendices.

Apparently, the first attempt in the Central Arctic to measure albedo in different spectral ranges was undertaken by Bryazgin and Koptev [11] in the red and near-infrared

regions of the spectrum at drifting station NP-6. The observations were taken with a standard Yanishevsky pyranometer whose glass dome was coated on the inside with a thin layer of asphalt lacquer. Its spectral transmission was restricted to the wavelength range 0.6 to 1.2 μm . The methods for measuring the albedo in this case were just the same as those used for the standard measurements of integrated albedo. Measurements of the integrated albedo were conducted along with those of the spectral albedo. Daily averaged values of the integral albedo, A , and of a "spectral" albedo, A^* , measured in the restricted spectral region (0.6–1.2 μm) are given in Table 26 for a variety of weather conditions and surface types.

Table 26. Mean daily values for integrated albedo A and "spectral" albedo A^* at NP-6 for various cloud conditions.

Day	April			May			June			July		
	Cloud Conditions	A	A*									
1				5/5 St	82	50	10/10 St	82	58	10/10 St	66	28
2				0/0	85	46	10/10 St	84	57	10/10 St	63	31
3				0/0	84	47	10/10 St	83	60	10/10 St	60	34
4				0/0	83	46	10/10 fog	82	51	10/10 St	55	38
5				4/0 Ci	88	42	0/0	83	52	3/1 Ac, St	48	34
6				8/8 Sc	83	50	10/10 St	80	56	10/10 Ac, St	50	29
7				0/0	84	48	10/10 Sc	74	41	2/0 Ac	52	29
8				2/0 Ci	84	44	9/9 Sc	78	49	10/10 fog	57	28
9				4/0 Ci	83	47	10/0 Ac	80	51	10/10 Ac, St	61	21
10				0/0	82	46	10/10 St	76	48	9/9 St	51	22
11				10/0 As	80	50	10/10 St	81	54	10/10 St	55	25
12				10/10 St	78	49	10/10 Sc	86	60	10/0 Ci	55	26
13				10/10 St	84	62	10/10 Sc	84	58	10/10 St	56	22
14	10/0 Ci	84	56	0/0	88	53	10/10 Sc	86	64	10/10 St	61	25
15	3/0 Ci	91	58	10/10 St	83	52	9/9 Sc	86	62	10/10 fog	61	29
16	1/0 Ci	90	57	10/10 St	84	56	10/10 Sc	85	59	10/10 fog	51	21
17	0/0	84	63	10/10 St	84	64	9/9 St	86	62	10/10 St	47	23
18	0/0	90	66	10/10 St	85	60	10/10 St	82	48	10/10 St	46	22
19	0/0	87	61	10/10 St	81	56	10/10 St	86	50	10/10 St	52	18
20	0/0	82	63	10/10 St	83	56	0/0	81	50	10/8 Ac, St	49	9
21	0/0	82	64	10/10 Ns	84	52	10/10 fog	79	45	10/10 St	50	14
22	0/0	80	62	10/10 St	83	54	10/10 Sc	75	40	10/10 St	48	20
23	4/0 Ci	86	62	10/10 St	84	58	10/10 Sc	73	39	10/10 St	44	25
24	5/0 Ci	80	66	10/10 Sc	84	59	10/10 Sc	75	34	9/9 St	55	42
25	0/0	85	44	10/10 Sc	84	60	10/10 St	72	30	10/10 St	57	31
26	2/0 Ci	86	52	10/10 Sc	84	58	9/9 St	76	46			
27	8/0 Ci	85	48	10/10 St	83	49	0/0	77	46			
28	2/0 Ci	84	54	10/10 St	82	54	10/10 fog	70	31			
29	10/0 As	82	50	2/2 Fs	82	49	10/10 Sc	68	31			
30	5/0 Ci	84	58	10/10 St	84	50	10/10 St	67	25			
31				10/10 St	83	61						

Note: 14 April–6 June: dry compact snow; 7–30 June: moist and wet snow; 1–4 July: melting snow and ice; 5–25 July: melting ice.

Daily variations of mean values of these two parameters for clear weather are presented in Figure 15(a) and for complete overcast in Figure 15(b). The only data included in this analysis were obtained for a single type of underlying surface (dry snow) whose temperature varied within the limits -5 to -35°C . Mean values were obtained from 94 sets of observations in clear weather and 125 sets under overcast conditions.

Unlike the values for A , the values for A^* show a steady decrease in diurnal variation for cloud-free weather with a change in the solar elevation from 5° to 25° . The difference ($A-A^*$) increased from 23% to 40%. The same characteristic pattern in the diurnal variation was also observed when upper-level clouds were present (see Figure 15b). It is most probable that this effect is related to a relative increase in the fraction of the incident solar spectrum with longer wavelengths as the solar elevation decreases. For measurements of the radiation fluxes in the spectral region of 0.6 – $1.2\ \mu\text{m}$, this also gives rise to an increase in the value of A^* in the morning and evening hours. When more dense low-level clouds were present, A^* showed no diurnal variation, and the difference between the integrated and "spectral" albedos was about 30% at all solar elevations.

Generalized data on the limits of variability of these two characteristics, A and A^* , for different types of snow, as well as ice and melt ponds, are shown in Figure 16. The maximum difference between the integrated and "spectral" albedo was observed for moist snow and was, on average, 35%.

Later at NP-10 in August–September 1962, the albedo measurements were carried out using a pyranometer with a red glass filter [52]. Unfortunately, it was not possible to reconstruct the spectral transmission characteristics of the filter that was used. The measurements with the filter showed pronounced daily variations such that the albedo decreased as the solar elevation increased. For the corresponding integrated albedo measurements, diurnal variations were not observed.

The only measurements of detailed spectral albedo, A_{λ} , at the NP drifting stations were performed in 1979 [45]. On NP-22 in June and August 1979, measurements of A_{λ} were carried out over a variety of surface conditions for a wide range of illumination conditions and degrees of cloudiness. On sunny days, measurements were made at solar elevations ranging from 10° to 37.5° , and on days with continuous overcast, around midday.

The spectral albedo was calculated using measurements of the upward and downward radiation fluxes made with a model K-3 spectrometer [38] with a spectral resolution of 20 nm over a range of wavelengths from 0.4 to $0.9\ \mu\text{m}$. Frosted quartz glass was used as an integrating element. For measurements of the hemispheric radiation fluxes, and hence for the albedo calculations, the integrating properties of the detector and, in particular, its angular characteristics are of critical importance. Laboratory studies of the angular characteristics of the frosted glass applied during the measurements have shown a significant deviation from a cosine dependence on zenith angle. The measured angular characteristics were taken into account during processing of the results of the measurements of the spectral radiation fluxes.

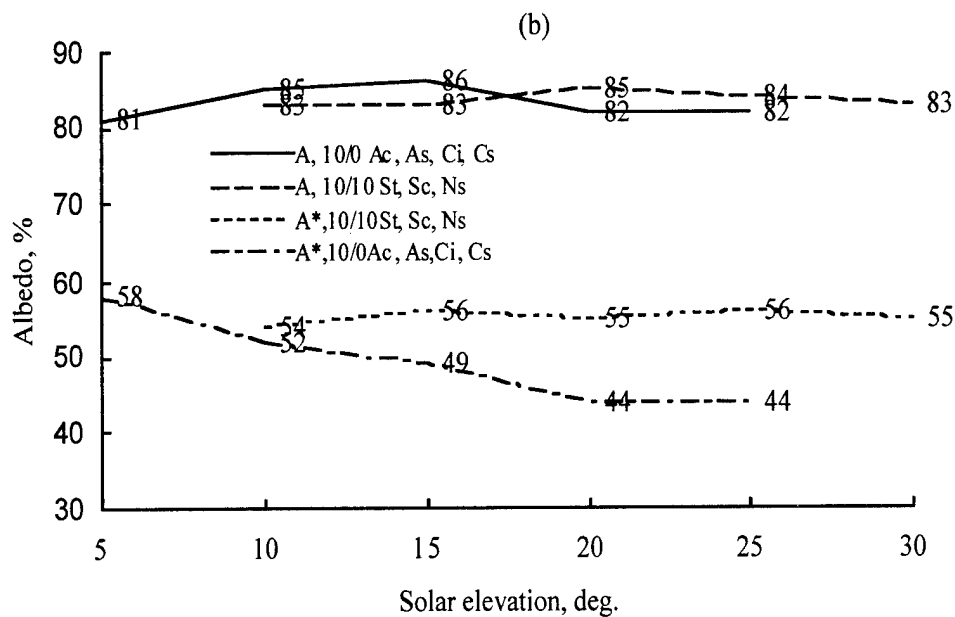
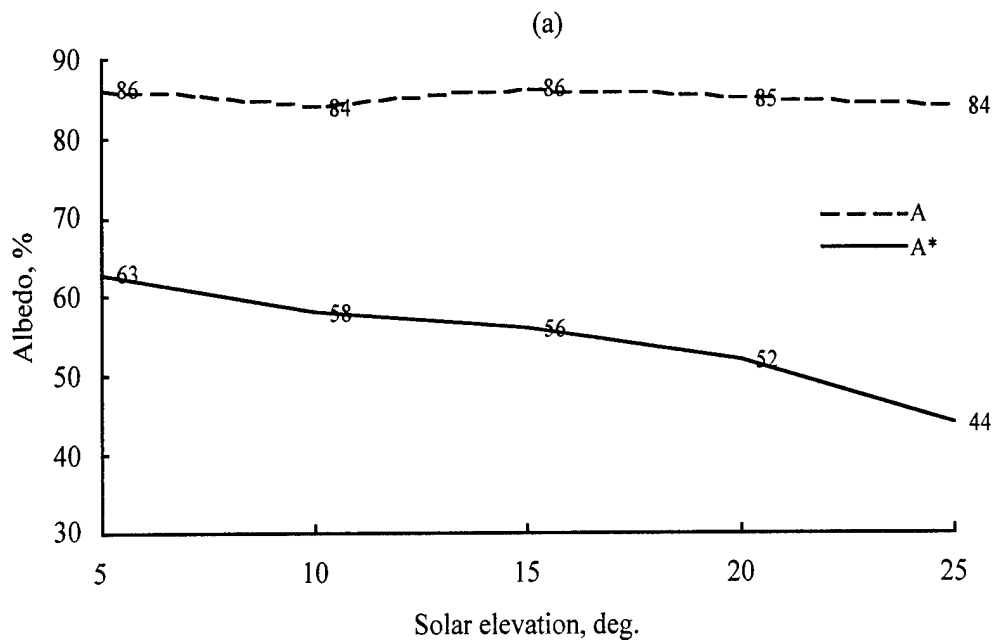


Figure 15. Diurnal variations of integrated albedo, A , and "spectral" albedo, A^* , for clear skies (a) and for cloudy skies (b).

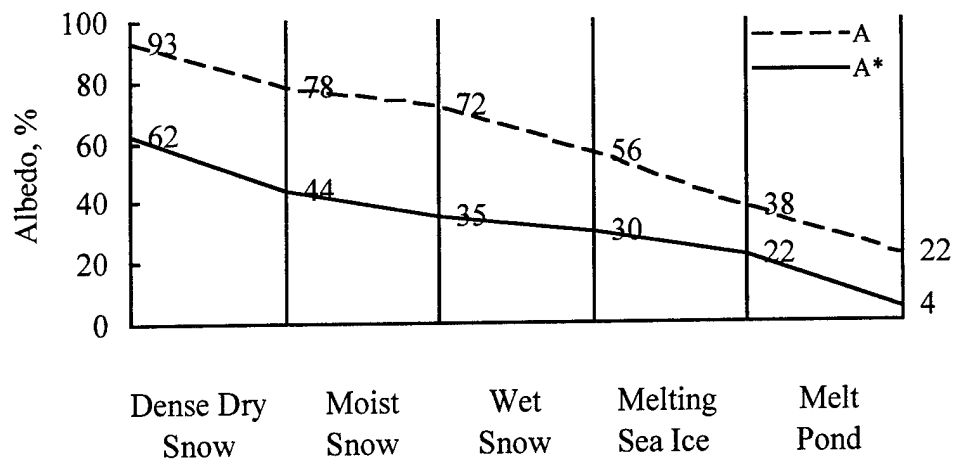


Figure 16. The limits of variability for the mean values of the integral albedo, A , and “spectral” albedo, A^* , for various surface types.

Measurements were conducted at a specially selected site at a distance of at least 500 m from the station structures. This site was one of the cleanest places on the station, least subjected to the influence of everyday activities of the personnel and technical operations. Shown in Figure 17 are the variations in the mean values of the spectral albedo A_λ for different types of snow surfaces. In the spectral region 0.5 to 0.7 μm , A_λ is essentially independent of wavelength. In the blue and infrared regions of the spectrum, a decrease is evident in the albedo measured for melting snow and firn. For dry snow, the decrease in A_λ is noticeable only for the infrared IR wavelengths.

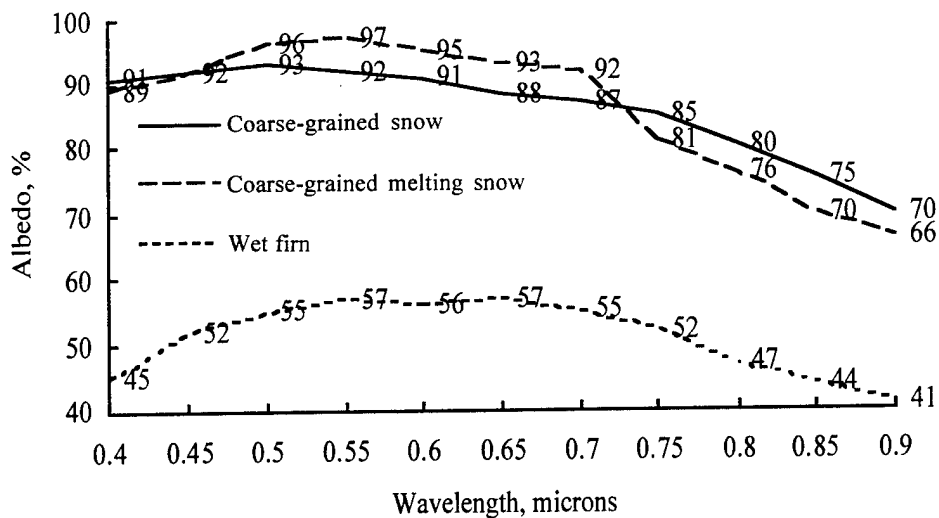


Figure 17. Spectral albedo of different types of snow surfaces versus wavelength.

The spectral albedo increased with the increase in solar elevation and reached its maximum value at noon at all wavelengths (see Table 27). This increase was monotonic, however, only in the red and IR regions of the spectrum. At wavelengths shorter than 0.6 μm , the increase was not monotonic. The last two lines of Table 27 show values measured in the afternoon. A relative decrease in A_λ was observed with increasing solar elevation while the character of the spectral dependence was preserved. The albedo decrease in the afternoon was connected with melting at the snow surface and with the formation of a water film on the snow grains.

Table 27. Diurnal variability of the spectral albedo, %.

Solar Elevation, deg.	Wavelength, μm									
	0.4	0.45	0.5	0.55	0.6	0.65	0.7	0.75	0.8	0.9
13.6	75	81	79	78	75	74	70	66	64	60
16.8	82	84	77	73	73	72	71	69	66	-
20.7	61	69	80	65	80	76	80	79	76	-
23.6	77	88	86	86	84	85	85	85	83	77
30.8	74	90	91	91	90	88	89	88	83	80
37.4	94	96	95	96	95	94	92	89	86	74
32.1	-	94	90	92	89	88	86	83	80	71
25.7	85	86	86	85	83	80	83	82	81	76

As with the observations of the integral albedo, the largest changes in the spectral albedo were related to changes in the physical characteristics of the snow cover before and during melting due to the creation of moisture. On the whole, these data on the spectral dependence of A_λ are consistent with our present understanding of the spectral albedo of snow-covered surfaces based on observations at temperate latitudes [25,26].

It is of interest to compare the results of measurements of the spectral albedo of the snow surface in the Arctic and the Antarctic. In 1984–1985 at the Antarctic stations Mirny, Vostok, and Molodyozhnaya, the spectral albedo was measured with a model K-3 spectrometer in the wavelength range 0.33 to 0.98 μm and by a model BAS-M spectrophotometer in the spectral range 0.4 to 1.1 μm [49]. At the coastal stations in the middle of summer, the albedo value was determined in many respects by the degree of snow wetness. Usually, the maximum value was observed around midday, and there was a corresponding minimum in the diurnal variation in the albedo. On the Antarctic plateau where the air temperatures are well below freezing even in the middle of summer, the changes in the snow cover were connected with ablation rather than with melting. Since there is no moistening of the snow surface at the inland Antarctic stations, the daily al-

bedo variations that are recorded in summer at the coastal stations are not expected to occur.

On the whole, the spectral reflection characteristics of the snow cover at the Russian Antarctic stations do not differ significantly from those observed at the McMurdo and South Pole stations [56] and over drifting ice in the Arctic. Variations in the spectral albedo values are primarily related to transformation of the surface characteristics under the influence of meteorological forcing and incident radiation.

In the summer months in the central Arctic Basin, a large variety of surface types is present, from dry fresh snow to open water. In this connection, a question arises whether the standard albedo observations at a single point are representative of substantially larger areas and the Arctic region as a whole. The albedo values measured above relatively dry locations at the continually maintained station sites turn out to be overestimates. This is confirmed by the results of albedo observations carried out from June through August 1958 at NP-6 using pyranometers mounted 1.5 to 12.0 m above the surface. During the period of snow-cover melting, the value measured with an albedometer at a height of 12 m was 10 to 12% lower than the results for the standard heights. This is because the albedometer at the greater height covered a larger area which included melt ponds and areas of ice. Beneath the standard albedometer, the surface was snow covered (sometimes including areas of bare ice). Before melting of the snow as well as afterward, when fresh snow fell, the albedo value measured at a height of 12 m was 3 to 5% less than that measured at the standard height. More correct results in this situation can be achieved by using the snow-line albedo observations of the various surfaces and calculating the relative areas occupied by each type. The generalized results of this type of observation have been presented by Marshunova and Chernigovskiy [35] and Chernigovskiy and Marshunova [52]. Table 28 gives the area-averaged albedo values calculated by M.M. Marshunova for June through August when taking into account the area of melt ponds. In general, no significant differences in the zonal distribution of the albedo values were found in the Arctic Basin.

Table 28. Mean albedo values in the Central Arctic, %.

North Lat.	June	July	August
90°	78	62	67
85°	78	60	67
80°	78	58	67
75°	73	57	67

6. SPATIAL VARIABILITY IN THE CHARACTERISTICS OF THE SNOW COVER IN THE ARCTIC BASIN

6.1 Methods for cataloging the data and for calculating the climatological characteristics based on the data from the drifting stations

The distribution of snow-cover characteristics for the Arctic Basin is not easy to obtain. The drifting stations do not shift a significant amount in the course of a month and this makes it possible to refer all data on the snow cover to the mean-coordinate point for a given month (or a 10-day period). During a year of drift, however, the stations move over hundreds of kilometers and sometimes traverse regions with different meteorological and circulation conditions. Hence it is not correct to refer the observations to the mean position of the station over a year.

Climatological processing of the observations at the drifting stations was carried out in the same way as for shipborne observations and was referenced to a square coordinate grid. The distinguishing feature here was that maps of monthly mean coordinates were prepared for all of the drifting stations. The number of the station and the year of its operation were indicated near each of the points [41]. The groupings were determined by averaging and combining the data for the different stations over the course of the years of observation based on these auxiliary charts. The advantage of this method, compared with ship-based data processing [42], is that when data are processed according to these groups of stations, the values obtained refer not to the center of the group (as ship-based data refer to the center of the square) but to the point determined by the mean coordinates of each group that includes a sufficient number of stations. Also, a single station can be used in adjacent groups; i.e., the groups overlap each other. This allows us to obtain information for intermediate regions and to increase the number of groups and the stations in them, i.e., to increase the interval over which the data can be averaged and at the same time improve the reliability of the characteristics of the regimes defined for the snow cover. In all, 10 groups were identified.

When such an approach is used from month to month, both the composition of the groups of stations and the mean position of the groups change, and no annual values can be obtained from them. It is also very difficult to assemble standard climatological tables for this compilation. To overcome this difficulty, monthly charts were prepared based on the calculated mean monthly values of the snow-cover characteristics. Data for each of the 12 months were interpolated onto a fixed coordinate grid consisting of 15 points. The annual sums and their mean values were then calculated at each of these points. These data characterize the annual variations of the various snow-cover parameters.

Mean coordinates were determined by simple arithmetic averaging. Only in the near-Pole area, in case the stations were situated on different sides of the Pole, was it inappropriate to perform this sort of averaging, and data for that entire group were simply refer-

enced to the Pole. If most of the stations in a group were located in a region of large longitude values ($\geq 300^\circ\text{E}$) and one (or even a few) had a very small longitude value, then 360° was added to the longitude of the latter (see the second line of Table 29). The mean longitude was then evaluated. The eight groups of stations used in calculating the multiyear mean values of the meteorological parameters for May are shown in Figure 18.

At most of the stations, the snow-cover characteristics were measured once every 10 days, but at some the interval was once a month. As a result, data processing was based on monthly data (using data from the third 10-day period of each month). Mean values of depth, density, water equivalent, and the dates of stable formation and disappearance of the snow cover were calculated from the data of every station composing each group. For analyzing multiyear variations of the parameters, the mean depths and snow densities obtained were plotted on a graph showing the annual variations. Based on this diagram, the depth and density of the snow cover were determined every 10 days, and the water equivalent of the snow was calculated for the end of the month.

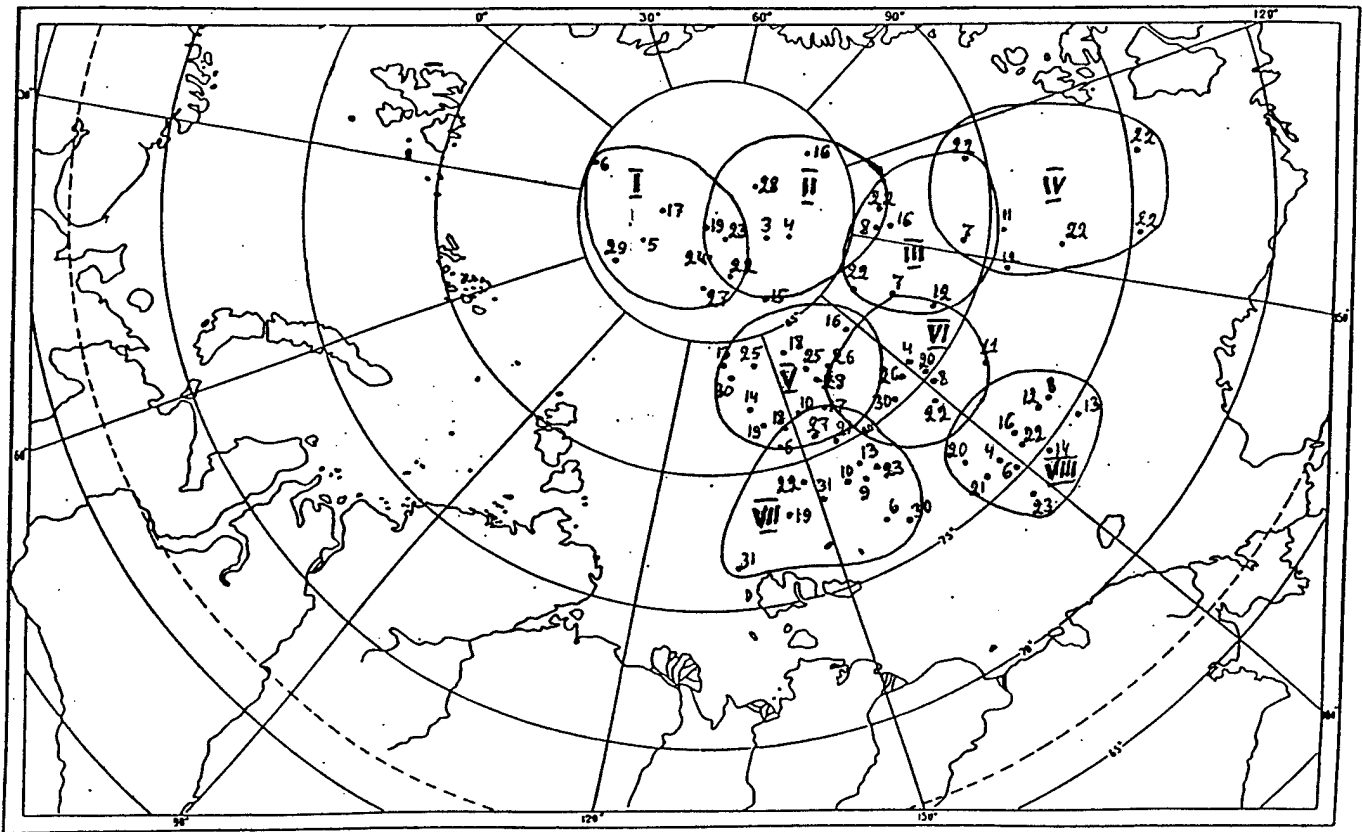


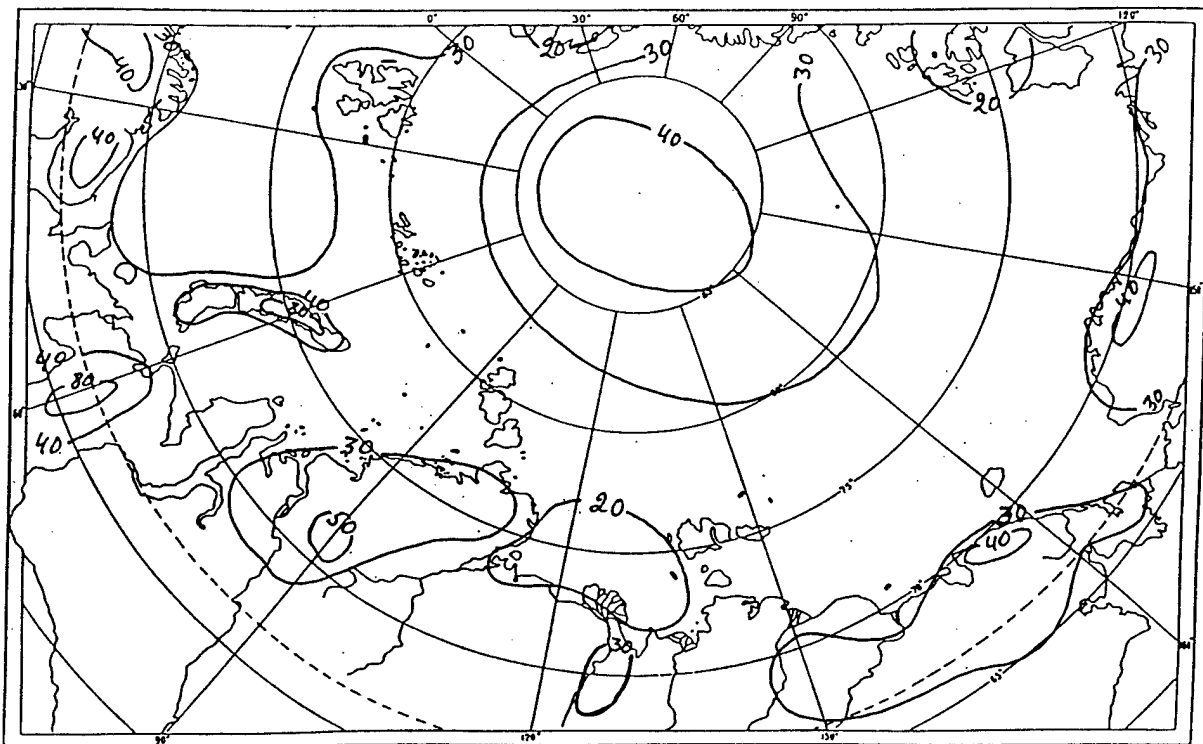
Figure 18. Eight groups of stations used for calculating multiyear mean values of the meteorological parameters for May. Arabic numbers associated with the points in each group indicate the numbers of the drifting stations.

Table 29. Determination of the mean coordinates of the groups of drifting stations.

Station	North Latitude	Longitude (0–360°)	
		Observed	Corrected
1st	88°14'	325°26'	325°26'
2nd	86°55'	6°57'	366°57'
3rd	86°19'	297°29'	297°29'
4th	88°23'	344°06'	344°06'
5th	85°45'	232°28'	232°28'
Total	434°36'	1206°28'	1566°26'
Mean	86°55'	241°17'	313°17'

6.2 Depth of the snow cover

Using the methods described above, we obtained multiyear mean depths of the snow cover and constructed monthly charts from September to June. Figure 19 presents a chart of the snow-cover depth distribution for May when the snow accumulation is at a maximum. When the climatological charts of the snow cover were constructed, the state of the ice was not taken into consideration.

**Figure 19.** Distribution of the snow-cover depth (cm) in the Arctic during May.

The onset of snow accumulation in the Arctic Basin occurs, as a rule, no earlier than the end of August. The annual variations in the snow-cover depth calculated from snow-line measurements and the observations at the meteorological sites in selected regions of the Arctic Basin are given in Figure 20. As can be seen, each of the regions has its own peculiarities in the annual variations of snow depth. The maximum snow-cover depth is basically observed in April to May except in the Canadian region, where it is observed in March. The highest rates of snow accumulation in the fall are observed in the Siberian region, where from September to October and from October to November the snow-cover depth increases, on average, by 7–8 cm. In the Pacific and Central regions, the monthly increase in the snow-cover depth is smaller, about 5 cm on average. During the following months, the rates of snow accumulation in all regions decrease. By the end of May, the process of snow accumulation ends, and densification and settling begin.

The multiyear mean results show that the maximum snow depth of 40 cm occurs during the third 10-day period of May. In the years with the maximum snow accumulation, the snow thicknesses reached 80–85 cm by the onset of melting; in the years with the minimum snow accumulation, it reached only 25 cm. Mean values of the snow depth at the intersection points of the coordinate grid are presented in Table 30.

In the initial and final months of the cold season, the snow depth was greater in the vicinity of the stations than at the meteorological sites. During the other months in all regions, greater snow depths were measured at the meteorological sites than on the snow lines. This indicates that in all regions of the Arctic Basin the snow that falls during the winter is redistributed to a significant degree by the wind, and as a result the fallen snow is systematically blown away from the snow survey lines.

Table 30. Seasonal progression of snow depth (cm) in the Arctic Basin at the coordinate points.

N. Lat.	E. Long.	Month									
		Sep.	Oct.	Nov.	Dec.	Jan.	Feb.	Mar.	Apr.	May	Jun.
Pole		20	24	30	30	33	34	36	39	42	32
85°	00°	12	18	23	28	30	31	36	41	42	27
85°	60°	11	16	22	26	27	29	31	33	34	25
85°	120°	15	20	24	26	28	30	32	34	35	28
85°	180°	22	21	26	28	29	31	34	36	38	32
85°	240°	21	21	27	30	31	31	37	38	41	32
85°	300°	18	22	26	28	31	33	41	42	42	38
80°	120°	8	16	19	22	23	24	26	28	29	19
80°	150°	11	18	21	26	27	30	32	33	35	28
80°	180°	15	21	26	28	28	31	33	35	36	31
80°	210°	17	21	26	27	29	31	32	34	35	30
80°	240°	11	18	22	23	24	25	28	28	29	20
75°	165°	8	14	24	25	28	29	31	33	33	20
75°	195°	9	14	23	25	26	29	31	32	32	20
75°	220°	6	13	22	23	24	25	27	28	29	20
Mean Value		14	18	24	26	28	30	32	34	36	27
rms Deviation		5	3	3	2	3	3	4	4	5	6

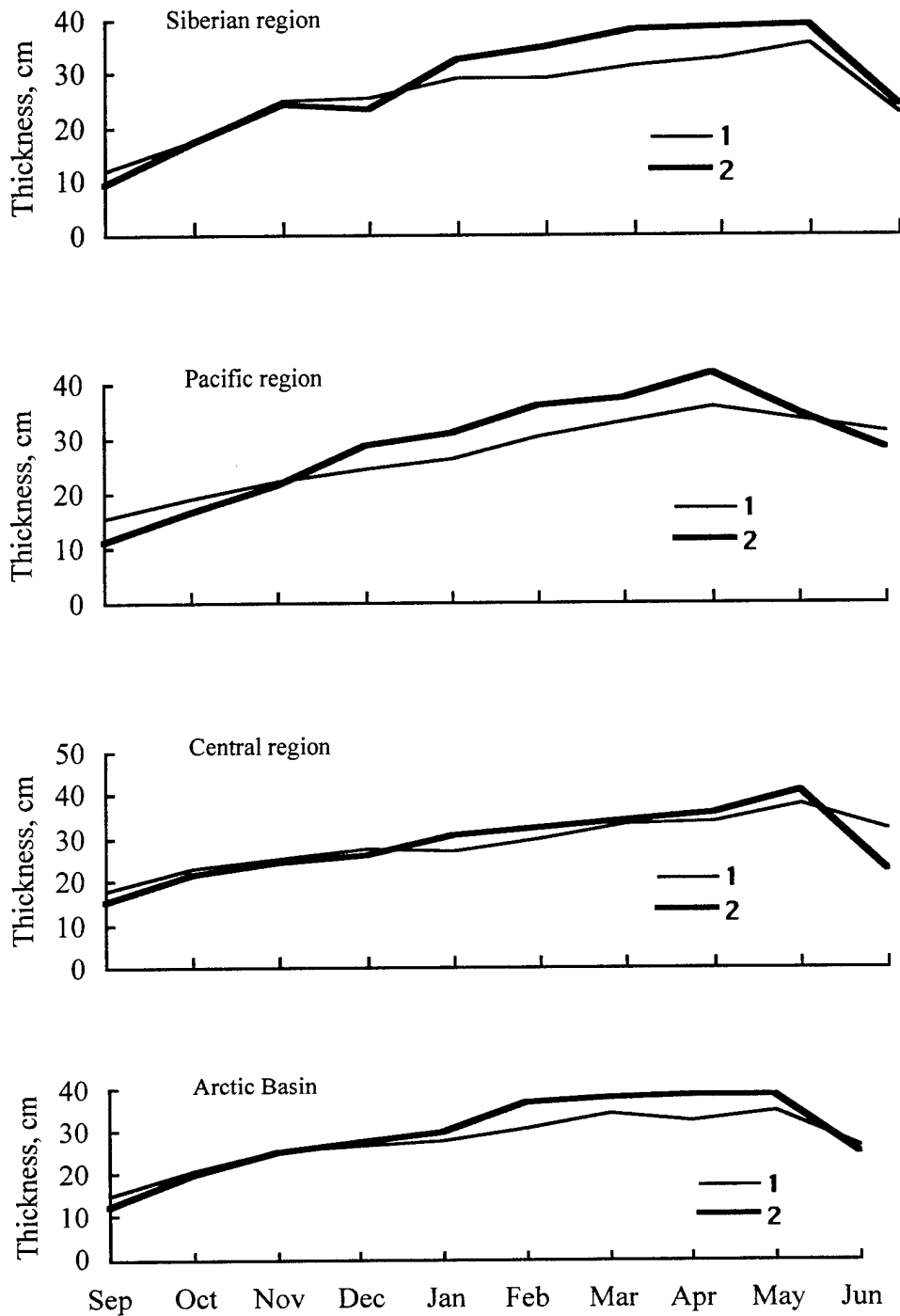


Figure 20. Annual progression of snow depth (cm) as calculated from the snow-line data and from the observations at the meteorological sites in the various regions of the Arctic Basin. 1- Thicknesses on the snow-line surveys. 2 - Thicknesses at the meteorological sites.

Figure 21 presents snow-depth data at NP-26 for three 10-day intervals in January 1984. The only differences between the three curves are that the smallest snow depths usually occur in the first 10-day period and the largest in the third period. Note, however, that on some parts of the snow line the snow depth in the first 10-day period exceeds that in the following periods. This effect emphasizes once again the important role of snow transport [18].

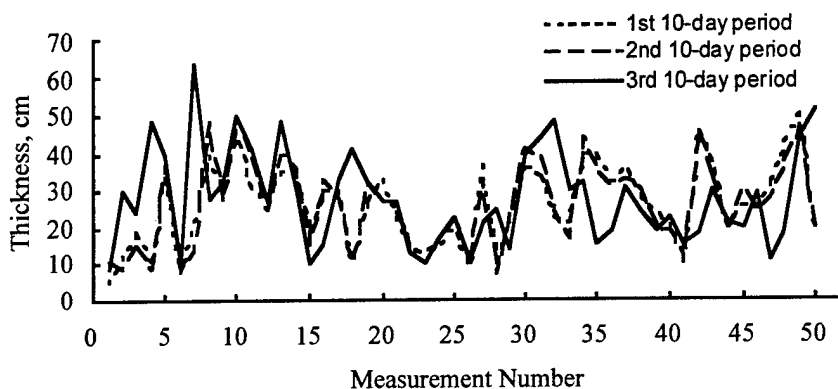


Figure 21. Snow-depth values for three 10-day intervals in January 1984 at NP-26.

An assessment of the spatial variability of snow depth in the Arctic Basin is difficult owing to the absence of continuous and long-term series of observations under stationary snow conditions. Only fragmentary snow-depth observations of limited duration are available from the meteorological sites using stakes and from the snow-line surveys at the drifting stations during the times they were in operation. The snow-line data make it possible to determine the variability of the snow depth in the vicinity of the stations. By using data from the snow-line surveys at all the drifting stations and by estimating the variability of measurements of the snow-cover depth during these surveys, an approximate picture of the spatial variability of the snow depth in the Arctic Basin can be obtained.

For direct estimates of the variability in the snow-cover depth at the drifting stations, root-mean-square (rms) deviations of the snow-cover depths were calculated based on the results of snow measurements for October (the beginning of snow accumulation), January (the middle of winter), and May (the end of snow accumulation) for all drifting stations. Since snow surveys were performed at 50 points on some stations and at 100 points on others, the error in the determination of the root-mean-square deviation was calculated from the formula

$$\delta_{\delta} = \frac{\delta}{\sqrt{2n}}.$$

Tables 31 to 33 present statistical characteristics for 100 and 50 points (selected from 100) for October, January, and May. The differences between the mean snow depths determined from the snow-line observations and from the measurements at the meteorological sites are also presented (last column, $X_{SL} - X_{MS}$). In October (when snow accumulation begins), the mean snow depths obtained from the snow-line observations at all stations (18 sets of measurements) are almost identical for both the 50 and 100 point samples—20.2 versus 20.1. The mean snow depth obtained from all available snow surveys (44 sets of measurements) practically coincides with the results for the set of 18 measurements (the difference is about 2%). The rms deviations are also close; their differences do not exceed 10–15%, on average. The snow-depth values measured at the meteorological sites are 15% greater, on average, than those obtained during the snow-line surveys.

In January (the middle of winter) and in May (the time of maximum snow accumulation), the accuracy of the measurements is steady; only the values of the snow depth and of the rms deviation change. Thus, the differences in the mean were 0.4 cm in January and 1.1 cm in May. As a result, the accuracy of measurements of the snow-cover depth along the 1000-m-long snow lines does not depend on whether 50 or 100 points were measured.

By comparing the rms deviations (σ), one can delineate the regions of the Arctic Basin that show predominantly larger or smaller variability. In October, the largest variability is observed near the central part of the Arctic Basin, where $\sigma = 17.2$ cm (NP-7, 1958). The lowest variability was recorded in the Beaufort Sea region and near the northern peripheries of the Arctic marginal seas (e.g., $\sigma = 3.1$ cm, NP-27, 1985).

In January, the standard deviations of the snow-cover depths increase, ranging from 4.8 cm (NP-22, 1982) to 20.2 cm (NP-10, 1962). In contrast to the situation in October, the region of large variability shifts westward and is located near the central Arctic Basin on the side of the Pacific sector. In addition, large σ values are observed in the southern part of the Arctic Basin. The regions of small variations in the snow-cover depth are located near the Canadian Arctic archipelago.

In May, during the largest amount of snow accumulation, the σ values for the snow depth are also the largest, ranging from 6.4 cm (NP-22, 1977) to 24.9 cm (NP-12, 1965). The zone of enhanced variability is clearly localized south of the central Arctic Basin in the Pacific sector.

The values for the variability parameters given in Tables 31–33 are probably connected with interannual variability in the amount of precipitation, which, in turn, results from annual and interannual variations of the synoptic processes over the Arctic Basin. To estimate the value of this variability over several decades, however, is not possible with the observations at hand.

Table 31. Statistical characteristics of snow depth from October snow-line data (cm).

NP Station	Year	N. Lat. (deg)	E. Long. (0-360°)	Mean	100 Points rms Deviation	rms Error	Mean	50 Points rms Deviation	rms Error	Difference of Mean Values ($X_{SL} - X_{MS}$)
7	1957	86.4	175.5	-	-	-	16.1	7.3	1.0	-14
7	1958	87.5	289.1	20.1	10.3	1.0	19.7	17.2	1.6	6
8	1959	78.1	183.5	-	-	-	20.6	9.3	1.3	6
8	1960	83.2	183.8	12.4	11.4	1.1	11.9	10.5	1.5	-2
8	1961	82.2	216.5	21.7	8.5	0.8	21.0	7.2	1.0	8
9	1960	82.9	153.8	16.5	9.6	1.0	16.6	9.1	1.3	-9
11	1962	82.3	210.5	15.7	9.3	0.9	16.8	10.0	1.4	6
12	1963	78.5	185.0	17.7	11.6	1.2	15.5	10.7	1.5	-2
13	1964	76.0	182.8	-	-	-	22.2	12.9	1.8	10
13	1965	80.5	150.9	12.3	6.7	0.7	11.6	6.6	0.9	2
14	1965	76.5	164.6	20.5	10.0	1.0	18.4	9.9	1.4	-9
15	1966	82.0	166.7	23.9	7.4	0.7	24.0	7.0	1.0	5
16	1968	79.2	180.9	20.2	12.0	1.2	22.4	12.6	1.8	7
16	1969	83.8	174.5	34.4	14.5	1.4	35.3	13.5	1.9	-5
16	1970	85.0	220.4	28.6	12.5	1.2	30.2	13.2	1.9	-7
16	1971	87.1	271.1	28.8	13.0	1.3	30.2	14.8	2.1	14
18	1970	79.4	154.5	22.3	6.1	0.6	23.0	7.2	1.0	-3
20	1970	77.3	184.8	18.0	7.6	0.8	17.2	8.0	1.1	-1
20	1971	80.4	188.1	27.0	9.4	0.9	25.0	8.6	1.2	3
22	1974	82.3	184.2	-	-	-	20.3	9.2	1.3	2
22	1975	83.3	204.0	-	-	-	28.9	8.4	1.2	-10
22	1976	84.3	233.8	-	-	-	20.5	5.8	0.8	-9
22	1977	78.2	322.0	-	-	-	26.1	12.3	1.7	9
22	1978	73.3	204.3	-	-	-	10.7	3.9	0.6	-6
22	1979	77.0	160.4	-	-	-	28.4	14.1	2.0	12
22	1980	80.8	153.7	-	-	-	20.7	9.1	1.3	11
22	1981	88.4	148.7	-	-	-	17.1	4.6	0.6	-6
23	1977	83.6	150.4	-	-	-	25.2	12.2	1.7	-5
23	1978	88.0	26.8	-	-	-	25.2	12.5	1.8	7
24	1978	78.2	157.6	-	-	-	19.4	10.7	1.5	8
25	1981	77.5	161.3	14.9	5.3	0.5	14.7	5.4	0.8	4
25	1982	85.5	184.3	-	-	-	32.9	12.3	1.7	10
25	1983	85.6	140.5	-	-	-	27.9	15.0	2.1	7
26	1983	79.0	176.7	-	-	-	17.9	8.0	1.1	10
27	1984	78.3	165.7	-	-	-	14.2	7.1	1.0	9
27	1985	81.6	149.8	8.7	2.8	0.3	8.1	3.1	0.4	2
27	1986	87.9	74.5	-	-	-	13.3	6.4	0.9	9
28	1986	80.9	167.4	-	-	-	21.7	10.0	1.4	12
28	1987	85.5	166.7	-	-	-	4.9	5.2	0.7	2
30	1988	76.0	167.0	-	-	-	21.9	11.3	1.6	9
30	1989	82.8	169.2	-	-	-	22.6	9.9	1.4	1
30	1990	84.0	125.5	-	-	-	20.2	8.2	1.2	10
31	1989	78.9	139.0	-	-	-	22.8	8.0	1.1	5
31	1990	73.2	138.2	-	-	-	12.5	6.5	0.9	5
Mean of 44 measurements				-	-	-	20.4	6.5	0.7	+3
Mean of 18 measurements				20.2	6.6	1.1	20.1	7.1	1.2	+1

Table 32. Statistical characteristics of snow depth from January snow-line data (cm).

NP Station	Year	N. Lat. (deg)	E. Long. (0-360°)	Mean	100 Points rms Deviation	rms Error	Mean	50 Points rms Deviation	rms Error	Difference of Mean Values ($X_{SL} - X_{MS}$)
5	1956	86.6	91.3	-	-	-	27.9	13.7	1.9	-15
7	1959	86.3	297.0	29.7	11.8	1.2	30.0	12.6	1.8	14
8	1960	77.5	186.8	-	-	-	28.5	12.1	1.7	-5
8	1961	83.8	201.3	15.6	12.0	1.2	16.3	11.5	1.6	-7
9	1961	85.9	174.2	17.7	10.8	1.1	17.1	12.0	1.7	-9
10	1962	75.8	170.1	36.6	21.1	2.1	36.5	20.2	2.9	-4
11	1963	81.3	217.8	24.5	14.5	1.4	28.2	14.9	2.1	15
12	1964	80.5	188.8	32.1	16.3	1.6	33.1	15.9	2.2	-30
13	1965	77.8	167.9	32.5	16.7	1.7	31.4	16.4	2.3	-1
15	1967	83.2	161.7	25.7	12.4	1.2	26.8	13.0	1.8	-6
16	1969	81.1	174.4	25.6	14.3	1.4	25.1	12.8	1.8	2
16	1970	84.3	200.9	35.9	15.0	1.5	38.3	14.5	2.0	-7
16	1971	86.0	236.5	38.4	17.1	1.7	39.3	17.1	2.4	-10
18	1971	82.5	148.9	22.3	8.5	0.8	22.1	9.7	1.4	-1
19	1970	76.5	155.2	22.3	13.5	1.3	21.1	10.2	1.4	6
19	1971	81.1	145.1	35.9	16.2	1.6	36.1	14.9	2.1	21
19	1972	87.3	131.2	26.4	19.3	1.9	25.2	13.1	1.8	12
20	1971	79.3	180.7	31.6	10.8	1.1	31.6	11.3	1.6	-2
20	1972	80.8	189.3	33.7	10.7	1.1	33.9	11.0	1.6	14
22	1975	82.5	190.8	-	-	-	27.2	9.4	1.3	-3
22	1976	74.6	216.2	-	-	-	35.8	5.9	0.8	-25
22	1977	82.8	232.1	-	-	-	27.7	7.2	1.0	-8
22	1978	76.1	227.7	-	-	-	34.6	15.3	2.2	6
22	1979	74.9	191.7	-	-	-	21.6	11.5	1.6	-31
22	1980	77.5	158.3	-	-	-	26.7	9.9	1.4	9
22	1981	83.0	152.5	-	-	-	31.1	10.1	1.4	9
22	1982	88.3	17.5	-	-	-	26.9	4.8	0.7	-1
23	1978	86.3	154.2	-	-	-	29.4	13.0	1.8	-9
24	1979	79.9	151.9	-	-	-	31.6	15.8	2.2	-12
25	1982	79.9	162.7	22.4	6.1	0.6	19.6	5.5	0.8	1
25	1983	84.8	204.3	-	-	-	33.2	11.6	1.6	15
25	1984	85.7	127.2	-	-	-	39.4	18.0	2.6	-
26	1984	80.6	175.6	-	-	-	26.3	11.9	1.7	11
25	1985	82.0	164.5	-	-	-	26.5	12.4	1.8	-14
27	1986	84.1	149.7	27.4	8.2	0.8	27.9	9.4	1.3	1
27	1987	88.6	10.2	-	-	-	14.0	11.4	1.7	-14
28	1987	80.8	169.6	-	-	-	30.2	12.7	1.8	7
28	1988	87.2	178.1	-	-	-	18.5	11.0	1.6	2
30	1988	74.6	174.6	-	-	-	26.2	12.6	1.8	17
30	1989	77.6	169.8	-	-	-	22.0	11.4	1.6	7
30	1990	82.6	150.8	-	-	-	29.9	15.8	2.2	1
30	1991	83.1	124.7	-	-	-	25.9	10.5	1.5	12
31	1989	77.1	155.3	-	-	-	30.4	9.6	1.4	0
31	1990	76.4	135.6	-	-	-	23.6	10.9	1.5	4
31	1991	72.4	145.0	-	-	-	25.6	13.7	1.9	15
Mean of 45 measurements				-	-	-	28.0	6.0	0.6	-0
Mean of 19 measurements				28.0	6.7	1.1	28.4	7.0	1.1	+0

Table 33. Statistical characteristics of snow depth from May snow-line data (cm).

NP Station	Year	N. Lat. (deg.)	E. Long. (0-360°)	Mean	100 Points rms Deviation	rms Error	Mean	50 Points rms Deviation	rms Error	Difference of Mean Values ($X_M - X_P$)
5	1955	82.7	152.9	-	-	-	49.5	13.1	1.8	-
7	1957	83.0	196.9	-	-	-	52.7	13.2	1.9	8
7	1958	86.3	210.0	27.3	12.7	1.3	27.2	9.6	1.4	-13
8	1959	76.7	193.1	-	-	-	26.3	13.0	1.8	-12
8	1960	79.9	180.4	-	-	-	35.3	14.3	2.0	-17
9	1960	77.7	164.3	45.2	14.3	1.4	43.2	13.0	1.8	-5
10	1962	78.1	159.9	42.0	20.6	2.1	43.2	18.7	2.6	-3
12	1963	77.1	191.2	38.0	20.7	2.1	42.1	21.3	3.0	14
12	1964	82.3	197.6	33.4	14.6	1.5	34.5	16.1	2.3	-7
13	1964	74.5	191.9	22.4	16.1	1.6	20.0	14.3	2.0	-1
12	1965	78.9	162.8	-	-	-	43.3	24.9	3.5	3
14	1965	74.9	182.3	22.4	14.4	1.4	19.3	13.6	1.9	3
16	1968	75.6	181.2	42.4	24.0	2.4	38.4	20.2	2.9	3
16	1969	82.2	177.0	40.7	19.5	1.9	42.1	19.9	2.8	19
16	1970	83.5	211.1	58.9	25.1	2.5	53.5	23.3	3.3	8
18	1970	80.5	151.7	-	-	-	23.2	15.8	2.2	-26
18	1971	83.6	159.6	33.0	14.9	1.5	35.3	16.6	2.3	-4
19	1971	81.7	149.7	43.7	24.0	2.4	41.0	18.1	2.6	19
19	1972	89.4	105.4	20.9	13.3	1.3	20.5	13.0	1.8	-11
20	1970	77.0	172.0	21.0	13.2	1.3	20.6	12.9	1.8	-7
20	1971	79.1	184.7	35.9	9.7	1.0	35.8	10.8	1.5	-5
22	1975	83.9	192.0	-	-	-	38.4	11.7	1.6	0
22	1976	83.2	219.9	-	-	-	55.1	6.8	1.0	-18
22	1977	81.8	233.1	-	-	-	34.2	6.4	0.9	-6
28	1987	82.3	167.5	-	-	-	21.6	13.1	1.8	-4
30	1988	76.4	166.2	-	-	-	32.8	12.5	1.8	16
30	1989	79.0	172.7	-	-	-	34.4	11.9	1.7	20
30	1990	83.2	140.1	-	-	-	28.1	9.8	1.4	-4
31	1989	77.9	151.6	-	-	-	44.0	10.3	1.5	-13
31	1990	76.4	133.8	-	-	-	28.5	12.9	1.8	11
Mean of 30 measurements				-	-	-	35.5	10.4	1.4	-1
Mean of 15 measurements				35.2	10.9	2.0	34.4	10.6	1.9	+1

Some understanding of the quantitative characteristics of the snow-cover distribution on undeformed ice can be obtained by plotting the frequency of occurrence of mean snow thickness versus area covered using drift-station data from the various years (Figure 22). This diagram shows that the entire mean-snow-thicknesses spectrum is lies within the bounds of 0 to 45 cm.

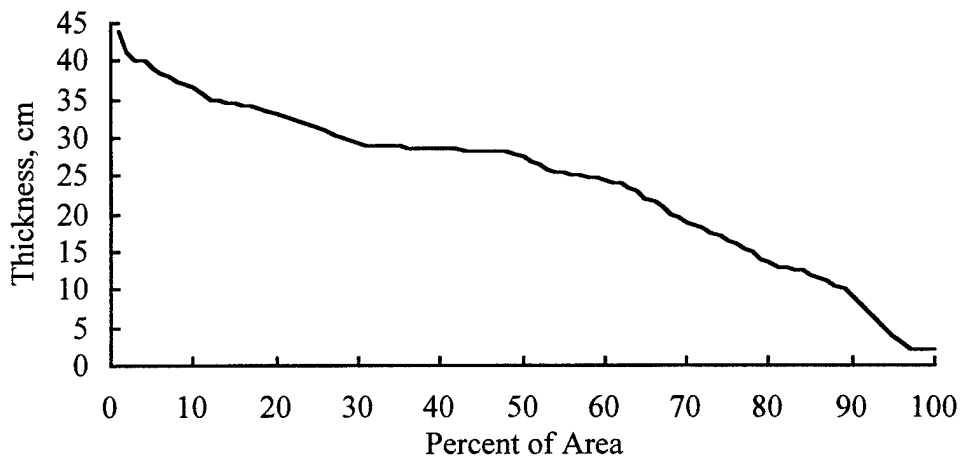


Figure 22. Curve showing the integrated (cumulative) snow-depth distribution.

On hummocked ice, snow accumulates between hummocks during episodes of blowing snow. In this case, the depth of the snow depends on the height of the pressure ridges and the distance between them. The average height is 82 cm. Table 34 gives the frequency distribution of snow depth for ridged ice.

Table 34 Frequency distribution of snow depths for ridged ice in the Arctic Basin.

Depth Range (cm)	Frequency of Occurrence (%)
0-50	27
51-75	31
76-100	26
>100	16

In the region near Greenland and in the central part of the Arctic Basin, the maximum depth of the snow cover on ridged ice at the end of winter ranges from 120 to 140 cm, and just off the edge of Greenland, it is as much as 160 to 180 cm. In other regions, it varies between 50 and 100 cm. On young ice, the ratio between the snow depth

on the windward side of pressure ridges and the depth on the leeward side is $2/3$ [12]. The dependence of the snow depth (h) on the height of pressure ridges (H) can be parameterized as

$$h = 0.11 H^{1.3}.$$

Snow ridges and sastrugi are typical forms for the snow cover on Arctic sea ice. The largest depths and also the greatest lengths of snow ridges have been observed in the Greenland and eastern Canadian regions of the Arctic Basin [47, 48]. Here, their heights range from 30 to 50 cm. In the other regions, the snow-ridge heights range from 29 to 40 cm. The smallest ridge heights, 10 to 20 cm, have been observed in the main shore-lead zone of the Beaufort Sea.

Sastrugi are narrow, elongated hillocks of snow extending in the direction of the wind. They are easily blown away when the wind changes direction, but new ones are formed almost immediately. The snow depths of sastrugi range from 20 to 50 cm, and the relative area they occupy from 10 to 25% [47].

The snow depth on the ice in the marginal seas is 1.5 times smaller than that on the ice in the Arctic Basin. This is because the ice in the marginal seas doesn't form until later in the season (October to November). The average snow depth on the young ice in these areas is 7 cm at the beginning of winter, 16 cm in January, and 23 cm in April and May.

In order to evaluate the role of the ice cover for shipping, it is necessary to take into account the snow-depth distribution on the ice. The snow-cover distribution on ice of different age categories has not yet been sufficiently studied. During the period when ice is growing, snow on the surface delays ice growth, and in the spring the snow cover delays ice melting. In summer, areas of anomalously thin or thick ice are preserved owing to the presence of the snow cover. On multiyear ice, however, this effect is not significant (to within ± 5 cm). The snow depth is less on level first-year ice than on multiyear ice. This explains why, for example, during the drift of M/V *Georgiy Sedov* from 26 October 1937 to 20 June 1939, the snow depths recorded at latitudes of 75° – 81° N at the beginning of the drift ranged from 3 cm (in October 1937) to 12 cm (in April 1938). Between January and June the next year at higher latitudes (85° – 86° N), the snow depths ranged from 22 to 28 cm. The results of the daily measurements of the snow and ice thickness over the entire drift of the *Sedov* are given in Appendix D. On fast ice near the islands and on the islands themselves, the snow depth is smaller than it is in the Arctic Basin (Table 35) [12, 39].

Table 35. Depth of the snow cover and ice thickness on fast ice (cm).

Age of Ice	Snow Thickness	Observation Period
Thin first-year ice, 30–70 cm	9	September–October
Thick first-year ice, 70–120 cm	14	October–February
Thick first-year ice, 120–200 cm	18	March–May

6.3 Snow density

The density of the snow cover is less variable than its depth. Fresh snow has the lowest density (50–90 kg/m³); the snow density after episodes of blowing snow is typically 170 kg/m³, and the highest density (500–550 kg/m³) is measured for melting snow and snow saturated with melting water.

Monthly charts of the spatial distribution of multiyear-mean snow densities were constructed based on the results of the snow-line surveys. The snow density changed little across the Arctic Basin, from 310 to 330 kg/m³. Over the course of the winter, however, the mean snow density increased from 200 to 360 kg/m³ (Table 36).

In the course of a year, the snow-cover density increases during the initial stages of snow accumulation, but from December to April it remains almost unchanged, with a value of about 300 kg/m³. Not until May and June does the density sharply increase again as a result of snow melting.

Table 36. The seasonal cycle of snow density in the Arctic Basin at the coordinate points (kg/m³).

N. Lat.	E. Long.	Month									
		Sep.	Oct.	Nov.	Dec.	Jan.	Feb.	Mar.	Apr.	May	Jun.
Pole		240	280	290	300	300	310	320	320	320	330
85°	00°	200	270	290	300	300	310	320	320	320	330
85°	60°	220	280	290	300	310	320	320	330	330	340
85°	120°	240	290	290	300	310	320	320	330	330	340
85°	180°	240	290	290	300	310	320	320	330	330	340
85°	240°	240	280	290	300	310	320	320	330	330	340
85°	300°	220	280	290	300	310	320	320	330	330	340
80°	120°	220	280	290	300	310	320	320	330	330	350
80°	150°	220	280	290	300	310	320	320	330	330	350
80°	180°	240	280	290	300	310	320	320	330	330	340
80°	210°	230	270	290	300	310	320	320	330	330	340
80°	240°	220	260	280	290	300	320	320	330	330	340
75°	165°	220	260	280	290	300	320	320	330	330	360
75°	195°	220	260	280	290	300	320	320	330	330	350
75°	220°	220	260	280	290	300	310	310	320	320	340
Mean		230	280	290	300	310	320	320	330	330	340
Std. deviation		12	11	5	5	5	4	3	4	4	8

6.4 The water equivalent of the snow cover

Because the water equivalent of the snow cover is proportional to the snow's depth and density, the spatial distribution of the water equivalent in the Arctic Basin is similar to the snow-depth distribution. In May the largest water equivalent, 120 mm, is observed in the Greenland region of the Arctic Basin, and the smallest is found in a region near the East-Siberian Sea.

Table 37 presents snow-cover water-equivalent data collected from October to May from all the drifting stations together with precipitation values calculated from data on the snow depth and density. The table contains the water-equivalent values, the differences from month to month, and the mean amount of precipitation for each month. The precipitation values have been corrected using the empirical methods described in [10]. Correction of precipitation values measured in the Arctic is necessary to eliminate measurement errors resulting from the effects of wind. For wind speeds up to 6 m/s, precipitation is underestimated. At wind speeds of 7 m/s and greater during blowing-snow events, "false," or excess, precipitation blows into the precipitation gauge. The daily precipitation measurements at the stations are corrected for precipitation gauge error due to wetting of the vessel walls. The correction equals 0.1 mm for measurements of solid precipitation and 0.2 mm for measurements of liquid precipitation. There is an additional instrumental error due to evaporation from the precipitation gauge during the exposure of the instrument. For a 12-hour exposure, this error is small—several times less than the measurement accuracy (between 0 and 5% of the amount of measured precipitation), and it was not included in the correction given here.

Table 37. Water equivalent of the snow cover and the amount of solid precipitation during the period October to May.

Characteristics	Month									Total
	Sep.	Oct.	Nov.	Dec.	Jan.	Feb.	Mar.	Apr.	May	
Depth of the Snow Cover, cm	13	18	23	26	28	30	32	34	36	-
Density of the Snow Cover, g/cm ³	0.23	0.28	0.29	0.30	0.31	0.32	0.32	0.33	0.33	-
Water Equivalent, mm	30	50	67	78	87	96	103	112	120	-
Difference in the Equivalent Values from Month to Month, mm	-	20	17	11	9	9	7	9	8	90
Amount of Precipitation Before Correction, mm	-	14	10	9	11	9	9	6	8	76
Amount of Precipitation After Correction, mm	-	20	17	12	10	9	7	8	9	92

The total solid precipitation from October to May, calculated from the water equivalent, is 90 mm. According to the uncorrected precipitation-gauge measurements, the total solid precipitation for this period was 76 mm. After the corrections to eliminate instrumental errors, the value was 92 mm per year. This is very close to the total precipitation obtained from the water equivalent of the snow cover for the winter.

The agreement between the water equivalent of the snow cover and the corrected values for the monthly precipitation confirms the correctness of the methods used to correct the precipitation observations.

6.5 Duration of the snow cover

Multiyear-mean dates of formation of stable snow cover and its disappearance were calculated using the methods described in Section 2. Shown below are the data for the North Pole. On average, the stable snow cover at the geographic Pole forms on 20 August and decays on 18 July.

Date	Formation	Decay
Mean	20 August	18 July
Earliest	Snow does not melt	2 July
Latest	8 September	Snow does not melt

Figures 23 and 24 are contours maps showing the dates of the autumn formation and spring decay of the snow cover. Formation of stable snow cover begins in the Arctic Basin during the last 10 days in August and rapidly spreads southward. A stable cover has already formed at 75°N, reaching the islands, on 11 September, and a stable snow cover is formed at the northern coastline of Russia and Alaska during the first 10 days in October.

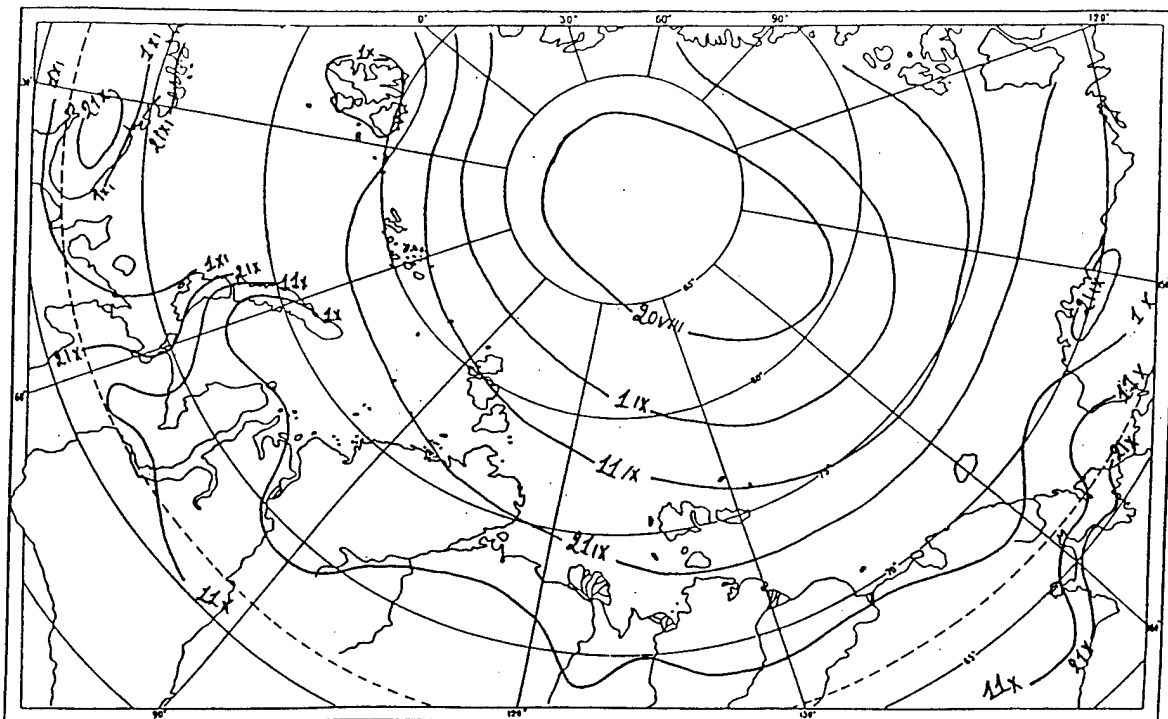


Figure 23. Dates of stable snow-cover formation. [Roman numerals denote the month; i.e., 21IX = 21 September.]

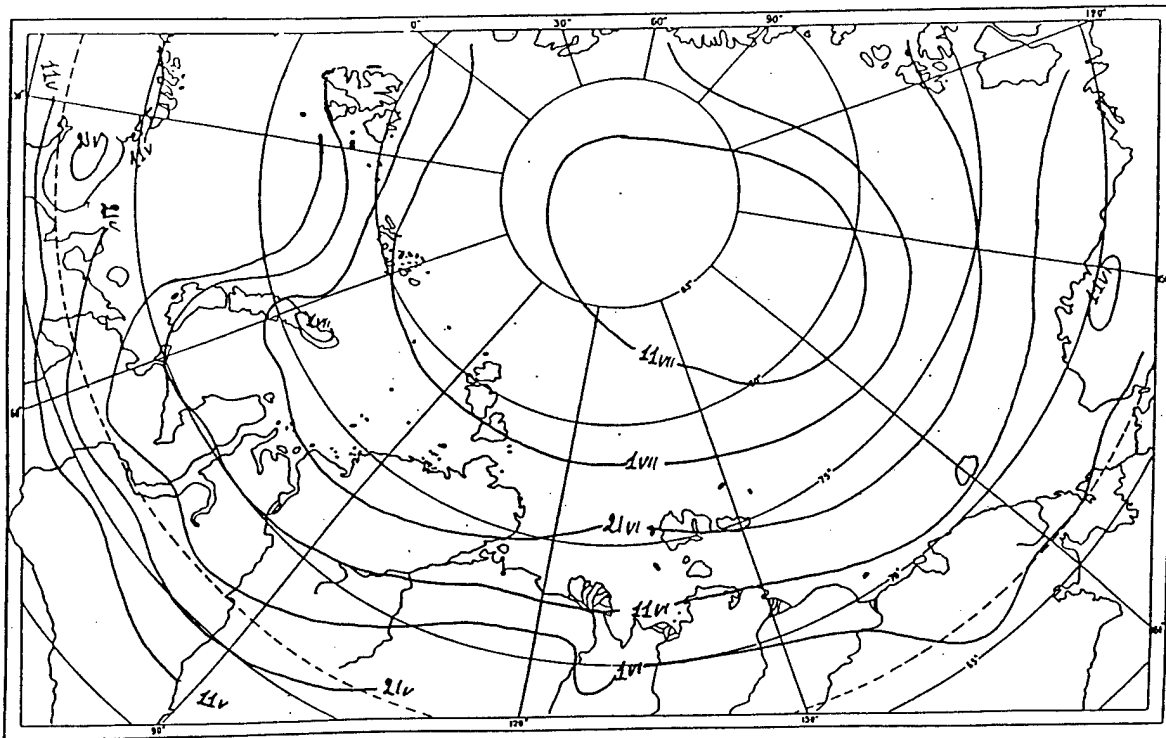


Figure 24. Dates of decay of the snow cover.

The decay of the snow cover begins in the south. At the Arctic coast, melting occurs during the first 10 days in June, but in the central Arctic it is delayed until the second 10 days in July. In this region, the snow cover did not melt completely in 25% of the cases.

The influence of melting of the snow cover on the air temperature is shown by the fact that in autumn the decrease in air temperature is greater when snow is present than when it is absent. In spring the reverse is found. The snow cover is responsible for the delay in the occurrence of above-freezing air temperatures. The greater the winter accumulation of snow, the later the air temperatures begin to rise above 0°C . This process is related to the fact that a larger amount of heat is required to melt a thicker snowpack, so it takes more time than for a thinner snow cover.

To illustrate this, Figure 25 presents a contour map showing the number of days in the Arctic Basin with snow cover. The number of days with a snow cover is greatest in the vicinity of the Pole—more than 350. This number decreases to the south. Across the Arctic islands, it is 300 days.

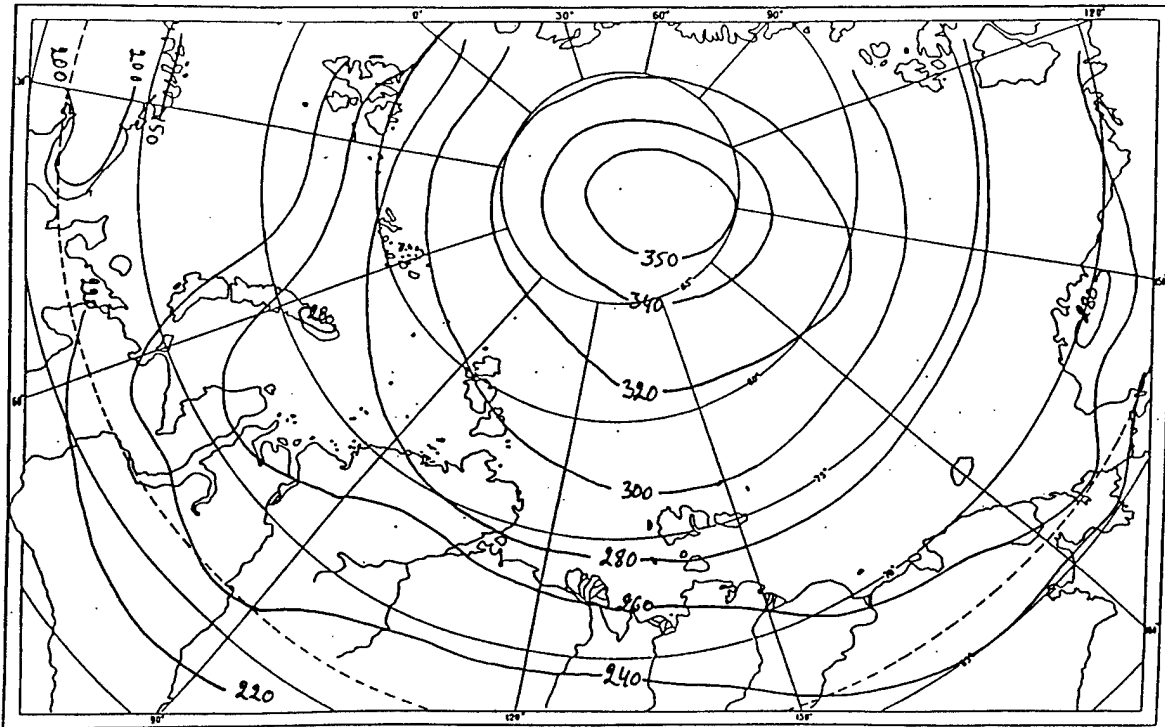


Figure 25. Number of days with a snow cover (per year).

6.6. Snow transport

The formation of the snow cover is greatly influenced by wind transport of the snow, especially for blowing-snow events, during which large volumes of snow are raised above the surface and transported over significant distances. In the Arctic Basin, blowing-snow events are recorded all year round. During blowing-snow events, snowflakes from the snow-cover surface are lifted up into the air by saltation (the difference in air pressure due to the change in the wind speed with height). In the wind speed range of 8 to 12 m/s, a gradual transition is observed from saltation to lifting of the snow particles by turbulence.

The snow transport rate (q) is the amount of snow (in grams) passing through a unit area (1 cm^2) perpendicular to the wind-flow direction per unit of time (minutes). Sometimes the magnitude of snow transport is defined by the concentration of solid phase per unit volume (g/m^3): The snow transport rate depends primarily on the wind speed. The higher the speed, the greater the rate of snow transport and the greater the height to which snow rises above the snow surface. A especially large amount of snow is transported in the air layer nearest the surface. There is a sharp decrease in the amount of the snow

transported with increasing height. This behavior is typical and is observed at all wind speeds that produce snow transport. A formula for the rate is proposed by Mel'nik [37]:

$$q = C U^3 \text{ g/cm}^2 \text{ min,}$$

where U is the wind speed in meters per second, and C is an empirical coefficient. In temperate latitudes, $C = 0.01$. For Arctic latitudes, it has not been determined.

At the Vavilov Dome glacier on the Severnaya Zemlya archipelago and at the Amderma station on the southwestern coast of the Kara Sea, experimental measurements of the snow-transport rate were carried out using the "Cyclone" drifting snow gauge during the winters of 1975–1976 and 1976–1977. In all, 400 comprehensive measurements were made during blowing-snow events at heights up to 5 m above the snow surface [9]. In fact, the values measured in the layer from 3 to 5 m turned out to be negligibly small compared with those at lower levels.

The results of these measurements are presented in Table 38. The last column of the table contains the values for $Q = \sum q_i \Delta h_i$. Physically, Q denotes the amount of snow (in grams) transported for 1 hour across a flat surface through an area with a transverse horizontal extent of 1 cm and a height of 5 m for the different wind speeds. For the entire layer from 0 to 3 m, the dependence of this value on the wind speed can be described by the formula

$$M = 0.80 U^{2.8}, \text{ g cm}^{-1} \text{ h}^{-1}$$

where U is the wind speed in meters per second. This formula can be used to estimate the volume of drifting snow transported across a contour of unit length during a blowing-snow event whose duration is τ :

$$V = M \tau / \rho.$$

Table 38. Rate of mean snow transport at different wind speeds.

Wind Speed (m/s) at 10-m Height	Snow Transport Rate (g/cm ² per hour) at Different Heights (cm)					Q
	0–1 cm	1–10 cm	10–100 cm	100–200 cm	200–300 cm	
6–8	86.5	86.4	9	8	2	191.9
9–10	150.1	153.0	72	50	10	435.1
11–13	325.0	202.5	162	90	20	799.5
14–16	520.5	304.2	378	220	60	1482.7
17–20	900.5	407.7	765	540	180	2793.2
21–25	1880.5	561.6	1503	1210	260	5415.1

7. TEMPORAL VARIABILITY OF SNOW-COVER CHARACTERISTICS IN THE ARCTIC BASIN

7.1 Technique for producing continuous series of observations from the drift-station data

In order to analyze interannual changes in the climatic characteristics, it is necessary to obtain a continuous series of observations at the standard meteorological stations. In the Arctic Basin, where the coordinates of the drift stations change every day, direct multiyear observational series at particular points are not possible. To some extent, the task of evaluating interannual changes in the snow-cover parameters is simplified because the area covered by the drift stations is limited. As a rule, the drift of a station is restricted to an area of the Arctic Basin whose climatic characteristics do not change very much. There are a few exceptions, specifically stations NP-1, NP-22, and NP-31 which during certain months of their drift were carried beyond the uniform climatic area.

To obtain the most reliable uninterrupted series of the individual meteorological components, special techniques were employed to refer the drift-station data to the mean coordinate point of all the stations ($82^{\circ}42'N$ latitude, $175^{\circ}00'E$ longitude). For the stations drifting in a zone within a radius of 400 km from this point, the actual data were used directly. For the other stations, the measured values of the snow-cover characteristics were reduced to that point according to the following scheme. For each specific year and month, isoline (isopleth) charts were constructed by including in the analysis the data from the coastal and island stations located around the boundary of the Arctic Basin. A total of 432 charts was produced, covering the entire observational period. The data from each specific drift station were interpolated along [parallel to] the isolines for the corresponding year and month to the point that had the mean coordinates of the drift of that station. For example, Figure 26 shows the isolines of snow-cover depth for May 1958 derived from the data from the island and coastal stations combined with the observations from the drift stations NP-6 and NP-7. For May 1958, the snow-depth isoline for 31 cm passes through the mean coordinate point given above for all stations. In this way, continuous series of monthly mean values were produced for snow-cover depths, the dates of snow-cover formation and decay, and the number of days when a snow cover was present. Similar series were also derived for total precipitation and air temperatures from 1954 to 1990.

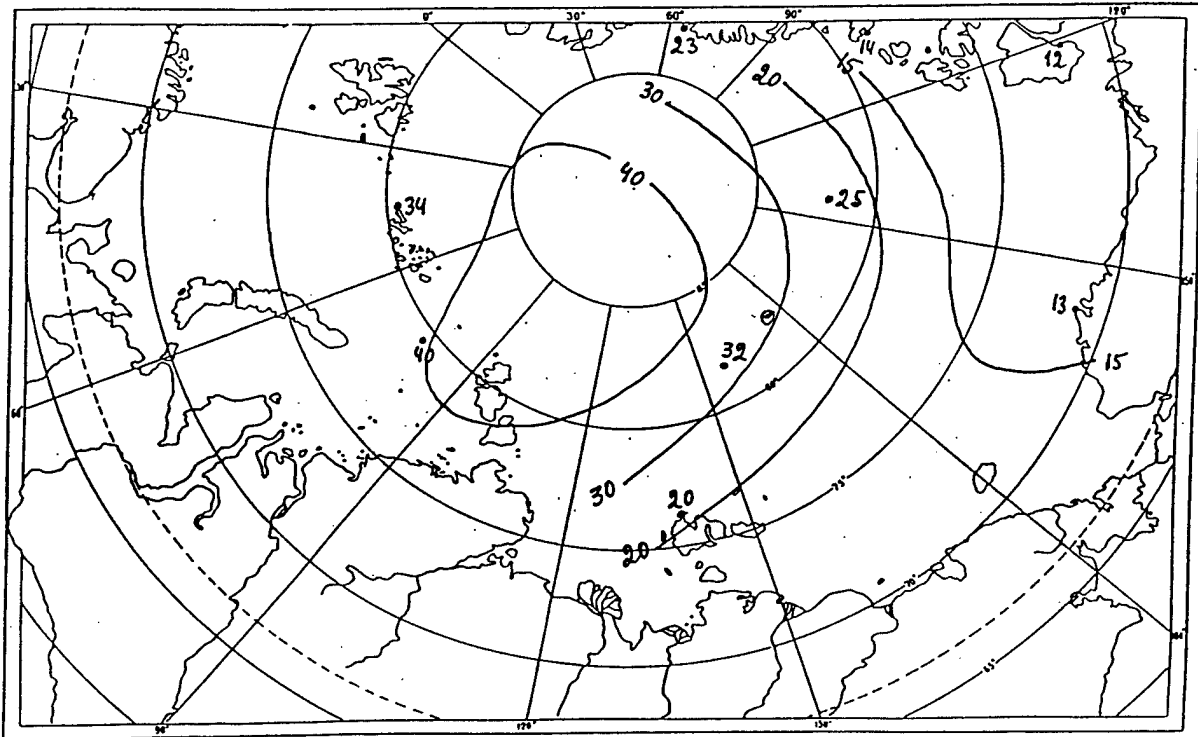


Figure 26. Map of the snow cover depth for May 1958 referenced to the central point of the drift of all NP stations.

7.2 Interannual variability of the snow-cover characteristics, precipitation, and air temperature

To estimate the changes in the snow-cover parameters during the period covered by the drift stations, the following quantities were analyzed: the interannual changes in the snow depth, the length of time a snow cover was present, and multiyear variations in the total precipitation and the air temperature.

The interannual variation in the number of days from 1954 to 1991 with a snow cover in the Arctic Basin is shown in Figure 27. Two distinct periods can be identified: from 1954 to 1975, when the duration of the snow cover decreased, and from 1976 forward, when it increased.

The values of the linear regression parameters for 1954 to 1975 showed that the number of days with snow decreased by 15 days (the slope of the regression is $B_x = -0.66$ day/year). The values for 1975 to 1991 showed an increase of 30 days ($B_x = 2.1$ days/year). The increase in snow-cover duration during the latter interval was produced by the combination of an earlier formation time (Figure 28) and a later decay time (Figure 29). From the mid-1980s on, however, the dates of snow-cover formation and de-

struction closely approached the mean values. For the whole period of operation of the drift stations, there are no systematic changes in snow-cover duration. As shown in Table 40, B_x is essentially zero for 1954 to 1991.

The minimum number of days with a snow cover in the Arctic Basin is 310, and it occurred in 1975 and 1987. The maximum, when the snow cover remained all summer, occurred in 1970 and 1983. Note that the minimum total precipitation during the cold period was recorded in 1975, and the maximum for the entire observational sequence was in 1983.

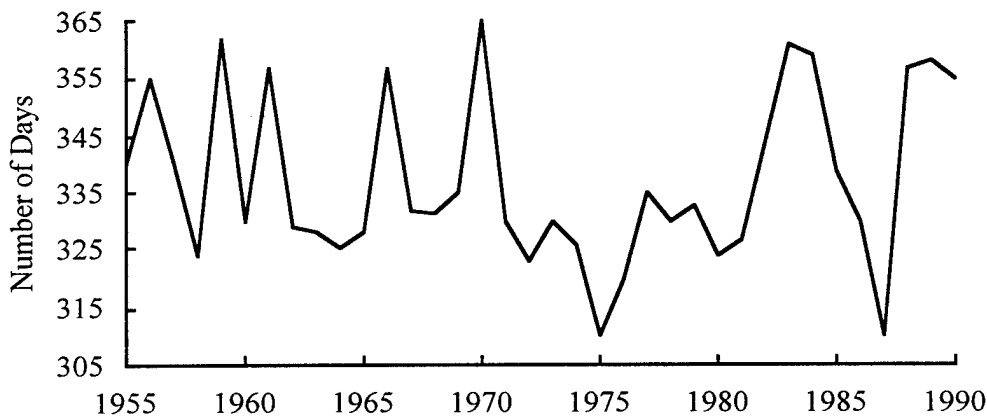


Figure 27. Number of the days with a snow cover in the Arctic Basin.

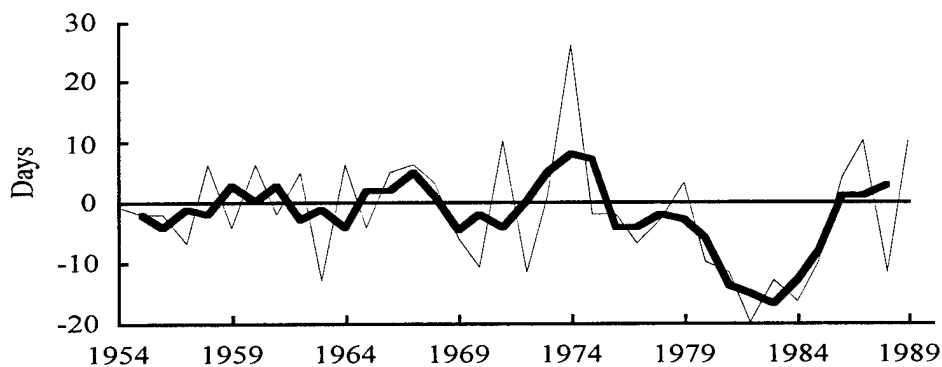


Figure 28. Anomalies [variations about the mean] in the dates of snow-cover formation; the thick line denotes a 3-year running mean.

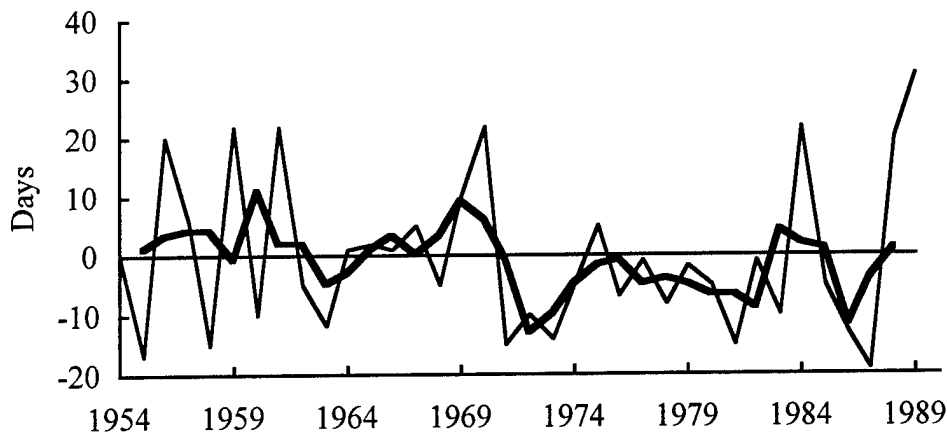


Figure 29. Anomalies [variations about the mean] in the dates of snow-cover destruction; the thick line denotes a 3-year running mean.

Table 40. Linear regression parameters of the interannual changes in snow-cover characteristics, yearly total precipitation, and temperature (1954–1991).

Parameter	B_x	$D, \%$
Snow cover depth in May	-0.53 cm/year	53
Anomalies of the snow-cover formation dates	-0.15 days/year	17
Anomalies of the snow-cover destruction dates	-0.18 days/year	15
Number of days with snow	0.05 days/year	3
Annual total precipitation	-0.27 mm/year	10
Total precipitation in the cold season (Sep.–Jun.)	-0.48 mm/year	19
Total precipitation in the warm season (Jul.–Aug.)	0.18 mm/year	11
Mean annual air temperature	0.002 °C/year	1
Average air temperature in the cold season	0.004 °C/year	>1
Average air temperature in the warm season	0.001 °C/year	>1

Note: B_x is slope of the regression in units of (parameter/year) and D is the percentage of the variation (dispersion) explained by the regression.

In Section 6 it was pointed out that snow-cover thickness in the Arctic Basin experiences considerable spatial variation. This spatial variability in the snow cover's thickness and its temporal variability at the mean coordinate point (82°42'N, 175°00'E) arise both from the annual variability in the snow depth in each of the specified snow-formation areas of the Arctic Basin and from the spatial variability in the snow depth across the Arctic Basin as a whole. The interannual rms deviations in snow depth in October, January, and May show distinctive variations from 1954 to 1991. In January and May, the rms devia-

tions in the first half of the period are high; toward the mid-70s, the values decrease, but later they increase again. In October, there is a weak linear decrease in the rms deviation values. The highest rms values of snow-cover variability were recorded in 1970 and 1980.

Figure 30 shows the interannual changes in the snow depth, smoothed with a 5-year running mean, observed at the meteorites at the beginning of the snow-formation period (October), in the middle of winter (January), and during the maximum snow accumulation in May. The snow thickness decreased from the mid-1950s to the mid-1960s, increased slowly until the mid-1970s, and then changed over and continued to decrease until the end of the record. The observed trend in snow depth over the whole period from 1954 to 1991 was a decrease. The interannual changes determined from the snow-line observations showed the same behavior. The decrease of the snow depth over this time interval explained by the linear regression was 19 cm.

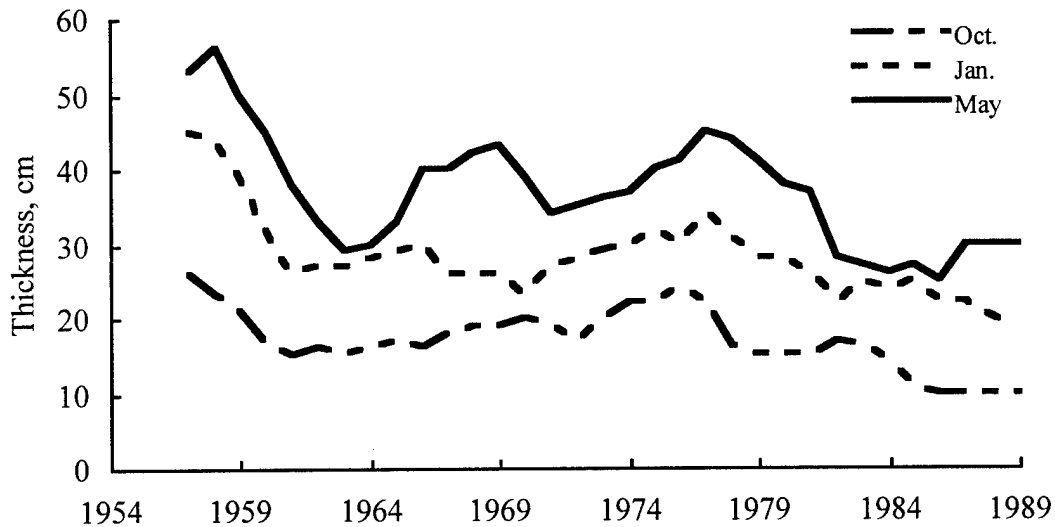


Figure 30. Snow-cover depth smoothed with a 5-year running mean.

The characteristics of the interannual changes in the duration of the snow cover are analogous in many ways to the changes in snow depth. From 1975 onward, however, the increasing duration of the snow cover was accompanied by a decrease in the snow's thickness.

The duration of the snow cover is related directly to the thickness of the snow at the beginning of the melt season. For the Arctic Basin, the distribution of precipitation throughout the year is irregular, depending on the specific conditions in each region: 70% of the total annual precipitation occurs in the cold season. Figure 31 shows the inter-

annual variation in the precipitation for the entire year and for the cold and warm parts of the year, smoothed with a 5-year running mean. The annual variability in the precipitation and the corresponding variability during the cold period are almost the same (their standard deviations are 28 and 27 mm, respectively), whereas the variability during the warm period is significantly less ($\sigma = 18$ mm). Throughout the total period of operation of the drift stations, the largest amount of precipitation (200 mm) in the Arctic Basin occurred in 1979 and the lowest (80 mm) in 1985. In the first case the anomaly was 2.0σ , and in the second -2.3σ .

Substantial decreases were observed in the precipitation during the cold part of the year from 1955 to 1965 (30 mm) and from 1968 to 1974 (60 mm). The record minimum for precipitation during the cold season was observed in 1974. The anomaly in this case was -2.7σ . Between 1974 and 1977, winter precipitation increased most sharply, by 100 mm (this amount is not evident in Figure 31 because of the smoothing). The last increase in snow-cover thickness in the Arctic Basin occurred during these years.

Precipitation during the warm season decreased from 1955 to 1965; after 1966, however, it began to increase slowly. From 1955 to 1990, as a whole, summer precipitation increased by 7 mm (see Table 40).

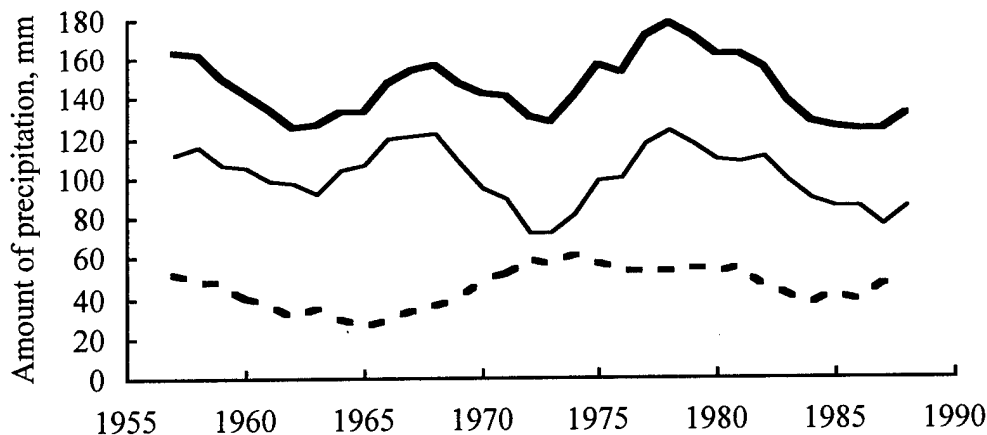


Figure 31. Amounts of precipitation smoothed with a 5-year running mean. The thick solid line is the yearly total, the thin solid line is the total for the cold season, and the dashed line is the total for the warm season.

The interannual variation in precipitation shows a decreasing trend, particularly for the cold season (Table 40). The decrease in precipitation in the Arctic Basin for the cold season showed a linear trend of 17 mm for the 36-year period.

A comparison of the interannual variation in snow-cover depths with the total annual precipitation confirms the recent tendency of a decrease in the annual and cold-season precipitation accompanied by a decrease in the thickness of the snow cover. At the same time, the increasing duration of the snow cover is explained by the weak increase in the amount of solid and mixed precipitation in the summer, as a result of which the number of days without snow in the summer is decreasing. The number of days with precipitation in July and August showed an increase up to 1990. Since 1965, the number of days with solid and mixed precipitation increased by 4 days in July and by 6 days in August.

The interannual variation of air temperature in the warm season shows a clear cycle (Figure 32). There are four well-defined segments of increasing temperature: 1956–1960, 1961–1965, 1969–1977, and 1980–1987, with corresponding maximum values in 1960, 1961–1965, 1969–1977, and 1980–1987, with corresponding maximum values in 1960,

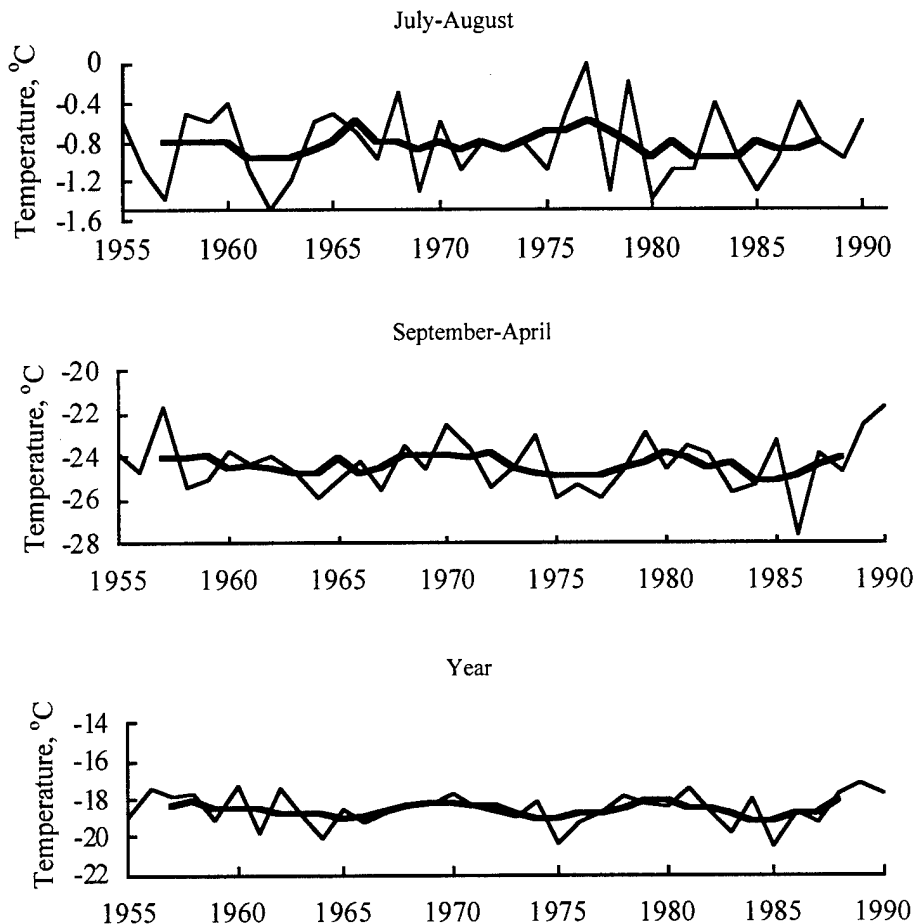


Figure 32. Interannual variability and 5-year running means of air temperatures in the Arctic Basin for the warm season, the cold season, and the annual average.

1965, 1977, and 1987. During the cold season, there were three distinct segments when the temperature was decreasing: 1956–1964, 1970–1975, and 1978–1986, with minimum values in 1964, 1975, and 1986. The lowest temperature, -27.6°C , was observed in 1986 [1]. The mean temperatures in the warm and cold seasons have standard deviations of 0.4 and 1.3°C , respectively, and the annual temperature has a standard deviation of 0.9°C . For the period 1955 to 1990 as a whole, the trends in the annual and seasonal air temperatures were essentially zero (see Table 40).

Spectral analysis of the intermonthly anomalies in snow depth, precipitation, and temperature revealed an 18-year periodicity in the snow depth and amount of precipitation and a 9-year periodicity in the temperature. There was also a half-year cycle in the precipitation variation, and a 9-year cycle in snow depth, as observed for the temperature. In addition to the principal oscillation periods noted above, a 2-year cycle appeared in each of the characteristics. To filter out the 2-year cycle, a 24-month smoothing was applied to the intermonthly series of air-temperature anomaly, snow-cover depth, and monthly amount of precipitation. The mutual correlation functions between the air temperature and the snow thickness and between the amount of precipitation and the snow thickness were then obtained (Figure 33). As shown in Figure 33, exclusion of the 2-year cycle makes it possible to illustrate the changes in the meteorological parameters under consideration more clearly.

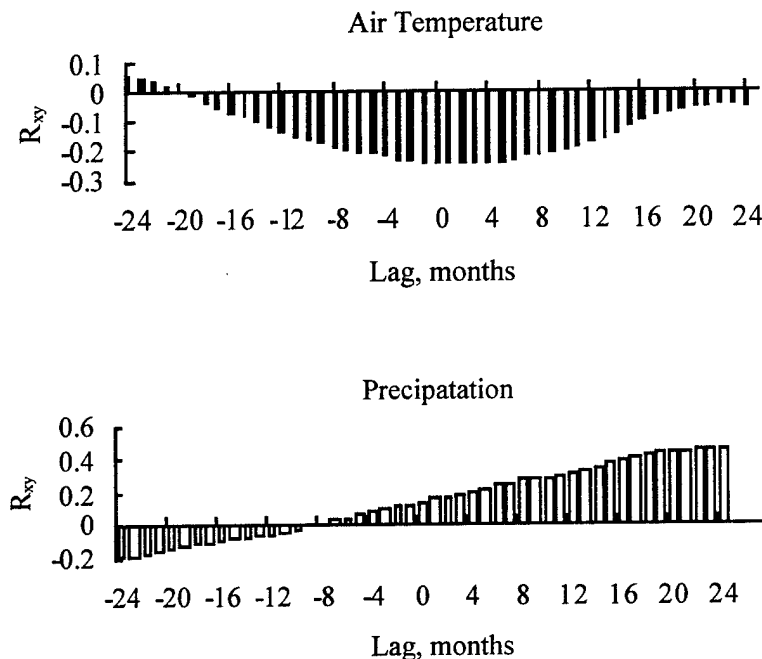


Figure 33. Correlation functions (R_{xy}) between variations of the smoothed intermonthly anomalies for (top) air temperature and snow thickness and (bottom) amount of precipitation and snow thickness.

The correlation functions show that the snow thickness reacts faster to changes in air temperature than to changes in precipitation: air-temperature changes lead snow-thickness changes by several months, but precipitation changes have a much larger time lag.

At the end of the 1980s, the interannual variations in snow-cover depth were similar to those in precipitation. The switch in the sign of the snow-depth changes is due both to the increasing air temperature and to the decreasing precipitation during that period of time. Both these processes can be explained by changes in the large-scale circulation processes in the northern hemisphere.

To estimate the fluctuations in the parameters of the circulation, we turn our attention to the distribution of the number of days that show Vangengeim-Girs circulation forms for the Atlantic-Eurasian (E, W, and C) and Pacific Ocean-American (Z, M1, and M2) sectors of the northern hemisphere [16]. The circulation forms E, C, M1, and M2 occur in areas where meridional circulation processes are prevalent. The W and Z forms occur in areas where zonal circulation is prevalent. An increase in the number of days with any of these circulation forms indicates changes in the exchange of heat and moisture between mid and high latitudes. For forms E, C, M1, and M2, more days indicate increased exchange, whereas for forms W and Z more days indicate a decrease. Table 41 shows the number of days per season and per year for each of these forms averaged over intervals of 11 years.

According to Table 41, important changes occurred in the interlatitude exchange during the operation of the drift stations. For the Pacific Ocean-American sector, the frequency of meridional circulation forms decreased from 1957 to 1991 and west-to-east transport increased; 1981 to 1991 saw the 100-year maximum in the number of days with eastern circulation form Z and the 100-year minima in meridional forms M1 and M2. In the Atlantic-Eurasian sector, meridional exchange intensified from 1970–1980, and the 100-year maximum in the number of days with circulation form E occurred; 1981 to 1991 saw a sudden change resulting in an increase in the west-to-east transport: the number of days with meridional circulation form E decreased, and the number of days with meridional circulation form C reached a 100-year minimum.

This confirms the long-term forecast predicting an increase in the western atmospheric circulation form in the 1990s and the beginning of the 21st century [23]. Because of the increase in zonal circulation, it is supposed that more cyclones will come into the Arctic Basin region, bringing more heat and precipitation. However, with an increase in the amount of precipitation, the thickness of the snow on the ice will also increase, which would decrease the transport of heat from the ocean to the atmosphere through the ice. Interaction of these two factors—an increase in cyclonic activity and a decrease in vertical heat transport through the ice—will give rise to further changes in the snow cover.

Table 41. Average number of days with the Vangengeim-Girs circulation forms. The entries in bold type indicate the maximum and minimum values.

Period	Form E	Form W	Form C	Form Z	Form M1	Form M2
Winter (December to February)						
1904—1914	34.8	39.8	16.2	23.4	13.2	53.4
1915—1925	45.3	34.8	9.9	24.0	11.1	54.9
1926—1936	47.7	22.2	20.1	25.5	7.8	56.7
1937—1947	45.3	25.8	18.9	27.3	8.1	48.6
1948—1958	42.3	30.3	17.4	21.1	25.8	43.2
1959—1969	42.0	21.9	26.1	22.5	18.6	48.9
1970—1980	52.8	16.5	20.7	38.1	14.7	37.2
1981—1991	37.2	33.6	25.2	43.5	10.2	36.1
Summer (July & August)						
1904—1914	18.9	37.6	35.5	36.1	15.0	10.2
1915—1925	22.8	42.4	26.8	31.6	53.5	6.9
1926—1936	37.0	33.7	21.3	34.3	52.6	5.1
1937—1947	39.7	20.1	32.2	33.1	37.9	21.0
1948—1958	37.6	25.6	28.2	27.7	43.0	21.3
1959—1969	46.6	21.0	24.4	32.5	31.9	27.6
1970—1980	59.2	14.1	18.7	35.5	30.7	25.8
1981—1991	56.2	16.8	19.0	42.2	22.2	27.4
Annual						
1904—1914	127.7	151.7	85.6	149.3	98.8	116.9
1915—1925	133.7	154.1	77.2	118.1	109.6	137.3
1926—1936	154.1	130.1	80.8	130.1	94.0	140.9
1937—1947	139.7	109.6	115.7	110.9	83.2	178.9
1948—1958	151.7	110.9	102.4	122.9	112.0	130.1
1959—1969	175.7	88.0	101.3	128.9	95.2	140.9
1970—1980	212.9	76.1	76.0	167.3	76.0	121.7
1981—1991	185.3	104.9	74.8	193.7	58.0	113.3

Significant changes are not expected in the snow-cover regime before 2005–2010. Oscillations will continue within the limits observed during the last 30 years, but there will be a trend toward a general increase in the depth of the snow cover on the ice. The number of days with snow cover will oscillate from about 300 to 365 without a significant trend.

8. SUMMARY

This investigation is the first detailed generalization of the standard experimental measurements of snow-cover characteristics in the Arctic Basin that were carried out over the working period of the North Pole drifting ice stations from 1954 to 1991. During this period, data were collected at the drift stations over a total of 848 station-months (sometimes two or three stations were operating simultaneously). The work was carried out using a single consistent methodology for each snow-cover characteristic studied.

The fundamental results presented in this monograph are based on data from three types of observations: snow-line surveys, snow-depth measurements at standard meteorological sites, and precipitation measurements. They differ not only because the instruments and methods employed were different, but also because the systematic errors were specific to each type of observation. The values of these systematic errors depend on a wide variety of factors, which influence the measured values in different ways. Among these are the orographic characteristics in the vicinity of the station, the direction and speed of the wind, the characteristics of the deposited snow, the type of precipitation, densification of the snow cover over the course of the winter, the effects of transport due to blowing snow (formation of snowdrifts, sastrugi, snow spits), and ablation.

As a result, the problem arises of how well the information obtained from a specific drifting ice floe represents the parameters of snow cover in general. In addition, there is the question of correct use of the observational results in models that call for the use of the snow-cover characteristics as input parameters.

In the ideal situation, the amount of precipitation within a sufficiently long period of time (10-day period, month, season, or year) should be the same as the water equivalent of the snow cover, and the snow deposited at the meteosites should be the same as that measured on the snow lines. In reality, the snow-cover thickness measured at the meteosites differs from that measured on the snow lines. The correlation coefficients between these measurements are 0.56 for October, 0.69 for January, and 0.61 for May. However, the interannual tendencies in their variations are similar: In both cases, the snow thickness at the time of maximum snow deposition in May decreased approximately 20 cm from 1954 to 1991. During this period, the amount of precipitation decreased by 30 mm, and the water content of the snow cover decreased by exactly the same value.

An important aspect of the analysis is that most of the data were collected in a climatically uniform region. The only exception was a small amount of the data collected at stations NP-1, NP-22, and NP-31, whose drift trajectories during certain months lay outside the boundaries of the uniform region.

The technique used for collecting the snow measurements provided an average of the results for all the snow lines over a sufficiently long time (10-day periods or months) to make it possible to minimize systematic errors. The basic problem in analyzing the

series of observations is that it is not possible to calculate the amount of spurious precipitation during blowing-snow events. Possibly part of the solution to this problem will be found in the process of developing a method to correct for it. For operational checks on the snow deposition, the snow thickness measurements at meteosites are very important.

Unfortunately, among all three types of observations (snow-line measurements, snow-thickness measurements at the meteosites, and precipitation measurements), it is impossible to calculate quantitatively the amount of snow that has accumulated between hummocks in the form of snowdrifts, sastrugi, etc. Attempts to obtain information of this sort have been made by Romanov [47]. According to his estimates of the area, thickness, and spatial distribution of the parts of the snow cover influenced by hummocks, the mean thickness of the snow cover should be increased by 10 to 15 cm. On this basis, it is also possible to improve the precision of that component of the Arctic fresh-water balance.

Within the period with stable snow cover, the integral surface albedo exceeds 0.8 as a rule. Changes in the mean monthly values are small and almost independent of latitude. In May the latitude dependence appears, in fact, to be connected with snow-cover melting. The minimum values of albedo in the Central Arctic Basin, a little more than 50%, are observed in July and August. When the new snow cover forms, the reflecting power of the surface increases again. The range of variation in the mean values of integrated albedo throughout the year is great—from 35% for snow saturated with water up to 88 % for new-fallen, clean, dry snow.

The maximum interannual changes in integrated albedo are observed in June and in September to October. They are related to the dates of snow formation and decay on the drifting sea ice. Comparison of the integrated and spectral albedos of different snow types measured at the NP drift stations, earlier in the Leningrad region, and in the Antarctic show systematic differences. The differences do not exceed the measurement error. For the spectral dependence of albedo, there is almost no variation over the range of wavelengths from 0.5 μm to 0.7 μm . At both longer and shorter wavelengths, the albedo decreases. Significant changes in the snow albedo values are related to changes in snow characteristics as the snow becomes moist and begins to melt in the spring and as new snow begins to form in the fall.

Two distinct intervals were observed in the atmospheric circulation processes at the drift stations (based on the Vangengeim-Girs classification): 1949 to 1971 was characterized by circulation forms E and C, and 1972 to the beginning of the 1990s was characterized primarily by circulation form E. These circulation forms are characterized primarily by meridional atmospheric fluxes. For this reason, the interannual characteristics of the cloud systems in the Arctic Basin, and consequently the precipitation, were quite stable from the 1950s to the beginning of the 1990s. Thus one can conclude that the data on snow-cover parameters collected on the snow lines at the NP drift stations are representative of the undeformed ice surfaces for almost the entire region.

The investigation of the spatial and temporal distribution of the snow-cover characteristics in the Arctic Basin made it possible to estimate the variabilities and to parameterize the regular behavior. Stable snow-cover formation in the Arctic Basin occurs, on average, on the 20th of August, and its decay occurs on the 18th of July. However, there were instances when the snow cover was preserved throughout the summer up to the beginning of the next period of snow deposition. By the end of the accumulation period, the snow-cover thickness reaches 30 to 40 cm. The snow density at the beginning of the accumulation period (September to October) is 200 to 220 kg/m³, and it increases up to 360 kg/m³ by the beginning of snow melt. Wet, melting snow has a density of 510 to 550 kg/m³. Density increases with increasing snow depth by about 70 to 75 kg/m³ for each 1 m of snow, reaching 460 kg/m³ for 3 m of dry snow in March and April. Melting of the snow cover begins at an air temperature of -4°C if the intensity of the solar radiation reaches at least 600 W/m². The penetration of solar radiation into snow is very small. The uppermost 5 cm of the snow intercepts 70 to 90% of the incident radiation. The solar radiation that exits the snow from the 5-cm level is 6 to 18% of the radiation incident on the snow surface.

Changes are continually taking place in the snow cover owing to evaporation, condensation of moisture, densification, and other processes. In the Arctic Basin, 48 mm of water equivalent evaporates in the course of a year, and 22 mm of moisture condenses on the snow surface (mainly as rime). On clear days, the temperature of the snow surface is 5 to 7°C lower than the air temperature, but on overcast days there is almost no difference.

For the first time, a technique has been developed for obtaining a continuous series of observations at the drift stations. These series are essential for investigating the interannual variability of the meteorological parameters.

Estimates have been obtained of the changes in snow-cover characteristics, precipitation, and air temperature over the total working period of drift stations in the Arctic Basin. According to the snow measurements for May, at the end of accumulation period, the snow-cover thickness decreased by 19 cm from 1954 to 1991. From 1976 to 1991, the number of days without snow decreased, and the duration of the snow-accumulation period increased correspondingly. This increase was the combined result of earlier formation of the snow cover and retardation of the date of its decay. As a whole over the entire working period of the drift stations, it is not possible to distinguish a significant change in the mean duration of the snow-covered period.

From 1954 to 1991, there was a decrease in the annual amount of precipitation in the Arctic Basin, basically due to changes in the winter. The decrease in the amount of precipitation during the cold period in the Arctic Basin over the 36-year interval was 17 mm. The interannual variations of air temperature from 1955 to 1990 for the different seasons and over the entire year showed no sign of significant long-term changes.

9. REFERENCES*

1. Alexandrov E. I. and Maystrova V. V., Comparison of atmospheric temperature changes of the polar regions, *Problemy Arktiki i Antarktiki*, 69 , pp. 38–52, 1995.
2. *Albedo and Angle Reflection Characteristics of Clouds and the Underlying Surface*, edited by Kondrat'yev, K. Ya. (-L, Gidrometeoizdat, 1981), 231 pp.
3. *Atlas of the Arctic*, Treshnikov A F. ed. (-L, GUGK [Main Administration for Geodesy and Cartography], 1985).
4. *Atlas of the World Water Balance* (-L, Gidrometeoizdat, 1974).
5. *Atlas of the Ocean: The Arctic Ocean*, Gorshkov S. G. ed. (MO SSSR [Ministry of Defense of the USSR], 1980).
6. Baskakov, G. A., The oceanic boundary of the Arctic, *Proc. AARI*, 304, pp. 36–58, 1971.
7. Bryazgin N. N., On the question of albedo of drifting ice, *Problemy Arktiki i Antarktiki* , 1, pp. 33–40, 1959.
8. Bryazgin N. N., The cloud cover in the Arctic, *Problemy Arktiki i Antarktiki*, 9, pp. 75–78, 1961.
9. Bryazgin N. N., Glaze ice and rime investigations in the Central Arctic, *Problemy Arktiki i Antarktiki*, 31, pp. 66–68, 1965.
10. Bryazgin N. N., Recommendations for the preparation of uniform series of monthly precipitation sums in regions of the USSR affected by snow storms (-L, AARI, 1980), 36 pp.
11. Bryazgin N. N. and Koptev A. P., On the spectral albedo of the ice-snow cover, *Problemy Arktiki i Antarktiki*, 31, pp. 79–83, 1969.
12. Buzuev A. Ya. and Dubovtsev V. F., Some regularities in the thickness of the snow and ice cover in the Arctic seas, *Meteorologiya i gidrologiya*, 3, pp. 54–60, 1978.
13. Buzuev A. Ya., Romanov I. P., and Fedyakov V. E., Variability of the snow distribution on Arctic sea ice, *Meteorologiya i gidrologiya*, 9, pp. 76–85, 1979.
14. Buinitsky V. Kh., Melting of the snow and ice cover in 1939, *Proc. Drift Glavsevmorputi Expedition on the Ice-Breaker G. Sedov* (-M,-L, Glavsevmorputi Publishing, 1951), pp. 90–98.

*All references are in Russian unless noted otherwise. -L = Leningrad, -M = Moscow.

15. Vaganov R. Kh., Gavrilov V. P., Kozlov A. I., Lebedev G. A., and Logvin A. I., *Range Methods for the Investigation of Sea Ice* (St. Petersburg, Gidrometeoizdat, 1993), 342 pp.
16. Girs A. A., The macrocirculation method for long-time meteorological forecasts (-L, Gidrometeoizdat, 1974), 488 pp.
17. Dem'yanov N. I., Ice observations at drift station "NP-4," in *Results of the Observations of the Drift Stations "NP-3" and "NP-4,"* Vol. 1 (-L, Gidrometeoizdat, 1957), pp. 399-43.
18. Dolgin I. M., Briazgin N. N., and Petrov L. S., The snow cover of the Arctic, *Proc. AARI*, 326, pp. 165-170, 1975.
19. Dyunin A. K., *Snow Evaporation* (Novosibirsk, 1961), 119 pp.
20. Kalitin N. N., Spectral albedo of the snow cover, *Series on Geography and Geophysics, Nos. 2 and 3* (Academy of Sciences of the USSR Publishing, 1938).
21. Karol' B. P., Radiation penetration into snow and ice on glaciers, in *International Geophysical Year* (-L, Leningrad University Publishing, 1960), pp. 151-160.
22. *Arctic Atlas of Climatology* (-L, Sea Transport Publishing, 1963).
23. *The Arctic Climatological Regime at the Boundary Between the 20th and 21st Centuries* (-L, Gidrometeoizdat, 1991), 200 pp.
24. Kozlov M. P., Results of the calculation of some mechanical characteristics of snow in the Arctic, in *Snow Cover, Its Distribution and the Role in the National Economy* (-M,-L, Academy of Sciences of USSR Publishers, 1962), pp. 47-54.
25. Kondrat'yev K. Ya., Mironova Z. F., and Daeva L.V., Spectral snow and plant cover albedos, in *International Geophysical Year* (-L, Leningrad University Publishing, 1960), pp. 35-58
26. Kondrat'yev K. Ya., Mironova Z. F., and Otto A. N., The spectral albedo of natural surfaces, *Problemy Fiziki Atmosferi*, 7(24), pp. 24-47, 1965.
27. Kopanev I. D., *Methods for Investigating the Snow Cover* (-L, Gidrometeoizdat, 1971), 228 pp.
28. Koptev A. P. and Piatnenkov B. L., Absorption and penetration of solar radiation into snow and ice in the Arctic, *Problemy Arktiki i Antarktiki*, 10, pp. 71-76, 1962.
29. Kuz'min P. P., Methods for the investigation of evaporation from the snow cover, *Proc. GGI*, 41(95), pp. 11-14, 1953.
30. Kuz'min P. P., *Physical Properties of the Snow Cover* (-L, Gidrometeoizdat, 1957), 205 pp.

31. Litvinov I. V., *Formation of Atmospheric Precipitation and Its Transformation on the Underlying Surface* (-L, Gidrometeoizdat, 1987), 232 pp.
32. Loshchilov V. S., The snow cover on the ice in the Central Arctic, *Problemy Arktiki i Antarktiki*, 7, pp. 36–45, 1964.
33. Marshunova M. S. and Mishin A. A., Handbook of the Radiation Regime of the Arctic Basin (Results from the Drift Stations), Radionov V.F. ed. (St. Petersburg, Gidrometeoizdat, 1994); Technical Report APL-UW TR 9413, Applied Physics Laboratory, University of Washington, Seattle, WA 98105-6698, December 1994, 66 pp. [in English].
34. Marshunova M. S. and Radionov V. F., Dynamics of the radiation climate of the Arctic, *Problemy Arktiki i Antarktiki*, 69, pp. 64–73, 1995.
35. Marshunova M. S. and Chernigovskiy N. T., Radiation Regime of the Foreign Arctic (-L, Gidrometeoizdat, 1976). (Translated from Russian by Indian National Scientific Documentation Centre, New Delhi, 180 pp.)
36. *Results of the Investigations at Drifting Stations NP-3 and NP-4*, Vol. 1 (-L, Gidrometeoizdat, 1957), 440 pp.
37. Mel'nik D. M., On the laws of snow transport and their use in snow warfare. *Tekhnika Zheleznikh Dorog*, 11, pp. 10–11, 1952.
38. Mikhailov V. V. and Voytov V. P., A universal spectrometer for the investigation of short-wave radiation fields in atmosphere, in *Problemy Fiziki Atmosfery*, 4, pp. 120–128, 1966.
39. Nazintsev Yu. L., On snow accumulation on the ice in the Kara Sea, *Proc. AARI*, 303, pp. 185–190, 1971.
40. *Instruction for Hydrometeorological Stations and Posts*, Vol. 3, Part 1 (-L, Gidrometeoizdat, 1985), 300 pp.
41. Prik Z. M., Mean position of the surface pressure and temperature fields in the Arctic, *Proc. AARI*, 217, pp. 5–69, 1959.
42. Prik. Z. M., Climatological analysis of the meteorological observations from the drift stations, *Proc. AARI*, 328, pp. 4–21, 1974.
43. Ragozin A. I. and Chukanin K. I., Mean trajectories and drift speeds of the pressure systems in the Eurasian Arctic and Subarctic, *Proc. AARI*, 217, pp. 35–64, 1959.
44. *Radiation in the Cloudy Atmosphere*, Feygel'son E. M. ed. (-L, Gidrometeoizdat, 1981), 280 pp.

45. Radionov V. F., Sakunov G. G., and Grishechkin V. S., Spectral albedo of the snow-covered surface using the data from drift station NP-22, in *First GARP Global Experiment*, Vol. 2, *Polar aerosol, heavy cloudiness, and radiation* (-L, Gidrometeoizdat, 1981), pp. 89–91.
46. *Radiation Characteristics of the Atmosphere and of the Earth's Surface*, Kondrat'yev K. Ya. ed. (-L, Girometeoizdat, 1981), 280 pp.
47. Romanov I. P., Ice cover of the Arctic Basin (St. Petersburg, AARI Reprint, 1992), 211 pp.
48. Romanov I. P., *Atlas of the Morphological Characteristics of Ice and Snow in the Arctic Basin* (St. Petersburg, AARI, 1993), 152 pp.
49. Sakunov G. G., Grishechkin V. S., Kovalenko A. P., and others, Spectral albedo of the Antarctic snow-covered surface, *Inform. Bulletin Soviet Antarctic Expedition*, 111, pp. 62–67, 1989.
50. Timerev A. A., Reflection characteristics of the surface of polar regions, *Proc. AARI*, 328, pp. 106–115, 1976.
51. Shamont'yev V. A., Ice observations on drift station "NP-3," in *Results of the Observations of the Drift Stations "NP-3 and NP-4,"* Vol. 1 (-L, Gidrometeoizdat, 1957), pp. 367–398
52. Chernigovskiy N. T. and Marshunova M. S., *The Climate of the Soviet Arctic (The Radiation Regime)* (-L, Gidrometeoizdat, 1965), 198 pp.
53. Yakovlev G. N., The snow cover on the drift ice of the Central Arctic, *Problemy Arktiki i Antarktiki*, 3, pp. 65–76, 1960.
54. Yanishevsky Yu. D., *Actinometric Instruments and Methods of Measurement* (-L, Gidrometeoizdat, 1957), 416 pp.
55. Yashina A. V., On the penetration of solar radiation into the snow cover, in *The Role of the Snow Cover in Natural Processes* (-M, Academy of Sciences Publishers, 1961), pp. 131–135.
56. Grenfell T. C., Warren S. G., and Mullen P. C., Reflection of solar radiation by the Antarctic snow surface at ultraviolet, visible, and near-infrared wavelengths, *J. Geophys. Res.*, 99(D9), pp. 18,669–18,684, 1994 [in English].
57. Kukla G. J. and Robinson P., Annual cycle of surface albedo, *Mon. Wea. Rev.*, 108(1), pp. 25–31, 1989 [in English].
58. Shapiro-Ledley, T., Variations in snow on ice: A mechanism for producing climate variations. *J. Geophys. Res.*, 98(D6), pp. 10,401–10,410, 1993 [in English].

Appendix A
Spectral albedo of the snow surface of
Koltushi (Leningrad Region) in March 1957
59°57'N. Lat., 30°42' E. Long

Date	Mean Solar Time	Cloudiness	State of the snow cover	Wavelength, nm																	Integ. Albed ^o						
				400	403	410	420	435	445	460	480	501	526	557	572	590	610	640	652	667		687	712	742	775	800	
1 4 Mar.	2	3	4	5	6	7	8	9	10	11	12	13	14	15	16	17	18	19	20	21	22	23	24	25	26	27	
	11-00	0/0	Snow Dense	80	82	83	80	78	78	76	74	73	73	72	70	70	69	67	67	68	70	70	74	74	74	80	
	12-00	0/0	Clean	61	61	77	78	79	77	79	-	70	71	71	69	72	73	71	72	73	71	72	74	72	75	79	
	13-00	0/0	Large grained	68	73	78	79	77	76	74	76	73	71	70	73	72	73	72	73	72	73	73	74	76	77	77	
	14-00	0/0,turbid		-	73	77	77	72	71	71	69	66	65	64	65	66	66	65	65	66	68	65	70	76	78	81	
15-00	0/0-1/0 Ci		-	62	66	67	67	68	71	70	70	69	67	67	65	-	65	65	64	64	-	63	62	-	62	78	
16-00		5/0-10/0 Ci	above	-	-	61	65	68	68	73	73	70	70	71	74	-	-	74	-	-	71	-	67	-	65	70	
			above	-	66	68	68	70	71	72	72	74	76	76	-	-	73	73	-	-	75	-	70	-	63	69	
		5/0-Ci,Ac		65	67	63	64	61	61	62	61	61	61	61	62	63	63	64	66	67	69	71	67	-	60	77	
		10/0 Ci,Ac	Dense, Clean	70	71	72	72	73	75	75	76	77	77	78	78	78	78	78	79	78	78	78	77	75	-	79	79
		10/0Ac,As	Large grained	67	70	77	67	63	66	69	-	74	-	74	60	-	71	-	-	-	-	68	-	67	-	-	76
6 Mar.	12-45	10/0 As,Cs	New snow,	83	-	77	-	-	-	79	-	73	-	-	-	78	-	-	-	-	68	-	69	-	-	82	
	13-15		dry,	-	85	83	80	80	80	79	78	77	80	-	83	82	80	82	-	-	81	-	81	-	80	80	
	14-00		loose	72	77	80	80	83	83	83	82	83	84	84	-	83	84	83	-	85	-	90	98	-	98	78	
	15-00		Same as above	-	73	-	80	-	80	-	73	-	76	-	73	-	-	76	-	-	81	-	-	-	-	82	
	16-00		Same as above	81	79	-	-	-	-	71	-	76	-	-	-	-	-	65	-	-	-	-	81	-	-	81	
7 Mar.	17-00		Same as above	-	76	73	73	73	74	71	70	68	66	64	62	-	63	67	-	-	67	-	69	-	-	78	
	9-20	0/0,turbid	Snow loose	77	80	82	80	79	80	78	78	77	76	76	75	-	75	75	-	76	77	-	77	-	77	73	
	10-00	0/0,turbid	dry, fine	73	78	78	86	84	81	78	78	76	75	75	73	-	73	71	-	69	69	-	70	-	69	76	
	11-00	0/0,turbid	grained,	-	79	83	80	78	76	76	76	74	74	73	72	-	70	68	-	69	66	-	68	-	68	76	
	12-00	0/0	as yesterday	76	74	72	70	69	68	70	67	66	65	65	64	64	65	62	63	63	65	64	62	-	(60)	72	
13-00	5/0 Ac-1/0 Ac	Same	72	73	74	71	75	-	74	74	75	75	74	-	77	77	77	-	-	79	-	72	-	(63)	76		
11 Mar.	9-30	10/10 Ns	Snow dry,	74	-	77	-	-	64	-	69	71	-	-	67	-	65	-	-	-	-	56	-	-	-	68	
	10-15	10/10 Ns	dirty, with	64	52	56	62	53	53	54	49	45	44	49	-	47	46	50	-	58	56	-	67	-	-	72	
	12-00	10/10 Ns	dark patches	69	68	-	69	67	67	67	-	53	60	-	-	61	-	61	-	-	-	-	-	-	-	73	
	14-00	10/0 Ac,Ci	after blizzard	55	56	54	63	62	62	55	57	59	60	59	-	58	60	60	-	58	59	-	70	-	67	68	
	15-00	10/0 Fc		-	-	56	59	58	58	52	40	42	60	53	-	-	54	-	-	-	52	-	-	-	-	63	
16-00	10/0 Fc	Same as above	-	56	59	58	68	71	66	56	78	68	-	-	-	60	51	-	-	76	-	68	-	-	73		
14 Mar.	9-50	10/0 Ac,Sc	Snow layered	61	-	67	-	66	-	70	-	66	65	67	-	66	-	68	-	68	56	-	57	-	-	69	
	11-00	10/0 Cs	dark, dense	61	-	68	69	63	63	64	-	61	61	63	-	63	-	67	-	66	58	-	74	-	-	72	
	12-00	10/0 Sc,Ac	fine-grained	63	-	77	73	62	64	69	68	67	67	67	-	77	-	78	-	82	85	-	-	-	-	68	
	13-00	10/0 Sc,As		61	-	65	75	65	65	66	69	70	72	75	-	79	-	83	-	88	-	-	-	-	-	69	
	13-10	10/10 As,Ns	crust,blizzard	57	-	60	64	70	72	72	72	73	73	74	-	75	-	72	-	74	74	-	62	-	-	71	

17 Mar.	10-00	1/0 Ci	Snow clean	65	66	64	62	61	61	61	60	60	61	59	58	61	70	71
	11-00	10/0 Cc	fine grained	69	68	65	62	62	62	62	63	63	65	64	65	65	65	69
	12-00	10/0 Cc,Ac	dense with	61	63	74	60	60	60	63	66	66	65	67	67	70	68	68
	13-00	10/0 Cc,As	patches of	75	67	67	69	68	68	68	68	68	71	76	76	75	70	70
	15-00	2/0 As-7/0 As	old snow	59	58	60	61	60	65	68	67	69	69	63	63	75	70	70
	16-00	10/0 As,Cs		60	75	65	77	73	73	73	75	75	75	64	64	67	66	66
	17-00	7/0 As	Same	72	71	72	72	76	76	76	78	79	79	64	67	67	67	67
18 Mar.	9-00	10/0 Ci	New fallen	73	71	69	68	68	68	68	68	68	68	77	77	62	79	79
	10-00	10/0 Cs,Ci	snow, clean	76	74	72	70	71	73	71	71	72	72	72	72	70	80	80
	11-00	10/0 Cs,Ci	fine grained	72	70	68	66	68	68	68	68	68	71	70	70	67	80	80
	12-00	10/0 Ci	with a wavy	65	71	68	69	68	68	68	70	69	68	72	60	68	80	80
	14-00	10/0 Cs,As	surface after	70	79	78	77	76	79	77	81	78	80	82	80	71	79	79
	15-00	10/0 Cs	blowing snow	64	70	76	79	79	80	80	78	80	80	81	70	74	80	80
	16-00	10/10 As,Ns		76	77	76	78	80	82	81	82	83	82	76	77	79	77	77
	17-00	10/0 As		64	66	82	78	74	77	80	83	82	84	85	85	74	78	78
20 Mar.	11-00	0/0	Snow dry,	67	72	73	72	72	70	70	68	68	71	73	73	66	77	77
		0/0,haze	dense,	69	72	72	70	70	70	70	70	70	70	71	71	66	77	77
			layered															
			wavy surface	64	67	71	72	74	72	71	72	72	73	73	74	86	79	79
			clean	61	66	71	69	68	67	68	69	70	72	74	73	(90)	80	80
				68	75	80	75	71	71	69	70	68	72	74	75	(74)	75	75
				68	75	77	68	71	74	72	73	75	73	72	63	(71)	75	75
			Same	74	75	74	79	72	77	75	77	77	71	75	80	(89)	74	74
21 Mar.	10-00	10/0 Ac,Cs,Ci	Snow layered	68	70	70	74	72	72	72	72	72	2	70	71	74	76	76
	11-00	10/0 Ac	dense, as	72	76	73	73	73	74	75	76	74	77	70	71	77	79	79
	12-00	10/0 Ac,Ce	yesterday,dry	70	72	73	70	70	71	73	72	72	75	73	72	77	76	76
	14-00	10/0 Ac,As		76	80	78	76	77	77	76	77	78	78	79	73	81	75	75
23 Mar.	10-45	0/0	New snow	75	80	81	80	80	81	78	80	89	89	90	90	84	83	83
	12-00	0/0	thin layer	83	83	81	79	77	76	75	74	77	76	77	78	84	83	83
	13-00	1/1 Cu	loose, dry	68	68	67	68	68	68	70	73	72	73	73	75	82	82	82
	14-00	0/0 weak	same	68	68	67	68	68	69	70	64	69	70	68	70	76	80	80
		winds																
	14-15	0/0	same	68	79	78	76	71	69	66	64	63	62	60	58	51	80	80
	15-00	0/0,trace	same	60	61	63	65	64	63	56	60	62	60	49	46	71	82	82
	16-00	0/0	same	60	62	64	65	66	66	64	63	60	67	67	69	71	80	80
	17-00	0/0	same	60	54	58	58	59	60	60	61	61	63	63	68	71	77	77
24 Mar.	9-00	0/0	Snow from	74	65	78	82	87	86	84	84	84	80	83	81	(72)	87	87
	10-00	0/0	yesterday,dry,	68	79	79	79	77	78	79	79	79	80	80	86	(74)	88	88
	11-00	1/0 Ci	fine grained	58	63	75	74	75	75	75	74	75	76	76	76	76	80	80
	12-00	1/0 Ci	wavy surface	70	60	65	66	67	68	68	70	72	70	70	70	73	84	84
	13-00	2/0 Ci	same	70	74	77	74	74	72	71	73	74	71	72	70	73	83	83
	15-00	10/0 Ci	same	67	66	67	67	68	66	68	68	66	62	66	65	66	80	80
	16-00	10/0 Ci	Same	67	66	67	67	68	66	68	68	66	62	66	65	66	80	80

Appendix B
Spectral albedo of the snow cover
Sablino (Leningrad Region), February to April 1958
59°40 N. Lat., 30°48 E. Long.

Date	Mean solar Time	Cloudiness	State of the snow cover	Wavelength, nm																	Total Albedo						
				400	403	410	420	435	445	460	480	501	526	557	572	590	610	640	652	667		687	712	742	775	800	
1 Feb.	2	3	4	5	6	7	8	9	10	11	12	13	14	15	16	17	18	19	20	21	22	23	24	25	26	27	
	11-15	0/0,haze	Snow clean	74	74	77	76	-	-	79	73	72	81	80	-	88	-	-	-	82	-	65	69	-	60	-	
	14-00	10/3 As,Fc	new fallen	-	74	79	76	-	66	83	63	74	64	70	-	74	58	73	-	-	-	68	65	-	72	-	
	15-00	10/4 As,Sc,Fc	loose	80	89	81	78	75	75	73	73	71	71	72	-	72	72	71	79	72	-	66	70	-	-	-	
11 Feb.	11-00	2/0 Sc	Snow dense	-	78	71	75	75	74	74	75	77	76	76	75	76	74	75	76	76	75	71	65	68	64	77	
	15-00	0/0	clean, fine-	82	85	77	74	75	65	72	70	60	64	66	66	60	68	81	77	73	69	61	71	78	-	89	
	16-00	3/0 Ci	grained, dry	71	76	78	82	78	75	74	75	76	77	65	67	69	68	67	73	73	78	67	-	-	-	74	
25 Feb.	10-00	8/0 Ci	Snow dry	74	75	72	72	63	63	62	62	62	63	64	61	60	60	60	60	64	64	65	69	72	-	-	
	11-00	5/0 Ci,blizzard	fine grained	74	63	59	51	71	67	70	73	71	66	60	67	68	77	75	59	67	66	73	-	59	65	-	
	12-00	2/0 Ci	clean	63	67	70	67	70	71	70	69	69	68	69	69	71	74	75	79	78	77	78	78	77	73	-	
	13-00	0/0	same	68	69	69	67	67	66	66	65	65	65	64	63	63	62	62	61	61	60	60	60	59	60	-	
	14-00	1/0 Ci	same	76	78	75	79	77	76	75	78	81	86	88	-	-	-	-	-	-	71	69	74	70	62	-	
	15-00	0/0	same	68	72	70	71	69	68	68	68	67	66	66	67	68	69	73	73	74	70	62	55	53	53	-	
	16-00	1/0 Ci	same	69	70	69	70	67	63	59	61	60	59	57	57	57	58	61	68	73	77	83	84	82	76	-	
26 Feb.	8-20	10/0 Cs,As	snow layered	89	87	87	87	87	87	87	87	87	84	84	84	84	83	82	81	81	80	75	76	77	-	-	
	9-20	10/0 Cs,As	dense, dry	82	82	78	78	72	74	79	78	80	81	81	80	81	85	86	-	76	76	72	72	74	-	-	
	12-00	10/0 As	fine grained	74	69	73	74	74	74	73	75	74	70	-	75	74	72	87	81	81	79	-	-	-	-	-	
	14-00	10/10 St	same	-	-	-	76	76	80	85	84	83	75	78	83	83	82	82	82	85	80	87	80	85	-	-	
	15-00	10/10 St	same	74	75	75	74	75	77	77	77	77	79	78	78	82	79	78	81	-	84	86	-	-	-	-	
4 Mar.	9-00	0/0,haze	snow dry	71	76	77	73	72	72	73	73	73	73	74	75	74	75	75	74	72	72	73	72	72	72	-	-
	12-00	2/0 Ci	dense	-	-	54	52	52	54	57	60	59	59	60	60	60	61	62	61	62	61	63	60	63	-	-	
	13-00	4/0 Ci	fine grained	-	-	54	62	72	75	72	73	67	65	52	55	53	42	46	50	51	52	55	56	52	53	-	
	14-00	3/0 Ci	same	58	60	62	62	62	58	57	56	55	54	54	53	58	59	61	61	62	62	58	57	57	59	-	
	16-00	9/0 Ac	same	65	69	69	70	72	72	72	73	73	74	73	73	72	72	72	74	77	83	82	77	76	72	-	
8 Mar.	12-00	1/0 Ci	new snow loose	65	63	63	65	64	64	71	70	69	69	67	66	65	64	61	58	57	58	57	56	54	74	-	
17 Mar.	8-00	0/0	densified by solar heating	-	-	-	55	56	59	67	65	65	67	67	68	68	68	70	72	69	67	63	64	-	-		
	10-00	0/0	snow dirty	58	62	65	72	70	70	69	55	55	55	51	53	64	66	63	-	-	65	62	64	60	70		
	11-00	0/0	damp, densified	61	65	63	63	63	68	66	65	64	65	65	66	63	64	65	65	67	67	63	65	61	66	70	
	12-00	0/0	same	63	65	66	69	69	68	68	66	65	65	65	65	65	64	64	63	69	72	75	77	77	-	70	
	14-00	0/0	same	53	57	57	60	61	62	62	63	66	64	64	64	64	63	63	63	66	67	68	70	70	-	69	
	16-00	0/0	same	57	61	62	64	67	68	69	75	75	73	73	72	72	72	72	72	77	78	80	80	78	-	71	
	17-00	0/0	same	63	65	65	67	65	69	82	-	81	80	80	74	76	77	80	81	81	81	81	83	86	-	72	

18 Mar.	14-00	1/0 Ci	14-00	64	62	63	63	61	60	59	57	59	61	60	64	60	58	54	58	70
	16-00	1/0 Ci	16-00	71	75	76	74	74	72	71	63	69	70	69	66	62	73	87	80	73
	17-00	0/0	17-00	63	70	84	84	84	84	80	82	81	79	79	86	87	81	80	-	83
19 Mar.	8-00	1/0 Ci	8-00	69	68	65	65	63	63	64	65	73	72	70	68	65	63	62	62	69
	9-00	0/0	9-00	61	67	71	69	68	68	68	67	67	70	71	71	70	69	69	62	68
	11-00	2/0 Ci	11-00	70	66	68	66	66	65	65	64	64	68	70	71	75	74	73	69	69
	12-00	1/0 Ci	12-00	64	63	64	64	64	64	63	63	62	62	60	59	58	58	59	62	69
	13-00	2/0 Ci	13-00	61	63	64	63	62	64	64	64	65	66	68	70	69	74	74	69	69
	14-00	5/0 Ci	14-00	62	60	62	62	61	62	62	61	60	59	59	58	57	55	58	61	69
	16-00	9/0 Ci	16-00	61	67	75	74	74	73	70	71	71	75	77	78	79	82	80	73	73
	17-00	9/0 Ci	17-00	63	66	69	68	67	66	66	66	64	63	59	58	54	65	66	68	76
21 Mar.	8-00	0/0	8-00	61	65	66	66	64	-	69	68	69	70	71	73	-	69	70	69	71
	10-00	0/0	10-00	57	58	60	60	56	62	63	62	62	60	61	61	61	57	-	-	68
	11-00	0/0	11-00	61	62	63	61	62	63	62	68	69	70	71	73	76	77	70	70	69
	12-00	0/0	12-00	63	62	64	62	62	62	62	61	61	68	68	69	72	72	72	72	70
	14-00	0/0	14-00	61	64	65	66	67	67	67	66	65	64	63	63	69	70	70	67	68
	16-00	0/0	16-00	63	61	76	73	68	67	67	63	66	71	66	68	72	71	71	-	73
	17-00	0/0	17-00	65	65	65	65	67	63	64	66	67	67	68	69	71	73	73	72	68
22 Mar.	9-15	0/0	9-15	67	68	69	69	68	68	67	67	68	67	67	66	65	63	65	65	67
	10-00	1/0 Ci	10-00	56	61	62	62	61	61	61	69	67	67	66	64	63	64	68	-	68
	11-00	1/0 Ci	11-00	65	64	64	64	63	62	62	65	70	70	70	70	69	68	62	61	68
	12-00	1/0 Ci	12-00	64	63	64	69	68	68	68	68	68	66	66	69	71	70	68	65	69
	13-00	2/0 Ci	13-00	58	61	67	65	65	64	65	67	68	70	72	71	70	70	70	64	68
	16-00	0/0	16-00	59	64	66	72	72	66	65	64	63	63	65	68	71	74	71	61	71
28 Mar.	11-00	2/0 Ac	11-00	64	65	66	67	68	67	68	68	68	67	67	64	62	62	61	62	72
	12-00	1/0 Ac	12-00	63	62	64	64	64	64	64	64	64	66	66	67	69	74	72	70	71
	13-00	1/0 Cu	13-00	74	75	76	75	76	77	77	76	80	81	84	87	94	95	90	94	71
	14-00	0/0	14-00	67	62	61	62	61	61	61	60	59	60	59	60	64	66	68	66	70
	16-00	0/0	16-00	59	62	61	62	64	64	63	64	61	60	63	66	68	70	72	66	73
	17-00	0/0	17-00	46	59	62	73	71	68	67	67	69	-	64	72	76	77	76	71	80
29 Mar.	9-20	10/0 Ac	9-20	70	72	64	75	63	64	65	66	67	65	69	69	68	71	52	-	60
	10-00	6/0 Ac	10-00	65	47	49	68	55	66	66	65	64	65	70	71	71	-	71	68	68
	12-20	5/0 Ac-3/0 Ac	12-20	70	69	71	72	73	76	80	80	80	82	82	82	83	82	84	87	69
	14-35	1/0 Cu	14-35	59	60	67	66	65	65	65	65	65	66	65	63	58	61	64	64	68
	16-00	3/2 Cu, Ci-	16-00	60	57	56	69	64	66	66	65	65	66	66	68	70	73	74	65	71
	17-00	5/1 Ci, Cu 5/2 Ci, Cu	17-00	67	69	72	75	70	68	68	66	65	62	64	67	68	66	58	56	-
31 Mar.	7-50	0/0	7-50	70	67	62	63	62	64	63	61	59	71	69	64	60	57	56	55	67
	9-00	0/0, turbid	9-00	64	68	61	60	59	62	59	58	55	55	53	58	65	65	59	-	63
	10-00	0/0, turbid	10-00	44	47	53	52	49	48	48	50	52	51	51	51	51	43	-	-	64
	11-00	0/0	11-00	63	61	59	59	58	59	59	59	59	63	64	66	66	67	66	-	66
	12-00	0/0	12-00	64	66	71	78	80	80	80	80	80	79	81	83	84	88	87	81	65
	13-00	0/0	13-00	75	74	72	72	74	77	78	77	74	72	72	73	74	77	79	71	63
	14-00	0/0	14-00	55	57	58	61	61	61	61	61	61	62	62	62	62	62	60	-	62
	15-50	0/0	15-50	51	52	56	65	66	67	67	67	67	63	60	68	72	73	74	-	64
	17-00	0/0	17-00	60	60	72	70	69	68	68	67	66	66	78	80	84	78	69	59	70

1 Apr.	8-00	2/0 Ci	snow dry	65	63	62	64	63	65	61	62	63	63	63	64	63	63	63	64	65	64	63	62	60	58	60	56	66
	9-00	2/0 Ci	dirty, porous	61	59	57	52	52	53	52	63	62	64	64	62	64	64	62	62	68	68	62	62	61	61	58	-	63
	10-00	2/0 Ci	granular	57	54	56	55	59	57	65	70	64	62	62	62	62	62	62	61	60	60	66	67	65	66	60	63	
	11-00	3/0 Ci-5/0 Ci	same	55	57	57	54	54	55	70	64	64	64	65	65	65	65	65	65	64	65	67	69	71	73	74	73	
	14-00	3/0 Ci	same	53	50	49	48	50	51	62	62	63	63	63	63	63	63	63	63	64	62	62	60	59	55	49	62	
	16-00	2/0 Ci	same	54	51	49	50	52	53	69	67	66	65	65	64	63	63	63	63	63	63	62	62	64	59	52	62	
	17-00	3/0 Ci	same	56	56	57	59	60	62	63	76	75	75	75	75	75	75	75	74	74	74	75	77	77	71	66	65	
	18-00		same	58	59	59	59	58	58	59	65	65	65	65	65	65	65	65	64	64	64	67	68	68	71	69	62	
4 Apr.	8-00	1/0 Ci	snow with	61	57	66	64	56	60	61	64	64	63	64	63	64	63	62	60	60	60	59	58	56	55	53	57	
	10-00	1/0 Ci	large crystals	64	63	62	57	56	65	58	60	59	59	59	59	59	59	59	59	59	59	61	62	60	60	60	52	
	11-00	2/0 Ci	dirty	58	58	58	58	59	59	60	61	62	62	62	62	62	62	62	63	63	63	66	67	68	68	69	52	
	12-00	1/0 Ci		61	60	59	59	59	59	59	60	60	61	61	62	62	62	62	62	62	62	62	63	63	65	66	65	
	13-00	1/0 Ci	snow wet	54	58	61	64	67	68	69	73	73	75	75	76	77	77	77	77	77	77	82	83	84	89	86	79	
	14-00	1/0 Ci	same	49	53	56	56	58	59	59	59	59	59	60	60	60	60	60	60	60	60	60	60	60	61	59	51	
8 Apr.	8-00	0/0	snow with	51	55	59	59	60	61	63	75	74	74	74	73	72	72	70	70	70	73	76	79	79	80	80	80	
	9-00	0/0	large crystals	58	57	57	62	62	63	62	56	55	54	55	58	59	59	59	59	59	59	76	82	87	89	82	78	
	10-00	1/0 Ac	dirty, melting	64	64	62	59	60	60	60	62	61	61	62	62	62	62	60	64	65	66	66	67	67	67	65	-	
	11-00	5/0 Ac	thin damp layer	55	56	60	62	62	60	61	63	58	60	62	63	63	63	63	63	63	63	61	60	59	59	60	49	
	12-00	3/3 Cu	same	54	56	57	58	59	60	64	64	64	63	65	65	65	66	66	66	66	67	66	63	62	62	60	49	
	14-00	8/8 Fe, Ac, Cb	same	45	51	60	-	48	56	-	-	-	-	52	-	-	56	56	56	56	-	54	-	57	-	53		
	16-00	7/7 Cu, Fe	same	43	42	41	38	38	39	38	51	50	48	48	47	46	46	46	46	46	46	50	49	47	44	45	50	
10 Apr.	10-00	4/0 Ci	snow porous	53	52	50	51	53	54	53	57	56	55	54	55	54	54	56	56	56	52	51	56	-	55	51	-	
	11-00	5/0 Cs-7/0 Ci	damp with	55	55	55	57	58	-	61	54	55	57	57	58	57	59	-	61	62	62	69	65	64	57	-	-	
	12-00	8/0 Cs, Cs	drops of	52	52	56	55	56	55	51	57	56	57	57	54	54	57	53	59	59	59	61	61	62	60	-	53	
	13-00	10/0 Cs, Cs	moisture, dirty	51	56	55	55	53	53	53	58	58	58	58	58	58	57	58	58	58	58	59	61	65	63	60	58	
	14-00	10/0 Cs, As	same	55	56	55	53	56	54	54	60	57	56	57	58	57	57	57	57	57	57	60	61	60	63	60	59	
	15-00	10/0 Cs, As	same	50	51	52	58	56	-	56	62	61	59	58	59	58	58	57	57	57	57	61	62	64	64	-	57	
	16-00	10/0 Cs, As	same	50	53	53	56	57	58	59	61	61	61	60	60	60	63	59	62	63	59	62	63	63	61	58	53	
	17-00	10/0 Cs, As	same	50	50	51	54	56	58	59	65	64	64	64	63	61	61	60	63	61	60	66	67	68	69	59	66	

Appendix D

Measurements of ice thickness (h_{ice}) and snow thickness (h_{snow})
during the cruise of the icebreaker *G. Sedov*

Date	h_{ice} (cm)	h_{snow} (cm)	deg N. Lat.	deg E. Long.
26.10.1937	27	3	75.6	131.3
27.10.	28	3	75.8	131.2
28.10.	29	2	75.9	131.1
29.10.	30	2	76.0	131.1
30.10.	31	2	76.1	131.2
31.10.	32	3	76.2	131.4
1.11.1937	33	3	76.2	131.5
2.11.	34	3	76.3	131.4
3.11.	35	3	76.3	131.9
6.11.	41	4	76.5	130.2
9.11.	43	8	76.9	129.3
12.11.	50	8	77.0	129.2
15.11.	53	8	76.5	130.1
19.11.	58	8	77.1	132.2
22.11.	60	8	77.4	133.3
25.11.	63	6	77.5	132.8
28.11.	65	6	77.6	133.3
1.12.1937	67	6	77.6	135.9
4.12.	70	6	77.8	138.6
7.12.	73	8	77.8	141.8
10.12.	75	8	78.1	140.8
15.12.	78	8	78.2	141.6
20.12.	88	8	78.3	142.3
25.12.	84	8	78.3	142.7
30.12.	88	8	78.3	141.5
4.01.1938	91	6	78.2	143.2
14.01.	104	6	78.2	147.3
24.01.	112	5	78.0	152.7
3.02.1938	125	5	77.9	151.7
13.02.	133	5	78.2	150.5
23.02.	138	5	78.3	151.4
5.03.1938	145	5	78.6	153.4
15.03.	157	5	78.7	152.6
20.03.	160	5	78.8	152.6
25.03.	166	5	78.8	152.5
30.03.	172	5	78.9	152.4
4.04.1938	172	5	79.2	151.7
9.04.	172	5	79.4	150.8
14.04.	176	5	79.5	150.4
19.04.	182	5	79.7	149.1
24.04.	185	6	79.9	147.6
4.05.1938	188	6	80.1	147.4
9.05.	191	6	80.2	145.3
14.05.	193	6	80.4	145.2
20.05.	193	12	80.5	144.6
25.05.	194	12	80.6	142.9
4.06.1938	195	12	81.1	141.7

REPORT DOCUMENTATION PAGE

Form Approved
OPM No. 0704-0188

Public reporting burden for this collection of information is estimated to average 1 hour per response, including the time for reviewing instructions, searching existing data sources, gathering and maintaining the data needed, and reviewing the collection of information. Send comments regarding this burden estimate or any other aspect of this collection of information, including suggestions for reducing this burden, to Washington Headquarters Services, Directorate for Information Operations and Reports, 1215 Jefferson Davis Highway, Suite 1204, Arlington, VA 22202-4302, and to the Office of Information and Regulatory Affairs, Office of Management and Budget, Washington, DC 20503.

1. AGENCY USE ONLY (Leave blank)		2. REPORT DATE March 1997	3. REPORT TYPE AND DATES COVERED Technical	
4. TITLE AND SUBTITLE The Snow Cover of the Arctic Basin			5. FUNDING NUMBERS NASA Grant NAGW-4382	
6. AUTHOR(S) V.F. Radionov, N.N. Bryazgin, and E.I. Alexandrov <i>Arctic and Antarctic Research Institute, a State Scientific Center of the Russian Federation, Russian Federal Service for Hydrometeorology and Environmental Monitoring</i>				
7. PERFORMING ORGANIZATION NAME(S) AND ADDRESS(ES) Applied Physics Laboratory University of Washington 1013 NE 40th Street Seattle, WA 98105-6698			8. PERFORMING ORGANIZATION REPORT NUMBER APL-UW TR 9701	
9. SPONSORING / MONITORING AGENCY NAME(S) AND ADDRESS(ES) National Aeronautics and Space Administration 300 E St. SW Washington, DC 20546			10. SPONSORING / MONITORING AGENCY REPORT NUMBER	
11. SUPPLEMENTARY NOTES				
12a. DISTRIBUTION / AVAILABILITY STATEMENT Distribution unlimited.			12b. DISTRIBUTION CODE	
13. ABSTRACT (Maximum 200 words) This monograph presents the results, reduction, and analysis of standardized observations of the precipitation and characteristics of the snow cover on the North Pole drifting stations maintained in the Arctic by the USSR from 1954 to 1991. The systematization of this unique set of observations and the resulting general conclusions, the completion of which involved the efforts of several dozen meteorologists, have made it possible for the first time to evaluate quantitatively the spatial and temporal variations of the parameters of the snow cover in the Arctic Basin. Along with cartographic materials, also presented in this monograph, this information can be used directly as input parameters in computer model to investigate a wide range of problems involving energy exchange in the ocean-atmosphere-cryosphere system and regional moisture exchange, as well as for climate research and the calculation of fresh water flux in the Arctic ocean.				
14. SUBJECT TERMS Snow cover, snow properties, Arctic Basin, Russian drifting stations, snow on sea ice			15. NUMBER OF PAGES 95	
			16. PRICE CODE	
17. SECURITY CLASSIFICATION OF REPORT Unclassified	18. SECURITY CLASSIFICATION OF THIS PAGE Unclassified	19. SECURITY CLASSIFICATION OF ABSTRACT Unclassified	20. LIMITATION OF ABSTRACT SAR	